

TECHNISCHE UNIVERSITÄT MÜNCHEN  
Fakultät für Chemie  
Institut für Organische Chemie und Biochemie  
Lehrstuhl für Organische Chemie II

# **Inhibition of Polo-like Kinase 1 by Small Molecules Targeting the Polo-Box Domain**

**Wolfgang Reindl**

Vollständiger Abdruck der von der Fakultät für Chemie  
der Technischen Universität München zur Erlangung  
des akademischen Grades eines

**Doktors der Naturwissenschaften (Dr. rer. nat.)**

genehmigten Dissertation.

Vorsitzender: Univ.-Prof. Dr. Christian Becker

Prüfer der Dissertation: 1. Univ.-Prof. Dr. Horst Kessler  
2. Univ.-Prof. Dr. Bernhard Küster

Die Dissertation wurde am 08.05.2008 bei der Technischen Universität München eingereicht und durch die Fakultät für Chemie am 18.06.2008 angenommen.



# Index

<b>1. Introduction.....</b>	<b>1</b>
<b>1.1 Protein-Protein Interactions.....</b>	<b>1</b>
<b>1.2 Modulation of Protein-Protein Interactions.....</b>	<b>1</b>
1.2.1 Antisense Techniques.....	2
1.2.2 Antibodies.....	2
1.2.3 Peptides and Peptidomimetics.....	3
1.2.4 Small Molecules.....	3
<b>1.3 The Mitotic Serine/Threonine Kinase Plk1.....</b>	<b>5</b>
1.3.1 Polo-like Kinases: an Overview.....	5
1.3.2 Structure of Plks.....	6
1.3.2.1 Overall Structure.....	6
1.3.2.2 The Kinase Domain.....	7
1.3.2.3 The Polo-Box Domain.....	8
1.3.3 Regulation and Mechanism of Plk1 Activity.....	9
1.3.3.1 Regulation of the Protein Level.....	9
1.3.3.2 Regulation of Plk1 Functions .....	9
1.3.3.3 Mechanism of Plk1 Activity .....	11
1.3.4 Cellular Functions of Polo-like Kinases.....	12
1.3.4.1 Multiple Cell-Cycle Functions of Plk1.....	12
1.3.4.2 The Roles of Plk2, Plk3 and Plk4.....	16
1.3.5 Plk1 and Cancer.....	16
1.3.6 Strategies for Plk1 Inhibition.....	17
1.3.6.1 Small Interfering RNAs (siRNAs) and Antisense Oligonucleotides (ASOs). 17	
1.3.6.2 Interfering Peptides.....	17
1.3.6.3 Small-Molecule Inhibitors.....	17
<b>1.4 Aims.....</b>	<b>20</b>
<b>2. Materials &amp; Methods.....</b>	<b>22</b>
<b>2.1 Materials.....</b>	<b>22</b>
2.1.1 Chemicals and Reagents.....	22
2.1.2 Chemical Libraries and Small Molecules.....	23
2.1.3 Kits, Markers and Miscellaneous Materials.....	23
2.1.4 Media, Buffers and Solutions.....	24
2.1.4.1 Bacterial Culture Media .....	24
2.1.4.2 Cell Culture Media.....	24
2.1.4.3 Frequently Used Buffers and Solutions .....	24

---

2.1.5 Bacterial Strains.....	26
2.1.6 Cell Lines.....	26
2.1.7 Primary Cloning Vectors and cDNAs .....	27
2.1.8 Primers.....	27
2.1.8.1 Cloning Primers.....	27
2.1.8.2 Mutagenesis Primers.....	28
2.1.9 Plasmids.....	28
2.1.9.1 Basic Vectors.....	28
2.1.9.2 Modified Vectors.....	29
2.1.10 Proteins.....	29
2.1.10.1 Enzymes.....	29
2.1.10.2 Antibodies.....	29
2.1.10.3 Recombinant Proteins.....	30
2.1.11 Peptides.....	30
<b>2.2 Molecular Biology Methods.....</b>	<b>31</b>
2.2.1 Microbiological Techniques.....	31
2.2.1.1 Cultivation and Maintenance of Bacterial Strains.....	31
2.2.1.2 Transformation of Competent <i>E. coli</i> Strains.....	31
2.2.1.3 Isolation of <i>E. coli</i> Plasmid DNA.....	31
2.2.2 DNA Amplification .....	31
2.2.2.1 Polymerase Chain Reaction (PCR).....	31
2.2.2.2 Mutagenesis PCR.....	32
2.2.3 Enzymatic Treatment of DNA.....	33
2.2.3.1 DNA Restriction with Endonucleases.....	33
2.2.3.2 Ligation of DNA Fragments.....	33
2.2.4 Agarose Gel Electrophoresis and DNA Purification.....	33
2.2.5 Sequencing.....	34
<b>2.3 Protein Isolation Methods.....</b>	<b>34</b>
2.3.1 Protein Expression.....	34
2.3.2 Protein Extraction.....	34
2.3.3 Protein Purification.....	34
2.3.3.1 His-tag Affinity Chromatography.....	35
2.3.3.2 MBP-tag Affinity Chromatography.....	35
2.3.4 Dialysis.....	35
2.3.5 Protein Stocks.....	36
<b>2.4 Protein Biochemistry Methods .....</b>	<b>36</b>
2.4.1 Determination of Protein Concentration.....	36
2.4.1.1 Bradford Protein Assay.....	36

---

2.4.1.2 BCA Protein Assay.....	36
2.4.2 SDS Polyacrylamide Gel Electrophoresis (SDS-PAGE).....	36
2.4.3 Western Blot / Immunoblot.....	37
<b>2.5 Eukaryotic Cell Culture Methods.....</b>	<b>38</b>
2.5.1 General Cell Culture Techniques.....	38
2.5.2 Transient Transfection of Mammalian Cells.....	38
2.5.3 Cell Lysis.....	38
<b>2.6 Cell Biology Methods .....</b>	<b>38</b>
2.6.1 Immunofluorescence .....	38
2.6.2 Determination of Mitotic Index and Mitotic Phases.....	39
2.6.3 Quantification of Plk1 Localization .....	39
<b>2.7 Fluorescence Polarization.....</b>	<b>39</b>
2.7.1 Binding Curves.....	40
2.7.2 Inhibition Curves .....	41
2.7.3 Z'-Factor.....	41
2.7.4 High-Throughput Screen.....	42
<b>3. Results.....</b>	<b>43</b>
<b>3.1 Fluorescence Polarization Assay.....</b>	<b>43</b>
3.1.1 Cloning, Expression and Purification of the Plk1 PBD.....	43
3.1.2 Establishment and Optimization of a FP-Based Binding Assay.....	44
3.1.2.1 Application of Fluorophore-Labeled Peptides.....	44
3.1.2.2 Determination of Optimal Buffer Conditions.....	46
3.1.2.3 Temporal Stability.....	47
3.1.3 Test of Inhibition and Binding Studies.....	48
3.1.4 Determination of the Z'-Factor.....	50
<b>3.2 High-Throughput Screen.....</b>	<b>51</b>
3.2.1 Screening Process.....	51
3.2.2 Validation of Primary Screening Data.....	52
3.2.3 Identification of Poloxin and Thymoquinone.....	54
<b>3.3 Specificity Profiles of Poloxin and Thymoquinone.....</b>	<b>55</b>
<b>3.4 Cellular Assays.....</b>	<b>59</b>
3.4.1 Transfection of the Plk1 PBD.....	59
3.4.1.1 PBD-Expression Increases the Mitotic Index.....	61
3.4.1.2 PBD-Expression Causes a Prometaphase-Arrest.....	61
3.4.1.3 Phenotype of PBD-transfected Cells.....	62
3.4.1.4 Plk1 Localization in PBD-transfected Cells.....	63

---

3.4.2 Effects of Poloxin and Thymoquinone.....	65
3.4.2.1 Determination of the Timepoint for Analysis of Effects.....	65
3.4.2.2 Influence of Poloxin and Thymoquinone on the Mitotic Index.....	65
3.4.2.3 The Mitotic Marker Protein Phospho-Cdc25C.....	67
3.4.2.4 Phase-Distribution of Cells Arrested by Poloxin and Thymoquinone.....	68
3.4.2.5 Phenotype Caused by Poloxin and Thymoquinone Treatment of Cells.....	69
3.4.2.6 Apoptosis.....	70
3.4.2.7 Plk1 Localization in Poloxin and Thymoquinone Treated Cells.....	71
3.4.2.8 Phosphorylation of BubR1.....	73
<b>3.5 Inhibition of the Plk2 PBD and Plk3 PBD.....</b>	<b>74</b>
<b>3.6 Inhibitory Mechanism of Poloxin and Thymoquinone.....</b>	<b>77</b>
<b>4. Discussion.....</b>	<b>78</b>
<b>4.1 Validation of the Plk1 PBD as Target for Small-Molecule Inhibitors.....</b>	<b>78</b>
<b>4.2 Assay Development.....</b>	<b>79</b>
4.2.1 A Homogeneous Assay Based on Fluorescence Polarization.....	79
4.2.2 Assay Controls and Z'-factor.....	81
4.2.3 Binding Studies.....	82
<b>4.3 Evaluation of the High-Throughput Screen.....</b>	<b>83</b>
4.3.1 Comparison of Different Screening Techniques.....	83
4.3.2 Analysis and Processing of Screening Data .....	84
4.3.3 Screening for Inhibitors of STAT5b .....	86
<b>4.4 Poloxin and Thymoquinone.....</b>	<b>87</b>
4.4.1 <i>In vitro</i> Characterization and Specificity Profiles.....	87
4.4.2 Cellular Activities.....	88
4.4.3 Binding Mechanism.....	90
<b>4.5 Relevance of the Identified Plk1 Inhibitors.....</b>	<b>91</b>
<b>4.6 Outlook.....</b>	<b>91</b>
<b>5. Summary.....</b>	<b>93</b>
<b>6. Abbreviation Index.....</b>	<b>94</b>
<b>7. Bibliography.....</b>	<b>95</b>
<b>8. Publications.....</b>	<b>109</b>
<b>9. Acknowledgements.....</b>	<b>110</b>

# 1. Introduction

## 1.1 Protein-Protein Interactions

One of the major challenges in biomedical research is to gain a thorough understanding of precisely how protein expression is translated into biological functions within a cell. It has become evident that instead of acting on their own, most proteins show activity as members of protein complexes (Gavin *et al.*, 2002). The cellular function of a particular protein may be dependent on the identity of its binding partners within a protein complex.

Involvement of protein-protein interactions and protein complexes has been shown to be crucial for a large number of vital processes, such as cell-cell communication (Yap *et al.*, 2007), cellular signal transduction (Jorissen *et al.*, 2003), cell cycle control (Nigg, 2001), or apoptosis and cell death (Okada & Mak, 2004).

For example, in EGFR (epidermal growth factor receptor) signaling, interaction of extracellular ligands with the membrane-bound receptor EGFR leads to the formation of a complex cellular network of adaptor proteins, like Grb2 (growth factor receptor binding protein 2), and effector proteins, for example the MAP or Akt kinases. This ultimately leads to the activation of transcription factors, like c-Myc or the STATs (signal transducers and activators of transcription), followed by subsequent transcription and expression of target proteins (Jorissen *et al.*, 2003).

The cell cycle, the series of events by which a cell replicates, is subject to regulation by a large number of protein complexes. The temporally- and spatially-restricted interaction of proteins and the formation of complexes on different cellular structures, such as centrosomes or kinetochores, allows cells a tight control of the whole process. The involvement of protein complexes in different mitotic checkpoints guarantees an error-free chromosome segregation (Nigg, 2001).

## 1.2 Modulation of Protein-Protein Interactions

As a result of the central role of protein complexes in cellular processes, aberrant or inappropriate protein-protein interactions hold the potential to cause pathological conditions, e.g. cancer. Modulation of protein functions or interactions therefore offers the possibility for the treatment of human diseases. There are several techniques available by which to interfere with protein function or inhibit protein-protein interactions. Protein expression can be blocked

at the mRNA-level using antisense techniques, or the functional activity of proteins and the formation of protein complexes can be blocked using antibodies, peptides or peptidomimetics, or small molecules. Each of these techniques has certain advantages. However, for application as therapeutics, the various techniques also have inherent drawbacks.

### **1.2.1 Antisense Techniques**

There are several antisense techniques available, the two most prominent being small interfering RNAs (siRNA) and antisense oligonucleotides (ASOs). These two techniques are used to block protein expression at the mRNA level.

siRNAs take advantage of the process of RNA interference (RNAi), a cellular mechanism for viral protection. An enzyme called Dicer recognizes and cleaves double-stranded RNA, resulting in the formation of 21-23 nucleotide long RNA molecules. These small RNAs can interact with the mRNA of certain proteins, which leads to subsequent degradation by the RISC (RNA-induced silencing complex) (Hammond, 2005). Therefore, application of siRNAs covering part of the sequence of the desired protein leads to silencing of this protein by RISC-mediated degradation of its mRNA.

ASOs are single-stranded DNA molecules with a length of 15-20 nucleotides, complementary to the mRNA of the desired protein. Binding to mRNA either blocks translation because of an arrest of ribosome function, or induces RNase H, an endonuclease which recognizes and cleaves RNA:DNA hybrids (Scherer & Rossi, 2003).

In summary, antisense techniques represent a tool for directed and effective silencing of single protein activities. However, there is restricted cellular uptake of siRNAs and ASOs, and in both cases RNA or DNA molecules are subject to rapid degradation by nucleases within the cell. Furthermore, gene silencing leads to an irreversible inhibition of protein expression and hence function, which is not always suitable for the investigation of essential proteins.

### **1.2.2 Antibodies**

Ever since development of the hybridoma technique (Kohler & Milstein, 1976), monoclonal antibodies have been an important tool for scientific and pharmaceutical research. Besides their well-documented functions for the immune system, antibodies can be used to interfere with signal transduction by blocking ligand-receptor or protein-protein interactions (Kim *et al.*, 2005).

The most important advantage of the use of monoclonal antibodies is the high degree of specificity for a certain antigen. Various antibodies have been established as promising anti-tumor agents. For example, Trastuzumab (Herceptin®) is used for the therapy of breast cancer. It blocks dimerization and subsequent signaling of the receptor HER-2, which is overexpressed in various breast cancer cell lines (Nahta & Esteva, 2006). Bevacizumab (Avastin®) recognizes VEGF (vascular endothelial growth factor) and inhibits tumor growth by blocking the formation of new blood vessels (Ferrara *et al.*, 2004). Cetuximab (Erbix®) is used as an inhibitor of the EGFR in head and neck cancers in the clinical setting (Goldberg, 2005).

One big drawback of antibodies as modulators of protein-protein interactions is the fact that they are located in the extracellular compartment only, restricting their application to extracellular receptors.

### 1.2.3 Peptides and Peptidomimetics

Peptides and peptidomimetics can also be employed for the inhibition of protein-protein interactions. If the interaction of interest is mediated by specific binding sites or known binding motifs, peptides can be designed according to the binding sequence. Proteins are then inhibited via competition for the binding site.

For example, the peptide cyclo(RGDf-N(Me)V-) (Cilengitide), was developed by the group of Prof. Horst Kessler at the Technical University of Munich and was shown to be an inhibitor of the tumor-associated integrin receptor  $\alpha_v\beta_3$ , which plays an important role for angiogenesis (Aumailley *et al.*, 1991; Dechantsreiter *et al.*, 1999; Meyer *et al.*, 2006). Cilengitide is currently undergoing clinical trials as an inhibitor of angiogenesis. Another example is a short synthetic peptide that was shown to inhibit the interaction between the tumor suppressor protein p53 and MDM2 (Picksley *et al.*, 1994).

Advantages of peptides as modulators are that their sequences can easily be optimized further, for example by phage display (Bottger *et al.*, 1996) or peptide screens (Elia *et al.*, 2003a), and that their inhibitory activity is reversible. However, cellular uptake of peptides is limited.

### 1.2.4 Small Molecules

In general, the term “small molecule” describes organic molecules with a molecular weight below 500 g/mol. These compounds can be of natural origin, modified natural products, or

synthetic substances. The molecular weight can sometimes exceed 500 g/mol, especially in the case of natural products (Lipinski *et al.*, 2001).

The development of small molecules as modulators of protein-protein inhibitors is subject to certain difficulties. One problem is the identification of lead structures for targeting protein-protein interactions, as only a small number of natural products modulators are known. In addition, the binding interface tends to be relatively flat with no obvious binding cavities for small molecules (Jones & Thornton, 1996; Berg, 2003), and the area of recognition sites in protein-protein complex is usually greater than 1100 Å<sup>2</sup> (Lo Conte *et al.*, 1999), which vastly exceeds the potential binding area of a low-molecular weight compound. This is why protein-protein interfaces used to be regarded as non-druggable by small molecules. However, it has been demonstrated that a minor fraction of the protein-protein interface residues in fact can account for the majority of the free energy of binding between proteins. These so called “hot spots” tend to cluster residues important for binding energy at the center of the protein-protein interface, and are surrounded by energetically less important amino acid residues that probably serve to occlude bulk solvent (Clackson & Wells, 1995; Bogan & Thorn, 1998; Berg, 2003).

Unlike all other presented techniques for the inhibition of protein-protein interactions, small molecules have the big advantage of excellent cellular uptake. A small molecule's potential for solubility and cell permeability is described by the “rule of 5” (Lipinski *et al.*, 2001). Poor absorption or permeation are likely if the following criteria are not met:

- molecular weight < 500 g/mol
- logP < 5
- H-bond acceptors (O- and N-atoms) < 10
- H-bond donors (OH- and NH-groups) < 5
- one rule may be violated

P is the partition coefficient, which describes the lipophilicity of a small molecule expressed as a ratio of octanol solubility to aqueous solubility. Substances meeting these criteria are likely to display good absorption or permeation. Compound classes that are substrates for biological transporters are exceptions to the rule.

Furthermore, small molecules can be used in a temporally-controlled manner, allowing for the study of timepoint-sensitive processes, such as those involved in the cell cycle.

Despite all primary doubts, the principal feasibility of using small organic molecules to target protein-protein interactions has been clearly demonstrated by a large number of compounds.

One example for a natural product used as a small-molecule inhibitor is the taxane paclitaxel (Taxol®) (Rowinsky, 1997), a diterpenoid isolated from the bark of the pacific yew tree (*Taxus brevifolia*), and its semi-synthetic derivative docetaxel (Taxotere®) (Guenard *et al.*, 1993). Both substances stabilize the interactions of the  $\beta$ -subunit of tubulin heterodimers, which enhances polymerization of tubulin into microtubules. As a consequence, microtubules cannot depolymerize during mitosis which leads to cell cycle arrest and apoptosis. Microtubule stabilization by taxanes has been approved for the treatment of a number of human cancers (Berg, 2003).

Furthermore, many of the FDA-approved cancer therapeutics are small molecules. Amongst the most prominent are imatinib (Gleevec®), gefitinib (Iressa®), erlotinib (Tarceva®), sorafenib (Nexavar®), and sunitinib (Sutent®).

## 1.3 The Mitotic Serine/Threonine Kinase Plk1

### 1.3.1 Polo-like Kinases: an Overview

The genomic stability of all eukaryotic organisms depends on accurate mitotic and meiotic cell divisions. Error-free segregation of chromosomes is a prerequisite for correct proliferation. Chromosomal imbalances can lead to cellular defects and cancer. The cell cycle is consequently a highly-regulated process. Especially in M-phase (mitosis followed by cytokinesis), where cells undergo a major reorganization of cellular architecture, a large network of regulator proteins and error-checkpoints orchestrates correct mitotic progression.

Several kinase families have been shown to play key roles in the regulation of M-phase, in particular cyclin-dependent kinases (CDKs), Aurora kinases, and Polo-like kinases (Plks). The latter are a family of serine/threonine kinases, and were first described in a screen for mutants affecting spindle pole behavior in *Drosophila melanogaster* (*polo*) (Sunkel & Glover, 1988; Llamazares *et al.*, 1991), which gave the name for this kinase family, and in *Saccharomyces cerevisiae* (*cdc5*) (Kitada *et al.*, 1993). Subsequently Plks have been found in many eukaryotes, for example in *Schizosaccharomyces pombe* (*Plp1p*) (Ohkura *et al.*, 1995), in *Caenorhabditis elegans* (*Plc1*, *Plc2*, *Plc3*) (Chase *et al.*, 2000a; Chase *et al.*, 2000b), and in *Xenopus laevis* (*Plx1*, *Plx2*, *Plx3*) (Descombes & Nigg, 1998; Qian *et al.*, 1998; Duncan *et al.*, 2001). In mammals, four Plks have been identified: Plk1 (Clay *et al.*, 1993; Lake & Jelinek, 1993; Holtrich *et al.*, 1994; Hamanaka *et al.*, 1994), Plk2 or SNK (serum-inducible kinase) (Simmons *et al.*, 1992), Plk3 or FNK / PRK (FGF-inducible kinase / proliferation-related

kinase) (Ouyang *et al.*, 1997; Holtrich *et al.*, 2000), and Plk4 or SAK (Fode *et al.*, 1994).

Plks have been shown to play key roles in various stages of mitosis, such as bipolar spindle formation, chromosome segregation and cytokinesis, and in ensuring the fidelity of checkpoint controls. Plk1 is the best-characterized Plk family member. Besides its multiple roles during mitosis, it has been shown that Plk1 is overexpressed in many types of human tumors and its expression is correlated with poor patient prognosis (Eckerdt *et al.*, 2005).

## 1.3.2 Structure of Plks

### 1.3.2.1 Overall Structure

All human Plks share a similar architecture, consisting of a highly conserved N-terminal serine/threonine kinase domain, and a C-terminal region containing one (Plk4) or two (Plk1, Plk2, Plk3) unique signature motif(s), termed polo-boxes, giving this domain the name polo-box domain (PBD) (Barr *et al.*, 2004; Strebhardt & Ullrich, 2006). The PBD is a protein-binding domain recognizing a S-(pS/pT)-(P/X) phosphomotif on substrates (Elia *et al.*, 2003a). Figure 1.1 schematically depicts the structures of the four human Plks.

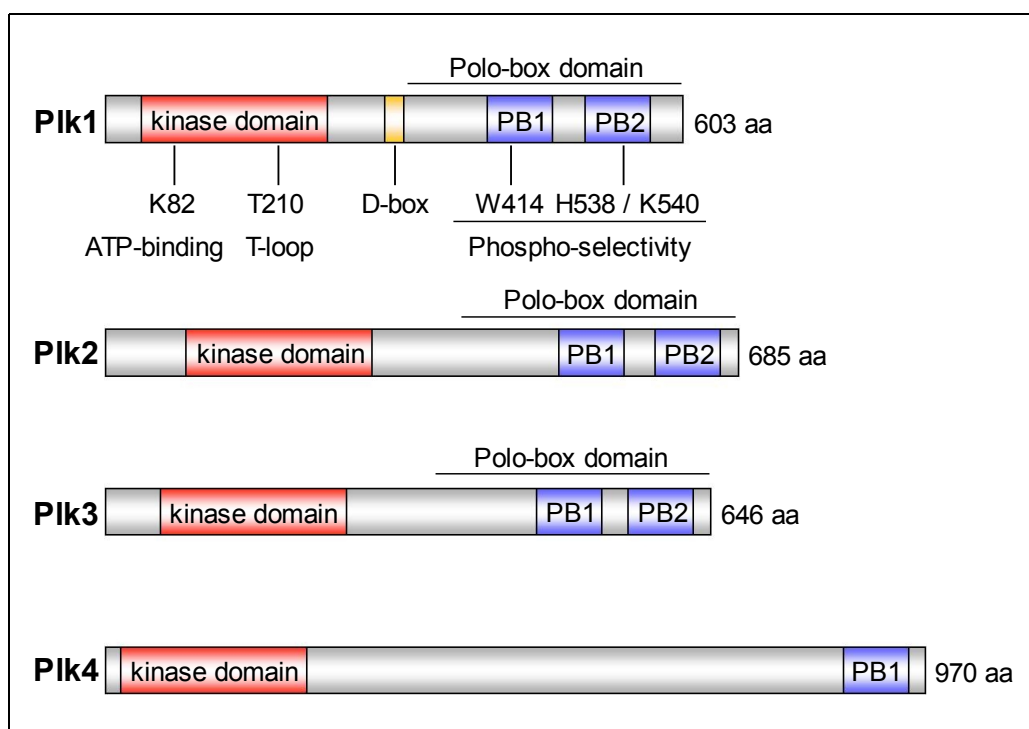


**Fig. 1.1: Schematic representation of the structures of the human Plks.** Protein lengths are given on the right (aa: amino acids). Positions of the kinase domain (red), the polo-box domain and the polo-boxes (PB; blue) are depicted. Residues important for enzymatic activity (K82, T210), for degradation (D-box; yellow), and for substrate recognition (W414, H538, K540) are given for Plk1. Adapted by permission from Macmillan Publishers Ltd: Strebhardt & Ullrich, *Nat Rev Cancer*, copyright 2006.

Several residues of Plk1 play important roles for regulation and activity: Lys82 is involved in ATP-binding and catalytic activity (Seong *et al.*, 2002). Phosphorylation of Thr210 leads to activation of Plk1 (Jang *et al.*, 2002b). Residues in the D-box mediate protein degradation (Lindon & Pines, 2004). Trp414, His538 and Lys540 are crucial for contacting the phosphate group within the binding motif on substrates (Elia *et al.*, 2003b). Residues with corresponding functions are also present in the other Plk family members (Strebhardt & Ullrich, 2006).

### 1.3.2.2 The Kinase Domain

The structure of a T210V mutant of the Plk1 kinase domain in complex with the non-hydrolyzable ATP analogue adenylylimidodiphosphate (AMPPNP) (Kothe *et al.*, 2007a), and the structure of the wildtype Plk1 kinase domain in complex with an ankyrin-repeat protein (Bandeiras *et al.*, 2008) revealed the typical kinase fold (Fig. 1.2).



**Fig. 1.2: Structure of the kinase domain.** The activation loop is shown in orange. Bound AMPPNP is shown as gray sticks. PDB ID: 2OU7 (Kothe *et al.*, 2007a).

The ATP binding site is located in a cleft, formed between the N-terminal lobe, composed predominantly of an antiparallel  $\beta$ -sheet, and the  $\alpha$ -helical C-terminal lobe. The two lobes are connected by a hinge region. The unphosphorylated activation loop is in an extended conformation (Kothe *et al.*, 2007a; Bandejas *et al.*, 2008).

Unique features of the Plk1 ATP binding site are the presence of a bulky phenylalanine at the bottom of the binding site combined with a smaller cysteine in the roof of the pocket (valine in many other kinases), a cluster of positively charged residues in the solvent-exposed area outside the adenine pocket, and an extra pocket created by Leu132 in the hinge region (Kothe *et al.*, 2007a).

It has been recently shown in co-crystallization studies that the specificity against non-Plks of the potent Plk1 kinase domain inhibitor BI 2536 (Lenart *et al.*, 2007; Steegmaier *et al.*, 2007) is due to interaction with the above-mentioned small binding-pocket generated by Leu132 (Kothe *et al.*, 2007b).

### 1.3.2.3 The Polo-Box Domain

The crystal structure of the Plk1 PBD in complex with a short phosphopeptide (Elia *et al.*, 2003b; Cheng *et al.*, 2003) is depicted in figure 1.3.

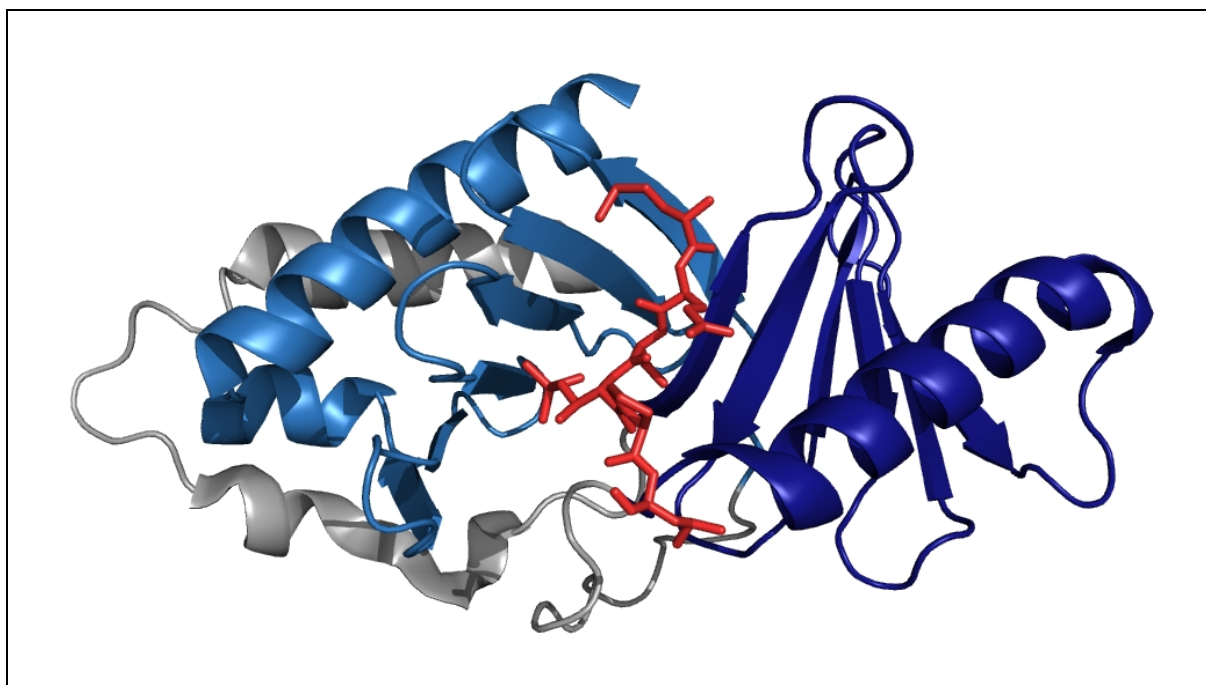


**Fig. 1.3: Structure of the PBD.** The two polo-boxes are depicted in light and dark blue. Gray indicates residues of the PBD, not part of the polo-boxes. The phosphopeptide (red; sticks) binds along the cleft between the two polo-boxes. PDB ID: 1Q4K (Cheng *et al.*, 2003).

It showed that the two polo-boxes, each of which exhibits folds based on a six-stranded  $\beta$ -sheet and an  $\alpha$ -helix, associate to form a 12-stranded  $\beta$ -sandwich domain. Phosphopeptides comprising an S-(pT/pS)-(P/X) motif (Elia *et al.*, 2003a) bind along a positively charged cleft between the two polo-boxes, the phosphate group making crucial contacts with Trp414, His538 and Lys540 (Elia *et al.*, 2003b; Cheng *et al.*, 2003). The same principle is applied with Plk2 and Plk3. For formation of the substrate binding cleft, Plk4 has to form homodimers (Leung *et al.*, 2002).

### 1.3.3 Regulation and Mechanism of Plk1 Activity

#### 1.3.3.1 Regulation of the Protein Level

Plk1 synthesis and activity, respectively, are regulated by Plk1 transcription and degradation. While Plk1 levels are low throughout G0-, G1- and S-phase, they show a strong increase during G2- and a peak in M-phase (Golsteyn *et al.*, 1994; Golsteyn *et al.*, 1995). As seen for Plo1p (Plk from *S. pombe*), where the dramatic rise in protein levels is due to a positive-feedback loop in which Plo1p phosphorylates and activates transcription factors leading to enhanced expression of Plo1p (Anderson *et al.*, 2002), a similar autoregulatory mechanism has been reported for human cells. The tumor suppressor protein p53 was identified as a key player for the precise restriction of Plk1 gene expression. As the activity of p53 is in turn controlled by Plk1, it contributes to the regulation of its own expression by the ability to render p53 inactive (Ando *et al.*, 2004; Martin & Strebhardt, 2006).

It has been shown that mitotic exit is dependent on the degradation of mitotic regulators (Morgan, 1999; Peters, 2002). Plk1 gets inactivated by proteolytic degradation through the ubiquitin-proteasome pathway at the end of mitosis. The main regulator involved in this process is a ubiquitin-ligase, termed anaphase-promoting complex/cyclosome (APC/C). The APC/C-Cdc20 complex promotes metaphase to anaphase transition, whereas the APC/C-Cdh1 complex takes over in late anaphase and is responsible for Plk1 degradation. The APC/C recognizes a destruction signal on Plk1 (D-box) which leads to subsequent proteolytic cleavage (Lindon & Pines, 2004).

In summary, Plk1 activity is restricted to mitosis by tight temporal control of its protein level.

#### 1.3.3.2 Regulation of Plk1 Functions

The PBD is involved in regulation of the catalytic domain. It folds back to the kinase domain and, by blocking the active site, keeps it in an autoinhibited state (Mundt *et al.*, 1997; Jang *et*

*al.*, 2002a). Two different mechanisms for the release from autoinhibition are discussed: stimulation of Plk1 activity by activating phosphorylations in the T-loop, and phosphopeptide/ligand binding to the PBD.

Like many other kinases, Plk1 contains a threonine (T210) in its activation loop (T-loop). In CDK2/cyclin A, for example, phosphorylation of the equivalent residue (Thr 160) leads to activation of the kinase (Russo *et al.*, 1996). It has been shown that Thr210 is a major phosphorylation site in activated Plk1. Substitution of Thr210 by the phosphomimetic amino acid aspartate leads to induction, while substitution with valine leads to inhibition of Plk1 activity (Jang *et al.*, 2002b). The human Ste20-like kinase (Slk) and serine/threonine kinase 10 (Stk10) have been identified as possible upstream kinases (Ellinger-Ziegelbauer *et al.*, 2000; Walter *et al.*, 2003; Johnson *et al.*, 2008). Therefore, phosphorylation of Thr210 appears to act as inducer of Plk1 activity.

The PBD binds to substrates containing a certain S-(pS/pT)-(P/X) binding motif (Elia *et al.*, 2003a). Upon binding to a ligand, the PBD folds away from the kinase domain, releasing autoinhibition of the kinase domain. However, PBD docking sites have to be established by so called “priming phosphorylations” before binding occurs (Elia *et al.*, 2003a). Reports have shown that CDK1/cyclin B can act as a priming kinase (Sillje & Nigg, 2003; Barr *et al.*, 2004), as well as other kinases (Rapley *et al.*, 2005; Rauh *et al.*, 2005), including Plk1 itself (Neef *et al.*, 2003; Kang *et al.*, 2006). Such a mechanism could serve as positive-feedback loop to concentrate Plk1 at required sites. Binding of the PBD to substrates not only activates

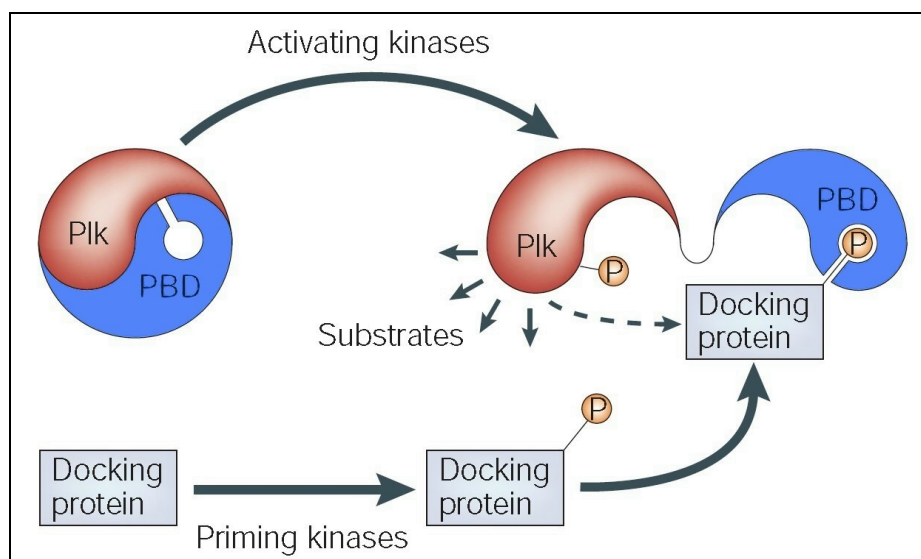


**Fig. 1.4: Mechanisms for the activation of Plk1.** The Plk1 kinase domain can be released from autoinhibition by phosphorylation of the T-loop by activating kinases or by binding of the PBD to primed docking proteins. Adapted by permission from Macmillan Publishers Ltd: Barr *et al.*, Nat Rev Mol Cell Biol, copyright 2004.

the kinase domain, it also targets Plk1 to various cellular structures (Elia *et al.*, 2003a). Thus, the mechanism of interaction with pre-phosphorylated substrates allows for temporal and spatial control of cellular Plk1 functions.

Figure 1.4 depicts the mechanisms for Plk1 activation.

### 1.3.3.3 Mechanism of Plk1 Activity

As reported by Hanisch *et al.*, 2006, two-different mechanisms of Plk1 activity have to be distinguished: PBD-dependent and PBD-independent functions.

PBD-dependent functions require pre-localization of Plk1 via the PBD to the cellular vicinity of substrate proteins, followed by subsequent phosphorylation of these targets. PBD-dependent functions also depend on correct localization of Plk1 to subcellular structures. By this mechanism, Plk1 activity is spatially controlled.

PBD-independent functions do not require prior PBD-mediated localization. Plk1 is probably activated by phosphorylation of T210 in the T-loop, followed by direct phosphorylation of target proteins.

Figure 1.5 shows a scheme for the two different mechanisms of Plk1 function.

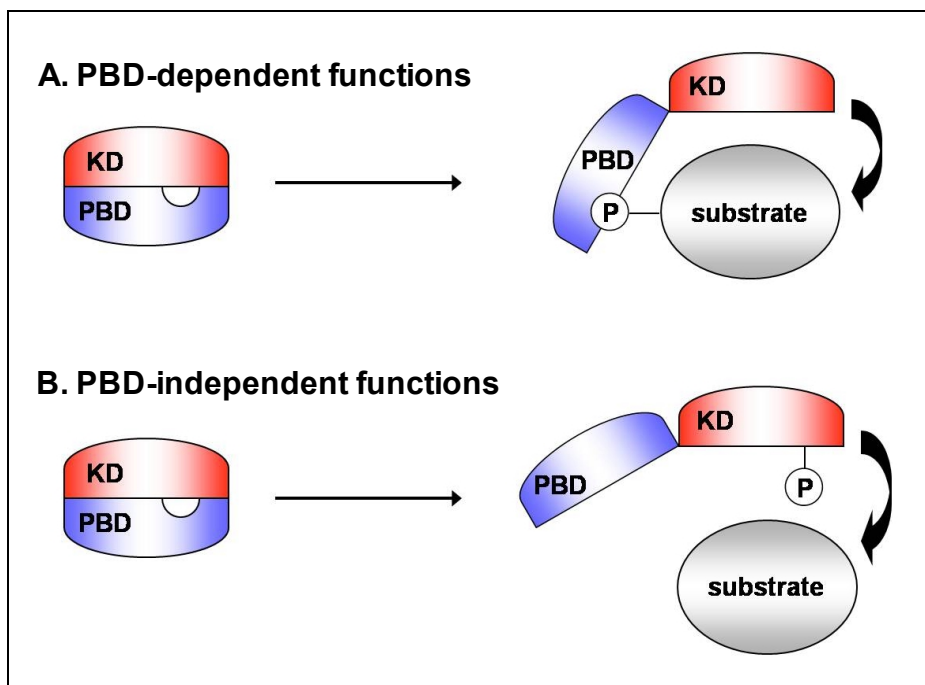


**Fig. 1.5: Two different mechanisms of Plk1 function.** A. PBD-dependent functions require pre-localization of Plk1 to primed substrates. Release of autoinhibition from the kinase domain (KD) is mediated by ligand-binding of the PBD. B. PBD-independent functions can be carried out without specific PBD-mediated localization. Relief from autoinhibition is achieved by phosphorylation of T210 in the T-loop of the kinase domain (KD). Curved black arrows symbolize phosphorylation reactions.

It was shown that inhibition of PBD-dependent functions by ectopic expression of the PBD leads to a checkpoint-dependent arrest with impaired chromosome congression (Hanisch *et al.*, 2006; Jiang *et al.*, 2006, Fink *et al.*, 2007). This is completely different from the phenotype observed for Plk1 depletion (Spankuch-Schmitt *et al.*, 2002b; Liu *et al.*, 2003) or inhibition of the kinase domain (Stevenson *et al.*, 2002; Liu *et al.*, 2005; Gumireddy *et al.*, 2005; McInnes *et al.*, 2006; Peters *et al.*, 2006; Lansing *et al.*, 2007; Lenart *et al.*, 2007; Steegmaier *et al.*, 2007; Santamaria *et al.*, 2007), which blocks both PBD-dependent and PBD-independent functions. Cells arrested in mitosis by depletion or enzymatic inactivation of Plk1 showed monoastral spindles, due to inhibition of centrosome maturation and separation. Therefore, the existence of these two mechanisms of Plk1 activity has considerable implications for Plk1 inhibitors. A PBD-specific inhibitor would be a valuable research tool for the differentiation of PBD-dependent and PBD-independent functions.

### **1.3.4 Cellular Functions of Polo-like Kinases**

#### **1.3.4.1 Multiple Cell-Cycle Functions of Plk1**

Plk1 is regarded as one of the key regulators of mitotic events, and it is essential for the maintenance of genomic stability. It is involved in virtually all steps of mitosis ranging from mitotic entry to cytokinesis (Barr *et al.*, 2004; van de Weerd & Medema, 2006).

#### **G2/M Transition**

Initiation of mitosis requires nuclear translocation and activation of the M-phase regulator Cdk1/Cyclin B. Its activity is primarily controlled by the concerted activity of the two kinases Wee1 and Myt1, and the phosphatase Cdc25C, which in turn are controlled by components of the DNA damage checkpoint. Before the onset of mitosis, Cdk1/Cyclin B is kept inactive by two phosphorylations on Thr14 and Tyr15, effected by Wee1 and Myt1. Cdk1/Cyclin B is activated as a consequence of phosphorylation of Wee1 and Myt1, which leads to their inhibition, and of Cdc25C, which gets activated and dephosphorylates Thr14 and Tyr15 of Cdk1/Cyclin B (Nigg, 2001).

It has been shown that Plk1 is involved in the phosphorylation of Wee1 and Myt1, which leads to their inactivation, and even SCF<sup>β-TrCP</sup>-mediated degradation of Wee1 (Watanabe *et al.*, 2004; Nakajima *et al.*, 2003). Plk1 also phosphorylates and activates Cdc25C (Roshak *et al.*, 2000). Once activated, Cdk1/Cyclin B triggers phosphorylation of Wee1, Myt1, Cdc25C and possibly Plk1 in a positive feedback loop (Barr *et al.*, 2004; Abrieu *et al.*, 1998).

### **DNA Damage Checkpoint**

As Plk1 is an activator of Cdk1/Cyclin B, and therefore a promoter of mitosis, it is involved in restarting the cell cycle after a DNA damage checkpoint mediated arrest in G2-phase.

One Plk1 target involved in the checkpoint is the tumor suppressor protein p53. On recovery from arrest, Plk1 phosphorylates and inactivates p53 (Ando *et al.*, 2004). Chk2 is another interaction partner of Plk1. During DNA damage, Chk2 is activated by the checkpoint kinases ATM and ATR. On checkpoint exit, Chk2 is bound and phosphorylated by Plk1, rendering it inactive (Tsvetkov, 2004; Tsvetkov *et al.*, 2005). Furthermore, Plk1 phosphorylates and inactivates the breast cancer susceptibility protein BRCA2, which is essential for the repair of DNA double-strand breaks (Lin *et al.*, 2003; Lee *et al.*, 2004). Therefore, Plk1 leads to a restart of the cell cycle after DNA damage by inactivation of crucial checkpoint proteins, while Plk1 in turn gets inactivated by ATM and ATR upon DNA damage (Tsvetkov, 2004).

### **Centrosome Maturation and Bipolar Spindle Formation**

Plk1 is involved in correct maturation of the centrosomes. Reduced Plk1 activity leads to aberrant spindle poles, which was found in a mutant screen in *D. melanogaster* and led to the discovery of the Plk family (Sunkel & Glover, 1988; Llamazares *et al.*, 1991). It was shown that Plk1 recruits the  $\gamma$ -tubulin ring complex ( $\gamma$ -TuRC) to the centrosomes, which increases the microtubule-nucleation activity required for spindle formation (Lane & Nigg, 1996). Nlp (ninein-like protein) interacts with the  $\gamma$ -TuRC in interphase, contributing to microtubule organization. At the onset of mitosis, its phosphorylation by Plk1 leads to dissociation from the centrosome, allowing the recruitment of other proteins serving as scaffolds for microtubule nucleation (Casenghi *et al.*, 2003; Casenghi *et al.*, 2005). The tubulin-stabilizing protein TCTP (translationally controlled tumor protein) is another substrate of Plk1. Phosphorylation of TCTP decreases its microtubule-stabilizing activity and promotes the increase in microtubule dynamics that occurs after metaphase (Yarm, 2002).

Formation of a bipolar spindle is essential for error-free chromosome segregation during mitosis. Plk1 was shown to be required for the formation of functional spindles. It was reported that Plk1 phosphorylates Kiz (Kizuna), which plays an important role for stabilization of mature centrosomes, spindle pole integrity and bipolar spindle formation (Oshimori *et al.*, 2006).

Recently, centrosome recruitment of Plk1 was shown to be dispensable for centrosome maturation and bipolar spindle formation, suggesting that the centrosomal functions of Plk1

are PBD-independent and Plk1 activity does not have to be specifically bound to centrosomes (Hanisch *et al.*, 2006).

### **Chromosome Alignment and Spindle Checkpoint**

Plk1 is implicated in chromosome alignment, since mislocalization of Plk1 in the cell leads to chromosome congression defects (Hanisch *et al.*, 2006).

Furthermore, Plk1 is required for the formation of stable microtubule-kinetochore interactions (van Vugt *et al.*, 2004a; Sumara *et al.*, 2004), and is involved in activation of the spindle checkpoint. The spindle checkpoint is a cellular mechanism that ensures fidelity of chromosome segregation by preventing cell-cycle progression until all chromosomes make bipolar spindle attachments and come under tension (Pinsky & Biggins, 2005). Plk1 contributes to this mechanism by creating the 3F3/2 phosphoepitope on kinetochores lacking tension, which leads to the recruitment and/or activation of several spindle checkpoint proteins, like Mad2, Hec1/Ndc80, BubR1, Cenp-E, or Nuf2 (Ahonen *et al.*, 2005; Wong & Fang, 2005; Wong & Fang, 2007). These proteins in turn block metaphase-to-anaphase transition by keeping the APC/C inactive (Fang *et al.*, 1998; Martin-Lluesma *et al.*, 2002) or enhancing correct stable kinetochore-microtubule attachment (DeLuca *et al.*, 2002; Lampson & Kapoor, 2005), ultimately leading to satisfaction of the spindle checkpoint.

### **Activation of APC/C and Chromosome Segregation**

Bipolar spindle attachment of all kinetochores leads to subsequent chromosome segregation. The main regulator for this process is the APC/C (Peters, 2002). The APC/C is tightly regulated. For example, Mad2 forms a complex with and sequesters Cdc20, an indispensable cofactor for the APC/C. On satisfaction of the spindle checkpoint, Mad2 dissociates from Cdc20, which subsequently forms a complex with the APC/C (Fang *et al.*, 1998). The involvement of Plk1 in activation of the APC/C was discovered recently (Schmidt *et al.*, 2005; Liu & Maller, 2005; Rauh *et al.*, 2005; Hansen *et al.*, 2006). In the proposed model in *Xenopus*, Plx1 phosphorylates Xerp1, also known as cytostatic factor (CF) (Emi1 in human cells), an inhibitor protein for the APC/C. Phosphorylation leads to inactivation of Xerp1, which releases the APC/C from the block. The activated APC/C-Cdc20 complex subsequently marks securin for degradation by the proteasome. This releases separase, which cleaves cohesin (a protein complex which holds chromatid arms together), leading to sister-chromatid separation and the onset of anaphase (Nasmyth, 2005).

Cohesin cleavage is also supported by Plk1. Phosphorylation of the cohesin subunit SA2 is

essential for dissociation of cohesin from chromosome arms in early mitosis, facilitating sister-chromatid resolution (Hauf *et al.*, 2005), whereas phosphorylation of the subunit Scc1 enhances its separase cleavage (Hornig & Uhlmann, 2004).

### Cytokinesis and Mitotic Exit

Plk1 has been implicated in cytokinesis, consistent with Plk1 localization to the central spindle/midbody in late mitosis (Donaldson *et al.*, 2001).

It has been shown that error-free cytokinesis depends on correct localization of Plk1 and interaction with the two mitotic kinesin-like proteins Mklp1/CHO1 and Mklp2 (Liu *et al.*, 2004; Neef *et al.*, 2003). Phosphorylation of NudC by Plk1 is required for the execution of cytokinesis. NudC mutants lacking the Plk1 phosphorylation site lead to cytokinesis defects and multinucleated cells (Zhou *et al.*, 2003).

It has also been shown that Plk1 regulates cytokinesis through Golgi-associated proteins. Plk1 phosphorylates the Golgi protein Nir2, mainly involved in remodeling of cytoskeletal elements. Nir2 phosphorylation by Plk1 is indispensable for the completion of cytokinesis (Litvak *et al.*, 2004).

Figure 1.6 summarizes the mitotic functions of Plk1.

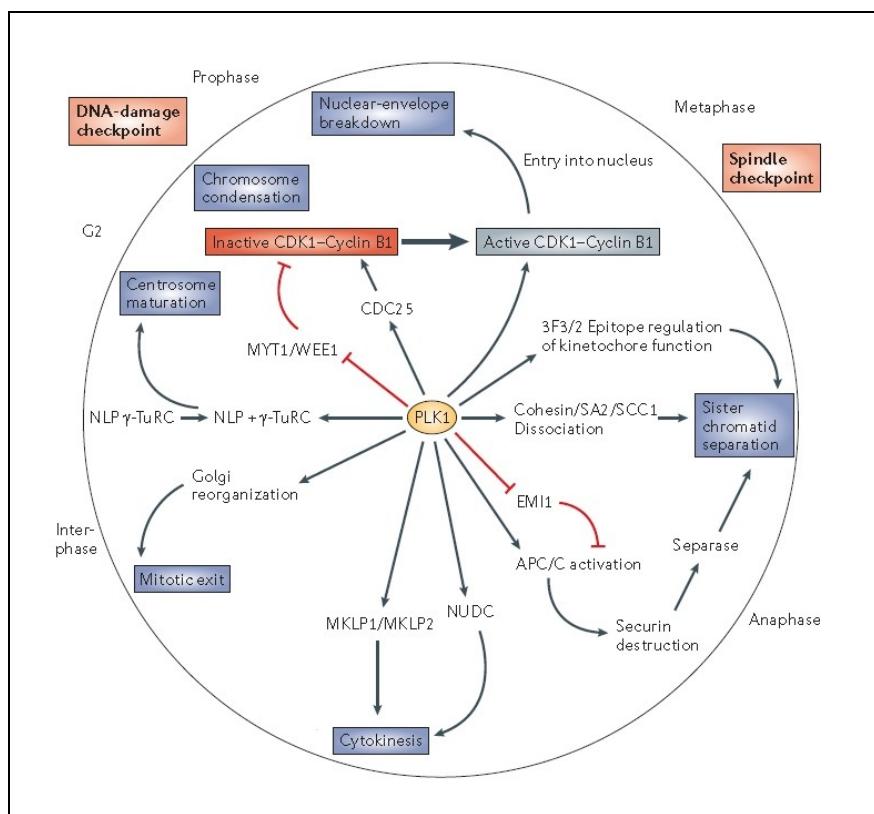


**Fig. 1.6: Mitotic functions of Plk1.** Adapted by permission from Macmillan Publishers Ltd: Strebhardt & Ullrich, *Nat Rev Cancer*, copyright 2006.

#### **1.3.4.2 The Roles of Plk2, Plk3 and Plk4**

##### **Plk2 / Snk**

Unlike Plk1, which shows its highest activity in G2- and M-phase (Golsteyn *et al.*, 1994; Golsteyn *et al.*, 1995), Plk2 was identified as an early-growth-response gene, which plays a role in G1- and early S-phase (Simmons *et al.*, 1992). There is evidence that Plk2 may be involved in centriole duplication during S-phase, since variations in Plk2 levels lead to incorrect numbers of centrosomes (Warnke *et al.*, 2004). Furthermore, Plk2 may also play a role in the DNA damage checkpoint, since Plk2 mRNA is induced by DNA-damaging agents (Burns *et al.*, 2003) However, it seems that Plk2 is a non-essential gene. Plk2<sup>-/-</sup> embryos are viable (Ma *et al.*, 2003), and Plk2 depletion in HeLa and U2OS cells does not alter progression through the cell cycle (Burns *et al.*, 2003).

##### **Plk3 / Fnk / Prk**

Plk3 protein levels remain relatively constant during the cell cycle (Bahassi *et al.*, 2002). Like Plk1, Plk3 has been linked to stress-response to DNA damage. However, Plk1 and Plk3 seem to have opposing functions in this process. Plk1 expression is downregulated, and Plk1 activity is inhibited by ATM/ATR phosphorylation (Ree *et al.*, 2003; Tsvetkov, 2004). In contrast, Plk3 activity is rapidly induced by ATM (Bahassi *et al.*, 2002). Known targets of Plk3 are p53 and Cdc25C (Xie *et al.*, 2001; Ouyang *et al.*, 1999). In this case Plk3 again exerts opposing functions to Plk1: Plk3 promotes p53 function (Xie *et al.*, 2001), and inhibits Cdc25C (Ouyang *et al.*, 1999).

##### **Plk4 / Sak**

Plk4 levels increase in late G1-phase, remain elevated during through S- and M-phase and decline in early G1-phase (Fode *et al.*, 1996). Like Plk1, Plk4 is essential for cell viability and proliferation (Fode *et al.*, 1994; Hudson *et al.*, 2001). Little is known about Plk4 functions. However, involvement of Plk4 in centriole duplication and biogenesis has been described recently (Habedanck *et al.*, 2005; Kleylein-Sohn *et al.*, 2007), suggesting an explanation for Plk4's crucial function in cell proliferation.

#### **1.3.5 Plk1 and Cancer**

Since Plk1 is a promoter of mitosis and cellular proliferation, it holds oncogenic potential. Indeed, Plk1 was found to be overexpressed in a broad range of human tumors, including non-small-cell lung cancer, oropharyngeal carcinoma, oesophageal carcinoma, gastric carcinoma,

melanoma, breast cancer, ovarian cancer, endometrial cancer, colorectal cancer, glioblastoma, papillary carcinoma, pancreatic cancer, prostate cancer, hepatoblastoma, and non-Hodgkin lymphoma. Plk1 is regarded as an adverse prognostic marker for cancer patients (Eckerdt *et al.*, 2005; Strebhardt & Ullrich, 2006).

The oncogenic potential of Plk1 is supported by several other studies: Overexpression of wildtype Plk1 results in mitotic defects and multi-nucleation (Mundt *et al.*, 1997; Jang *et al.*, 2002a). Expression of the hyperactive T210D mutant of Plk1 can override the DNA damage checkpoint (Smits *et al.*, 2000; van Vugt *et al.*, 2004b). Furthermore, the p53 tumor suppressor is phosphorylated by Plk1, which inhibits the pro-apoptotic functions of p53 (Ando *et al.*, 2004). Inhibition of Plk1 functions by various approaches (see 1.3.6) leads to the induction of apoptosis in tumor cells. Therefore Plk1 is regarded as a therapeutic target for the treatment of human cancers.

### **1.3.6 Strategies for Plk1 Inhibition**

Because of its implications in tumor development, there have been numerous studies describing various approaches for Plk1 inhibition.

#### **1.3.6.1 Small Interfering RNAs (siRNAs) and Antisense Oligonucleotides (ASOs)**

Various studies have uniformly shown that interference with Plk1 expression using siRNA or ASOs leads to decreased Plk1 mRNA and protein-levels, resulting in reduced cellular proliferation, cell cycle arrest and apoptosis in various cancer cell lines. Furthermore, tumorigenesis in xenograft mouse models was reduced (Spankuch-Schmitt *et al.*, 2002a, Spankuch-Schmitt *et al.*, 2002b; Liu & Erikson, 2003; Guan *et al.*, 2005).

#### **1.3.6.2 Interfering Peptides**

A peptide derived from the sequence of polo-box 1 (aa 410-429) was used to block endogenous Plk1 binding sites, resulting in decreased proliferation and apoptosis of several tumor cell lines. To allow for cellular uptake, the peptide was fused to an antennapedia peptide, which was reported to enter cells via nonendocytotic, and receptor-/transporter-independent pathways (Yuan *et al.*, 2002).

#### **1.3.6.3 Small-Molecule Inhibitors**

The first identified small-molecule Plk1 inhibitor was the marine natural product Scytonemin,

a pigment isolated from cyanobacteria. It inhibited recombinant Plk1 with an  $IC_{50}$  of 2  $\mu$ M via a proposed mixed competition mechanism. However, various other kinases were blocked with equal potency: Myt1, Chk1, Cdk1/Cyclin B, or PKC $\beta$ 2 (Stevenson *et al.*, 2002).

The widely used PI3-kinase inhibitor Wortmannin was also found to potently inhibit Plk1 ( $IC_{50}$  = 24 nM) by an ATP-competitive mechanism. However, several other kinases, e.g. Plk3 are also inhibited by Wortmannin (Liu *et al.*, 2005; Liu *et al.*, 2007).

ON01910 has been shown to be an inhibitor of Plk1 activity via a non-ATP-competitive mode ( $IC_{50}$  = 9-10 nM). The presence of ON01910 caused mitotic arrest in a wide range of human tumors, characterized by spindle abnormalities and induction of apoptosis. Tumor growth was inhibited in animal models. Several other kinases were also inhibited: Abl, Flt-1, PDGFR, Src, Fyn, and Plk2. ON01910 is currently being explored in clinical settings (Gumireddy *et al.*, 2005).

An *in silico* docking screen performed by Cyclacel led to the identification of the ATP-competitor Cyclapolin-1, a benzothiazole N-oxide. Cyclapolin-1 inhibited Plk1 with an  $IC_{50}$  of approximately 20 nM, causing spindle collapse in HeLa and *Drosophila* S2 cells, which is typical for Plk1 inhibition. Only minor effects were seen on a panel of 20 other kinases. A small fraction of cells was arrested in mitosis, suggesting the cell cycle may also be affected in G1/S (McInnes *et al.*, 2006).

DAP-81 was synthesized using a diaminopyrimidine as the basic scaffold, and inhibited Plk1 with an  $IC_{50}$  of 0.9  $\mu$ M. No selectivity data was shown, but DAP-81 causes spindle collapse, leading to monopolar spindles, consistent with Plk1 inhibition (Davis-Ward *et al.*, 2004; Peters *et al.*, 2006).

The leflunomide metabolite analog LFM-A13 has been identified as a Plk1 inhibitor ( $IC_{50}$  = 10.3  $\mu$ M). LFM-A13 showed anti-proliferative activity against human breast cancer cells. However, LFM-A13 also inhibited Plk3 and Bruton's tyrosine kinase (BTK), for which it was originally designed (Mahajan *et al.*, 1999; Uckun *et al.*, 2007).

GlaxoSmithKline identified Compound 1, a thiophene benzimidazole, as a low-nanomolar ATP-competitive inhibitor of Plk1 and Plk3. Compound 1 caused a mitotic arrest with spindle defects, resulting in apoptosis and inhibition of proliferation in several tumor cell lines (Lansing *et al.*, 2007).

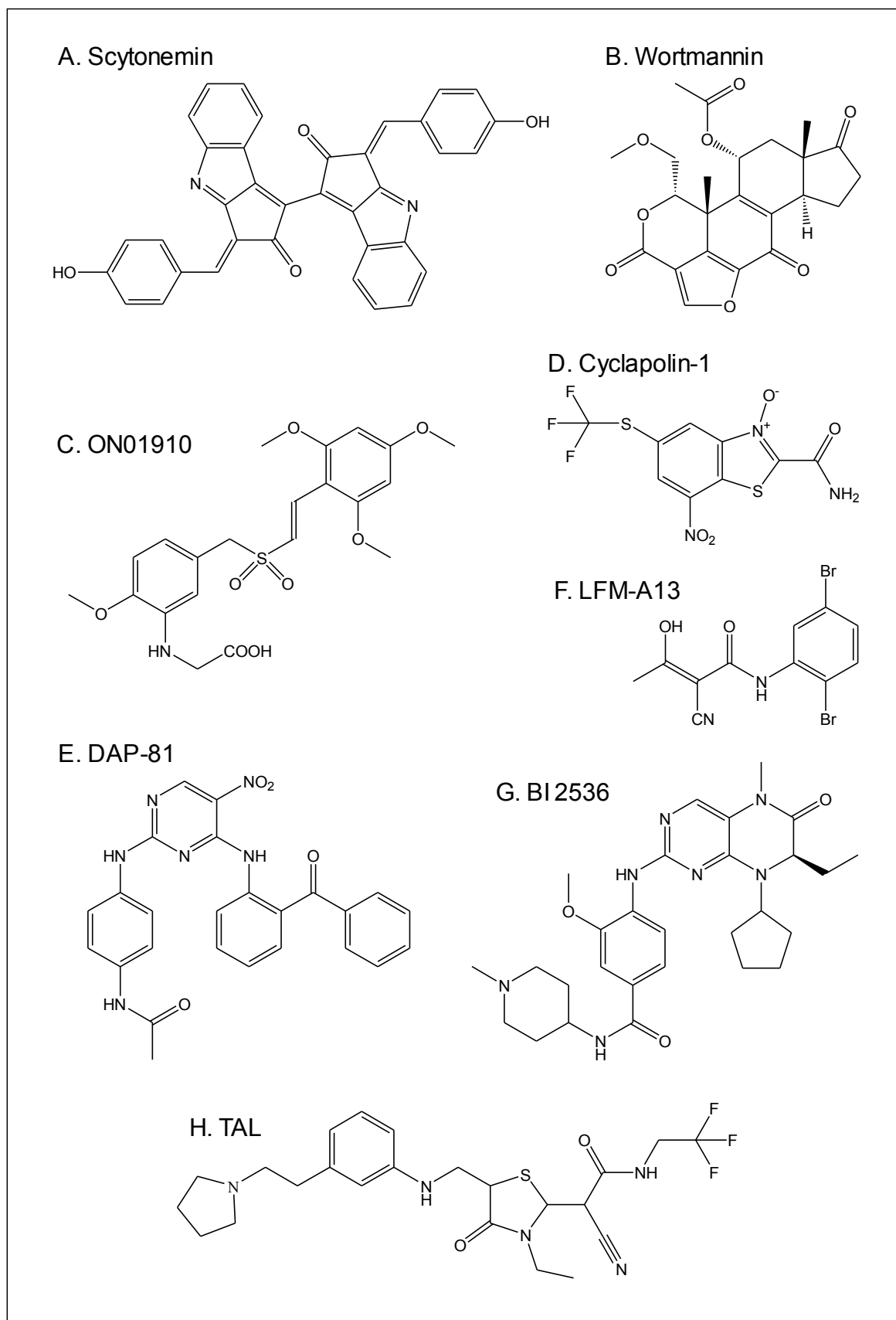


**Fig. 1.7: Structures of published Plk1 inhibitors.**

BI 2536 is a novel highly-effective Plk1 inhibitor ( $IC_{50} = 1$  nM) developed by Boehringer Ingelheim, based on dihydropteridinone. Plk2 ( $IC_{50} = 4$  nM) and Plk3 ( $IC_{50} = 9$  nM) were also inhibited to some extent, but no other kinase was inhibited from a panel of 63 kinases. All observed cellular effects and phenotypes were consistent with Plk1 inhibition (Lenart *et al.*, 2007). BI 2536 was also highly active against a large panel of human tumors and progressed into clinical studies (Steggmaier *et al.*, 2007). As shown in crystallography studies, BI 2536 competes for the ATP binding site (Kothe *et al.*, 2007b).

Recently ZK-Thiazolidinone (TAL), a Plk1 inhibitor ( $IC_{50} = 19$  nM) developed by Bayer Schering Pharma, was published. TAL also inhibited Plk2, Plk3 and Plk4, but showed no significant activity on a panel of 93 other kinases. TAL was validated in a large variety of cellular assays and showed effects and phenotypes consistent with Plk1 inhibition (Santamaria *et al.*, 2007).

Figure 1.7 shows the structures of the described Plk1 inhibitors. The structure of Compound 1 by GlaxoSmithKline has not been disclosed.

In summary, nearly all published Plk1 inhibitors act as ATP-competitors, targeting the kinase domain (exception: ON01910, unknown mechanism), resulting mostly in monopolar spindels, mitotic arrest and apoptosis of cancer cell lines.

## 1.4 Aims

Plk1 is one of the key enzymes for mitotic regulation and maintenance of genomic stability. It is involved in most steps of mitosis and has functions for checkpoint control. Overexpression of Plk1 leads to tumorigenesis and has prognostic potential in cancer, validating Plk1 as a therapeutic target. Plk1 is therefore an interesting target for inhibition studies, which might yield a broader picture of Plk1's role in cell cycle control, leading to a better global understanding of mitosis and the cell cycle. Plk1 inhibition also represents an important anti-tumor therapy.

The aim of this thesis was a new approach towards Plk1 inhibition: Identification of inhibitors for the Plk1 polo-box domain (PBD). Up to now, all published Plk1 inhibitors target the function of the kinase domain. PBD-specific inhibitors would have two important advantages. Firstly, they could be used as valuable new Plk1 research tools, since they would allow a clear distinction between PBD-dependent and PBD-independent functions with a temporal control. Secondly, they would represent an alternative strategy, by which to target Plk1 in tumors.

Since there are approximately 400 serine/threonine kinases, all sharing a similar kinase domain fold (Manning *et al.*, 2002), but only 4 Plks containing a PBD, PBD-targeted inhibitors have the potential to be much more specific than kinase domain inhibitors (Fig. 1.8).

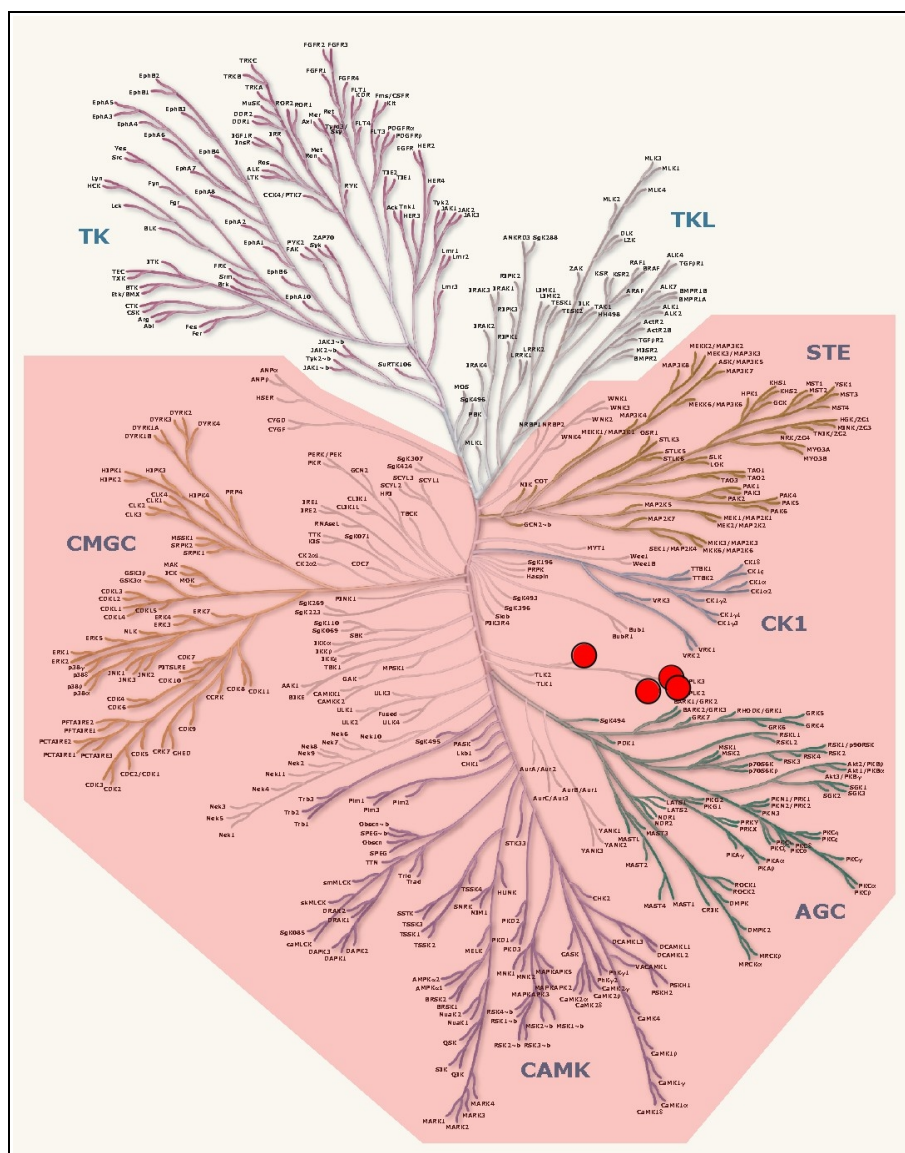


**Fig. 1.8: Schematic depiction of the human kinome.** Serine/threonine kinases are highlighted in light red. The 4 Plks are marked with red dots. Group names: TK: tyrosine kinase; TKL: tyrosine kinase-like; STE: homologs of yeast Sterile 7, Sterile 11, Sterile 20 kinases; CK1: casein kinase; AGC: containing PKA, PKG, PKC families; CAMK: calcium/calmodulin-dependent protein kinase; CMGC: containing CDK, MAPK, GSK3, CLK families. Adapted by permission from Cell Signaling Technology, Inc.: Manning *et al.*, Science, copyright 2002.

PBD-specific inhibitors will be identified in a high-throughput screen based on an *in vitro* fluorescence polarization assay. Potential candidate molecules will subsequently be analyzed for specificity and cellular effects consistent with inhibition of the Plk1 PBD.

## 2. Materials & Methods

### 2.1 Materials

#### 2.1.1 Chemicals and Reagents

Acetic acid	Fluka (Buchs, SUI)
Acrylamide	Serva (Heidelberg)
Agar (Difco™)	BD Biosciences (Heidelberg)
Agarose	Eurogentec (Köln)
Ampicillin	Roche (Mannheim)
Antipain	Fluka (Buchs, SUI)
Aphidicolin	Sigma-Aldrich (Steinheim)
Aprotinin	Sigma-Aldrich (Steinheim)
Bisacrylamide	Serva (Heidelberg)
Bovine $\gamma$ -globulin	Sigma-Aldrich (Steinheim)
Bovine serum albumin (BSA)	Sigma-Aldrich (Steinheim)
Chloramphenicol	Calbiochem (Schwalbach)
Deoxy nucleotide (dA/G/C/TTP)	Amersham (Freiburg)
4',6-diamidino-2-phenylindole hydrochloride (DAPI)	Roche (Mannheim)
Dimethyl sulfoxide (DMSO)	Riedel-de Haën (Seelze)
Dimethyl sulfoxide (DMSO), anhydrous	Sigma-Aldrich (Steinheim)
Dithiothreitol (DTT)	Sigma-Aldrich (Steinheim)
Ethanol p.a.	Riedel-de Haën (Seelze)
Ethidium bromide	Roth (Karlsruhe)
4-(2-Hydroxyethyl)piperazine-1-ethanesulfonic acid (HEPES)	Biomol (Hamburg)
Isopropanol	Fluka (Buchs, SUI)
Isopropyl thiogalactopyranoside (IPTG)	Fermentas (St. Leon-Rot)
Kanamycin	Invitrogen (Karlsruhe)
Leupeptin	Serva (Heidelberg)
Methanol	Fisher Scientific (Schwerte)
N,N,N',N'-Tetramethylethylenediamine (TEMED)	Serva (Heidelberg)
Nocodazole	Sigma-Aldrich (Steinheim)
Nonidet® P-40 Substitute (NP-40)	Fluka (Buchs, SUI)
NZ amine	Sigma-Aldrich (Steinheim)
Pepstatin	Roche (Mannheim)
Phenylmethanesulfonyl fluoride (PMSF)	Sigma-Aldrich (Steinheim)
Serva Blue R	Serva (Heidelberg)
Sodium dodecyl sulfate (SDS)	Serva (Heidelberg)
Sodium orthovanadate	Sigma-Aldrich (Steinheim)
Tris	Sigma-Aldrich (Steinheim)
Triton X-100	Roth (Karlsruhe)
Tryptone (Bacto™)	BD Biosciences (Heidelberg)
Tween 20	Sigma-Aldrich (Steinheim)
Western Lightning™ Chemoluminescence Reagent Plus	PerkinElmer (Boston, USA)
Yeast extract (Bacto™)	BD Biosciences (Heidelberg)

All other chemicals were purchased from Merck (Darmstadt) at quality level p.a.

### 2.1.2 Chemical Libraries and Small Molecules

For high-throughput screening 22,461 compounds were used: Chemically diverse libraries from ChemDiv (San Diego, USA; 8298 compounds), Maybridge (Trevillet, UK; HitsKit: 9000 compounds), and 5,163 miscellaneous compounds

Poloxin ([2-methyl-4-oxo-5-(propan-2-yl) cyclohexa-2,5-dien-1-ylidene] amino 2-methyl benzoate) was purchased from ChemDiv (San Diego, USA; compound code 1436-0018) and purified by reversed phase HPLC. Identity and purity were furthermore verified by mass spectrometry and 400 MHz <sup>1</sup>H-NMR (> 97%). Thymoquinone was purchased from Sigma-Aldrich, and its identity and purity were verified by mass spectrometry and 400 MHz <sup>1</sup>H-NMR (> 97%).

### 2.1.3 Kits, Markers and Miscellaneous Materials

Amylose resin	New England Biolabs (Frankfurt)
BCA™ Protein Assay Kit	Pierce (Rockford, USA)
Bio-Rad Protein Assay	Bio-Rad (München)
Cell culture dishes/flasks	BD Falcon (Heidelberg)
	Corning Inc. (Corning, USA)
Chromatography paper 3MM	Whatman (Dassel)
Coverslips	Hartenstein (Würzburg)
CryoTube™ vials	Nunc (Roskilde, DK)
Fluoromount-G	Southern Biotech (Birmingham, USA)
His•Bind® resin	Novagen (Madison, USA)
Hyperfilm™	Amersham (Freiburg)
Kaleidoscope™ protein marker	Bio-Rad (München)
Millex®-HA 0.45 µm sterile filter	Millipore (Schwalbach)
Parafilm	Pechiney Plastic Packaging (Chicago, USA)
Plastic ware	BD Falcon (Heidelberg)
	Eppendorf (Wesseling-Berzdorf)
	Greiner bio-one (Frickenhausen)
	Nunc (Roskilde, DK)
Poly-Prep® chromatography columns	Bio-Rad (München)
Protran® nitrocellulose transfer membrane	Whatman (Dassel)
QIAGEN® Plasmid Maxi Kit	Qiagen (Hilden)
QIAprep® Spin Miniprep Kit	Qiagen (Hilden)
QIAquick® Gel Extraction Kit	Qiagen (Hilden)
QuikChange® II Site-Directed Mutagenesis Kit	Stratagene (Heidelberg)
Screening plates	Corning Inc. (Corning, USA)
	Thermo Fisher (Schwerte)
SmartLadder DNA marker	Eurogentec (Köln)
Spectra/Por® dialysis membrane	Spectrum Laboratories (Rancho Dominguez, USA)

## 2.1.4 Media, Buffers and Solutions

### 2.1.4.1 Bacterial Culture Media

Luria-Bertani broth (LB) (1 L)	10 g	Tryptone
	5 g	Yeast extract
	10 g	NaCl
	pH 7.0	
NZY <sup>+</sup> broth (1 L)	10 g	NZ amine
	5 g	Yeast extract
	5 g	NaCl
	pH 7.5	
	added after autoclaving (filter-sterilized):	
	12.5 ml	of 1 M MgCl <sub>2</sub>
	12.5 ml	of 1 M MgSO <sub>4</sub>
	20 ml	of 20 % (w/v) glucose

For solid culture media 12 g agar was added to 1 L of medium (LB agar).

All media were autoclaved and filter-sterilized antibiotics were added afterwards at the following final concentrations: 100 µg/ml ampicillin, 50 µg/ml kanamycin, 34 µg/ml chloramphenicol.

### 2.1.4.2 Cell Culture Media

The medium used for cell culture in this thesis was Dulbecco's Modified Eagle Medium (DMEM) supplemented with 4.5 mg/ml glucose (high glucose), 2 mM L-glutamine, 1 mM sodium pyruvate, 10 % fetal calf serum (FCS), 100 U/mL penicillin, and 100 µg/mL streptomycin. DMEM and additives were purchased from GIBCO/Invitrogen (Karlsruhe), L-glutamine and penicillin/ streptomycin from PAA (Pasching, AUT).

Long-term stocks of cells were set up in cryo medium consisting of 90 % FCS and 10 % DMSO and stored under liquid nitrogen.

### 2.1.4.3 Frequently Used Buffers and Solutions

All buffers and solutions were prepared with bi-distilled water.

Acrylamide solution (30/0,8)	30 % (w/v)	Acrylamide
	0.8 % (w/v)	Bisacrylamide
Amylose resin buffer	20 mM	Tris/HCl, pH 7.5
	200 mM	NaCl
	1 mM	EDTA
Amylose resin elution buffer	20 mM	Tris/HCl, pH 7.5
	200 mM	NaCl
	1 mM	EDTA
	10 mM	Maltose

Coomassie R-250 solution	0.25 % (w/v) 45 % 10 %	Serva Blue R Methanol Acetic acid
DNA loading buffer (6x)	30 % 0.3 % 0.3 % 100 mM	Glycerol Bromophenole blue Xylene cyanol EDTA
His-tag binding buffer	20 mM 500 mM 5 mM	Tris/HCl, pH 8.0 NaCl Imidazole
His-tag wash buffer	20 mM 500 mM 60 / 200 mM	Tris/HCl, pH 8.0 NaCl Imidazole
His-tag elution buffer	20 mM 500 mM 1 M	Tris/HCl, pH 8.0 NaCl Imidazole
Laemmli buffer (3x)	10 mM 3 % 20 % 0.05 % 3 %	EDTA SDS Glycerol Bromophenole blue $\beta$ -Mercaptoethanol
Lysis buffer	50 mM 150 mM 1 mM 10 % 1 % 10 mM 2 mM 1 mM 0.5 mM	HEPES, pH 7.5 NaCl EDTA Glycerol Triton X-100 $\text{Na}_2\text{P}_2\text{O}_7 \cdot 10 \text{H}_2\text{O}$ $\text{Na}_3\text{VO}_4$ Aprotinin PMSF
NET-gelatine	50 mM 150 mM 5 mM 0.05 % 0.25 % (w/v)	Tris/HCl, pH 7.5 NaCl EDTA Triton X-100 Gelatine
PBS(T)	137 mM 2.7 mM 8.1 mM 1.5 mM (0.1 % pH 7.4	NaCl KCl $\text{Na}_2\text{HPO}_4$ $\text{KH}_2\text{PO}_4$ Tween 20)

Transblot-SD buffer	50 mM	Tris/HCl pH 7.5
	40 mM	Glycine
	20 %	Methanol
	0.004 %	SDS
Strip buffer	62.5 mM	Tris/HCl, pH 6.8
	2 %	SDS
	0.83 %	$\beta$ -Mercaptoethanol
TBE buffer	89 mM	Tris/HCl, pH 8.0
	89 mM	Boric acid
	3 mM	EDTA
TBS(T)	25 mM	Tris/HCl, pH 7.6
	137 mM	NaCl
	2.7 mM	KCl
	(0.1 %)	Tween-20)
TE (10/0,1)	10 mM	Tris/HCl, pH 8.0
	1 mM	EDTA
Tris-Glycin-SDS buffer	25 mM	Tris/HCl, pH 8.8
	192 mM	Glycine
	1 %	SDS

### 2.1.5 Bacterial Strains

The *E. coli* strains in table 2.1 were used for transformations, plasmid amplifications (DH5 $\alpha$ ) and for protein expression (Rosetta<sup>TM</sup>).

**Tab. 2.1: Used bacterial strains**

Strain	Properties/Genotype	Source
DH5 $\alpha$	F <sup>-</sup> $\phi$ 80dlacZM15 (lacZYA-argF)U169 deoR recA1 endA1 hsdR17(r <sup>-</sup> k <sup>-</sup> m <sup>-</sup> k <sup>+</sup> ) phoA supE44 thi-1 gyrA96 relA1 $\lambda$ <sup>-</sup>	Invitrogen (Karlsruhe)
Rosetta <sup>TM</sup> (DE3)	BL21 derivatives, express 6 additional tRNAs rarely occurring in <i>E. coli</i> ; F <sup>-</sup> ompT hsdS <sub>B</sub> (r <sub>B</sub> <sup>-</sup> m <sub>B</sub> <sup>-</sup> ) gal dcm (DE3) pRARE (Cam <sup>R</sup> )	Novagen (Madison, USA)

### 2.1.6 Cell Lines

The cervix adenocarcinoma cell line HeLa (ATCC CCL-2) was used for all cellular experiments in this thesis.

### 2.1.7 Primary Cloning Vectors and cDNAs

Plk1 and Plk1 PBD were cloned by PCR with the vector pRK5-PLKtag as template, which had been produced by Katja Specht (Max Planck Institute of Biochemistry, Martinsried).

All other proteins produced in this thesis were primarily cloned by PCR using cDNA from either placenta or HeLa S3 cells. cDNAs were previously isolated by Tatjana Knyazeva (Max Planck Institute of Biochemistry, Martinsried).

### 2.1.8 Primers

Primers were either used to clone the cDNA of proteins (see 2.2.2.1) or to introduce mutations into the DNA sequence of a protein coding for single amino acid exchanges (see 2.2.2.2). All primers were purchased from Sigma-Genosys (Steinheim).

#### 2.1.8.1 Cloning Primers

Application: Cloning of wildtype Plk1 and the Plk1 polo-box domain (PBD; aa 326-603)

Sequence:

Plk1-1-fwd	ATTGGCCGGCCGATGAGTGCTGCAGTGA
Plk1-326-fwd	ATTGGCCGGCCGATGTCGATTGCTCCAGCAGCCTGGA
Plk1-603-rev	ATTGGCGCGCCGAGGCCTTGAGACGGTTGCTGG

Application: Cloning of the Plk2 PBD (aa 355-685)

Sequence:

Plk2-355-fwd	ATTGGCCGGCCGATGCACTTATCAAGCCCAGCTAAGAA
Plk2-685-rev	ATTGGCGCGCCGCGTTACATCTTTGTAAGAGCATGTTTCAGG

Application: Cloning of the Plk3 PBD (aa 335-646)

Sequence:

Plk3-335-fwd	ATTGGCCGGCCGATGACACCCCCCAACCCAGCTAGGAGTC
Plk3-646-rev	ATTGGCGCGCCGCTGGGCTGCGGTCCCGGAG

Application: Cloning of the Chk2 forkhead-associated domain (FHA; aa 1-225)

Sequence:

Chk2-1-fwd	ATTGGCCGGCCGATGTCTCGGGAGTCGGATGTTGA
Chk2-225-rev	ATTGGCGCGCCGTTTTTGACATGATGTATTCATCTCTTAATGC

Application: Cloning of 14-3-3 $\zeta$

Sequence:

14-3-3 $\zeta$ -fwd	ATTGGCCGGCCGATGGATAAAAATGAGCTGGTTCAG
14-3-3 $\zeta$ -rev	ATTGGCGCGCCGCATTTTCCCCTCCTTCTCCTGCTTC

All cloning primers are given in the 5'→3' direction. Primers were designed in such a way that all forward (fwd) primers introduced a *FseI* restriction site (GGCCGGCC) at the 5'-side, reverse (rev) primers an *AscI* restriction site (GGCGCGCC) at the 3'-side of the cloned cDNA.

Primer design was done using the Amplify v1.2 software for Macintosh (Engels, 1993)

including the following rules: The melting temperature ( $T_M$ ) of a primer should be between 60 and 72 °C; There should be no more than two guanines and cytosines or one thymidin at the 3'-end of a primer; The content of the bases guanine and cytosine should be between 40 and 60 %. Furthermore, primers were designed not to contain self-complementary regions which could lead to the formation of secondary structures.

### 2.1.8.2 Mutagenesis Primers

Application: Introduction of a mutation into the cDNA of the Plk1 PBD coding for the amino acid exchange W414F

Sequence:

*sense* Plk1-W414F      CTTCTGGGTCAGCAAG**TTT**GTGGACTATTCGGACAAG  
*antisense* Plk1-W414F    CTTGTCCGAATAGTCCACAA**ACT**TGCTGACCCAGAAG

Application: Introduction of two mutations into the cDNA of the Plk1 PBD coding for the amino acid exchanges H538A / K540A

Sequence:

*sense* Plk1-H538A/K540A  
    CTTCTTCCAGGAT**GCCACCGCGCT**CATCTTGTGCC  
*antisense* Plk1-H538A/K540A  
    GGCACAAGATGAG**CGCGGTGGC**ATCCTGGAAGAAG

All mutagenesis primers are given in the 5'→3' direction. The sites coding for the amino acid exchanges are shown in bold.

Mutagenesis primers were designed with PrimerX (<http://www.bioinformatics.org/primerx/>) using “QuikChange Site-Directed Mutagenesis Kit by Stratagene” as the mutagenesis protocol and standard settings. Special attention was given to ensure that the mutated codons created were of frequent *E. coli* codon usage.

## 2.1.9 Plasmids

### 2.1.9.1 Basic Vectors

All of the following basic vectors (Tab. 2.2) were provided by Thomas Mayer (University of Konstanz) or Olaf Stemmann (Max Planck Institute of Biochemistry, Martinsried).

**Tab. 2.2: Used basic vectors**

Vector	Properties
pET28a-10His-FA (“pET28a”)	Modified pET28a expression vector (Novagen; Madison, USA); Kan <sup>r</sup> N-terminal 10x His-tag, <i>lacI</i> coding sequence, T7 promotor, <i>FseI</i> and <i>AscI</i> restriction sites
pMAL-C-6His-FA (“pMAL-C”)	Combination and modification of pMAL-C (New England Biolabs; Frankfurt) and pQE-70 (Qiagen; Hilden) expression vectors; Amp <sup>r</sup> , N-terminal MBP-tag and C-terminal 6x His-tag, <i>lacI</i> coding sequence, <i>tac</i> promotor, <i>FseI</i> and <i>AscI</i> restriction sites
pCS2-MT-FA (“pCS2-MT”)	Modified pCS2-MT expression/transfection vector; Amp <sup>r</sup> , N-terminal 6x myc epitope tag, sCMV promotor, <i>FseI</i> and <i>AscI</i> restriction sites

### 2.1.9.2 Modified Vectors

The following vectors (Tab. 2.3) were produced during this work by cloning of cDNA or mutations into basic vectors.

**Tab. 2.3: Used modified vectors**

Vector	Cloned Inserts
pMAL-C/Plk1	cDNA of the human Plk1
pET28a/Plk1 PBD	cDNA of the human Plk1 PBD (aa 326-603)
pET28a/Plk1 PBD FAA	cDNA of the human Plk1 PBD (aa 326-603) with introduced mutations coding for W414F, H538A, K540A
pMAL-C/Plk2 PBD	cDNA of the human Plk2 PBD (aa 355-685)
pMAL-C/Plk3 PBD	cDNA of the human Plk3 PBD (aa 335-646)
pET28a/Chk2 FHA	cDNA of the human Chk2 FHA domain (aa 1-225)
pET28a/14-3-3 $\zeta$	cDNA of human 14-3-3 $\zeta$
pCS2-MT/Plk1 PBD	cDNA of the human Plk1 PBD (aa 326-603)
pCS2-MT/Plk1 PBD FAA	cDNA of the human Plk1 PBD (aa 326-603) with introduced mutations coding for W414F, H538A, K540A
pCS2-MT/Plk2 PBD	cDNA of the human Plk1 PBD (aa 355-685)
pCS2-MT/Plk3 PBD	cDNA of the human Plk1 PBD (aa 335-646)

## 2.1.10 Proteins

### 2.1.10.1 Enzymes

<i>Pfu</i> DNA Polymerase	Fermentas (St. Leon-Rot)
<i>PfuUltra</i> <sup>TM</sup> High-Fidelity DNA Polymerase	Stratagene (Heidelberg)
Restriction Enzymes	Fermentas (St. Leon-Rot)
	New England Biolabs (Frankfurt)
T4 DNA Ligase	Fermentas (St. Leon-Rot)
Trypsin	GIBCO/Invitrogen (Karlsruhe)

### 2.1.10.2 Antibodies

In this thesis, antibodies were used for Western blot and immunofluorescence experiments (Tab. 2.4).

**Tab. 2.4: Used antibodies**

Immunoblot Antibodies	Properties	Source
anti-myc (9E10)	mouse, monoclonal	Santa Cruz (Santa Cruz, USA)
anti-Cdc25C (C-20)	rabbit, polyclonal	Santa Cruz (Santa Cruz, USA)
anti-BubR1 (clone 9)	mouse, monoclonal	BD Biosciences (Heidelberg)
anti-Plk1, NT	rabbit, polyclonal	Upstate (Lake Placid, USA)
anti-actin	rabbit, polyclonal	Sigma-Aldrich (Steinheim)
anti-mouse HRP conjugate	goat, polyclonal	Dako (Hamburg)
anti-rabbit HRP conjugate	swine, polyclonal	Dako (Hamburg)

Tab. 2.4: continued

Immunofluorescence Antibodies	Properties	Source
anti- $\gamma$ -tubulin (clone GTU-88)	mouse, monoclonal	Sigma-Aldrich (Steinheim)
anti- $\alpha$ -tubulin (clone DM1A) FITC conjugate	mouse, monoclonal	Sigma-Aldrich (Steinheim)
anti-Plk1 (ab14209)	rabbit, polyclonal	Abcam (Cambridge, UK)
Alexa Fluor® 546 anti-mouse	goat, polyclonal	Molecular Probes (Karlsruhe)
Alexa Fluor® 488 anti-rabbit	goat, polyclonal	Molecular Probes (Karlsruhe)

### 2.1.10.3 Recombinant Proteins

Some recombinant proteins were not produced in this thesis but provided by the following sources:

The Pin1 WW domain (aa 1-162) was provided by Martin Gräber (this group).

The Src-homology 2 domains (SH2) of STAT1 (aa 135-712), STAT3 (aa 135-712), STAT5b (aa 136-704), and Lck (aa 121-226) have been described (Schust & Berg, 2004 and Schust *et al.*, 2006).

### 2.1.11 Peptides

Peptides (Tab. 2.5) were synthesized and purified using standard Fmoc chemistry by the core facility of the Max Planck Institute of Biochemistry (Martinsried), and by Peptide Specialty Laboratories (Heidelberg). Coupling to 5-carboxyfluorescein (5-CF) was performed via N,N'-diisopropylcarbodiimide (DIC)/1-hydroxy-benzotriazole (HOBt) activation in N,N-dimethylformamide (DMF) or via the NHS-ester. Unless stated otherwise (Ac: Acetyl), peptides were synthesized with an N-terminal amino group and a C-terminal carboxyl group. Peptides were analyzed by HPLC and MS and showed purity >95 %.

Tab. 2.5: Used peptides

Sequence	Properties
5-CF-ASpTPLNGAKK	Plk1-binding fluoropeptide 1
GPMQSpTPL-K(5-CF)-NH <sub>2</sub>	Plk1-binding fluoropeptide 2
5-CF-MQSpTPLNG	Plk1-binding fluoropeptide 3
5-CF-GPMQSpTPLNG	Plk1-binding fluoropeptide 4
MAGPMQSpTPLNGAKK	High-affinity Plk1-binding peptide
MAGPMQSTPLNGAKK	Unphosphorylated high-affinity Plk1-binding peptide
Ac-ASpTPLNGAKK	Plk1-binding peptide reduced to SpTP-motif
Ac-ASpSPLNGAYKK	Plk1-binding peptide reduced to SpSP-motif
MAGPMSQDPLNGAKK	High-affinity Plk1-binding peptide with pT→D exchange
MAGPMSQEPLNGAKK	High-affinity Plk1-binding peptide with pT→E exchange
5-CF-GPMQTSpTPKNG	Plk2-binding fluoropeptide
5-CF-GPLATSpTPKNG	Plk3-binding fluoropeptide
5-CF-GHFDpTYLIRR	Chk2-binding fluoropeptide
Ac-GHFDpTYLIRR	Chk2-binding peptide
5-CF-GWFYpSPRLKK	Pin1-binding fluoropeptide
5-CF-GARSHpSYPACK	14-3-3 $\zeta$ -binding fluoropeptide

Tab. 2.5: continued

Sequence	Properties
5-CF-GpYDKPHVL	STAT1-binding fluoropeptide
5-CF-GpYLPQTV-NH <sub>2</sub>	STAT3-binding fluoropeptide
5-CF-GpYLVLDKW	STAT5b-binding fluoropeptide
5-CF-GpYEEIP	Lck-binding fluoropeptide

## 2.2 Molecular Biology Methods

### 2.2.1 Microbiological Techniques

#### 2.2.1.1 Cultivation and Maintenance of Bacterial Strains

*E. coli* strains were grown at 37 °C overnight either in liquid LB medium or on LB agar plates containing the appropriate antibiotics.

For short-term storage, *E. coli* cultures were kept on LB agar plates at 4 °C. For long-term conservation glycerol stocks were set up by mixing 750 µl of a 3 ml overnight culture with 500 µl 50 % (v/v) glycerol and stored in CryoTube™ vials at -80 °C.

#### 2.2.1.2 Transformation of Competent *E. coli* Strains

For transformation of *E. coli* DH5α, 50 µl of cells were thawed and mixed with either 1 µl (30-100 ng) of isolated plasmid DNA (see 2.2.1.3) or 3 µl (5-15 ng) of a ligase reaction (see 2.2.3.2). Mixed samples were incubated for 30 minutes on ice, followed by a 45 second heat shock at 42 °C and another incubation on ice for 2 minutes. Then 500 µl of antibiotic-free LB medium was added and samples were incubated for 1 hour at 37 °C on a rotating wheel. Afterwards, 100 µl of culture volume were plated on LB agar plates containing the appropriate antibiotics and incubated overnight at 37 °C.

For transformation of *E. coli* Rosetta™ (DE3), 1 µl (10ng) of plasmid DNA was incubated with 9 µl of cells for 5 minutes on ice. The pre-incubated samples were heat-shocked for 30 seconds at 42 °C, cooled down for 2 minutes on ice and after addition of 50 µl LB medium without antibiotics incubated for 1 hour at 37 °C on a rotating wheel. The whole sample was subsequently plated on LB agar plates with the respective antibiotics and incubated overnight at 37 °C.

#### 2.2.1.3 Isolation of *E. coli* Plasmid DNA

Small amounts of plasmid DNA (0.5-10 µg) were extracted from 3 ml overnight cultures using the QIAprep® Spin Miniprep Kit.

For larger amounts (300-1000 µg) and higher purity, plasmids were isolated out of a 200 ml culture volume using the QIAGEN® Plasmid Maxi Kit.

All plasmid preparations were carried out according to the corresponding kit manual.

### 2.2.2 DNA Amplification

#### 2.2.2.1 Polymerase Chain Reaction (PCR)

PCR is a fast and efficient method for *in vitro* amplification of a certain piece of DNA (Mullis & Faloona, 1987). A DNA segment flanked by a pair of primers (forward and reverse primer;

see 2.1.8.1) is exponentially amplified by a repeated cycle of denaturation, primer annealing and polymerase-driven primer elongation.

The following standard PCR reaction was used:

5 $\mu$ l	10x <i>Pfu</i> buffer (provided with <i>Pfu</i> DNA polymerase)
4 $\mu$ l	25mM MgCl <sub>2</sub>
1 $\mu$ l	sample DNA (50-100 ng plasmid or 1 $\mu$ g cDNA)
1 $\mu$ l	forward primer (10 pmol/ $\mu$ l)
1 $\mu$ l	reverse primer (10 pmol/ $\mu$ l)
1 $\mu$ l	dNTP mix (dA/G/C/TTP; 10 mM)
0.5 $\mu$ l	<i>Pfu</i> DNA polymerase (2.5 U/ $\mu$ l)
36.5 $\mu$ l	H <sub>2</sub> O

PCR reactions were carried out in 0.5 ml PCR tubes in a Progene thermal cycler (Techne; Stone, UK) using the following program (T<sub>M</sub>: primer melting temperature):

Denaturation:	5 min @ 95 °C	
Amplification cycle:	30 sec @ 95 °C (Denaturation)	35x
	30 sec @ T <sub>M</sub> – 5 °C (Annealing)	
	2 min @ 72 °C (Elongation)	
Final elongation:	5 min @ 72 °C	

The results of PCR reactions were analysed on agarose gels (see 2.2.4). Positive PCR products were subsequently cut out of the gel and purified (see 2.2.4).

### 2.2.2.2 Mutagenesis PCR

The QuikChange® II Site-Directed Mutagenesis Kit was used to introduce mutations into a protein's cDNA that code for single amino acid exchanges.

The principle of this method is that a plasmid containing the non-mutated cDNA as template and a pair of complementary primers (*sense* and *antisense* primer; see 2.1.8.2) carrying the desired mutations are used to PCR-amplify the whole plasmid and at the same time introduce the mutations into the protein's cDNA. The endonuclease *DpnI* is specific for methylated DNA. As the template plasmid was isolated from *E. coli* DH5 $\alpha$  its DNA is methylated and is therefore susceptible to *DpnI* digestion. Hence *DpnI* cleaves the template plasmid only and leaves the unmethylated newly synthesized plasmid carrying the desired mutations.

The mutagenesis PCR was run according to the corresponding kit manual:

5 $\mu$ l	10x reaction buffer
1 $\mu$ l	dsDNA template (approx. 10 ng)
1 $\mu$ l	<i>sense</i> primer (approx. 125 ng)
1 $\mu$ l	<i>antisense</i> primer (approx. 125 ng)
1 $\mu$ l	dNTP mix
3 $\mu$ l	QuikSolution™ reagent
0.5 $\mu$ l	<i>PfuUltra</i> ™ High-Fidelity DNA polymerase (2.5 U/ $\mu$ l)
37.5 $\mu$ l	H <sub>2</sub> O

PCR reactions were carried out in 0.5 ml PCR tubes in a Progene thermal cycler (Techne; Stone, UK) using the following program:

Denaturation:	1 min @ 95 °C	
Amplification cycle:	50 sec @ 95 °C (Denaturation)	18x
	50 sec @ 60 °C (Annealing)	
	x min @ 68 °C (Elongation)	
Final elongation:	7 min @ 68 °C	

The elongation time (x) was calculated as 1 minute per kb of plasmid length.

After the PCR the samples were restriction digested with 10 U of the endonuclease *DpnI*. 2 µl of digested PCR product was subsequently transformed into DH5α. Single colonies were restreaked and used for plasmid preparations (see 2.2.1.3). To check for positive mutagenesis results, isolated plasmids were sequenced (see 2.2.5).

## 2.2.3 Enzymatic Treatment of DNA

### 2.2.3.1 DNA Restriction with Endonucleases

For a restriction digest, approximately 0.5-2 µg of DNA (PCR fragment or plasmid) was mixed with 5-10 U per endonuclease in a reaction buffer recommended by the manufacturer. Some endonucleases required the addition of BSA. When incubating with two restriction enzymes at the same time buffer conditions guaranteeing at least 50 % activity for each enzyme were applied. Restriction samples were incubated for 3 hours at 37 °C and subsequently purified via agarose gel extraction (see 2.2.4).

### 2.2.3.2 Ligation of DNA Fragments

DNA fragments were ligated with a correspondingly cut vector in T4 DNA ligation buffer (provided with T4 DNA Ligase) using 5 U of T4 DNA Ligase. Approximately 15-40 ng of vector were used. The required amount of inserted DNA fragment was calculated according to the following formula:

$$\left( \frac{\text{amount of insert}}{\text{insert length}} \right) / \left( \frac{\text{amount of vector}}{\text{vector length}} \right) = 3$$

Ligations were carried out for 2 hours at 16 °C. 3 µl of ligation reaction were subsequently transformed into *E. coli* DH5α (see 2.2.1.2). Plasmids were isolated from transformed clones and ligations controlled by sequencing (see 2.2.5).

## 2.2.4 Agarose Gel Electrophoresis and DNA Purification

Plasmids and DNA fragments were separated on 1 % agarose gels containing 0.01 % (v/v) ethidium bromide (Sambrook *et al.*, 1989). DNA samples were mixed with DNA loading buffer and put into the agarose gel. Electrophoresis was performed in TBE buffer at 80 V for 60-90 minutes.

DNA bands were visualized on a transilluminator at 302 nm (intercalating ethidium bromide fluoresces orange when exposed to UV light) and photographs were taken with the IDA gel documentation system (Raytest; Straubenhardt). The size of separated DNA bands was monitored via the Smart Ladder DNA marker.

If DNA samples had to be used for further experiments they were separated on 1 % agarose

gels and visualized with a Dark Reader® (Clare Chemical Research; Dolores, USA) at 460 nm to avoid introducing mutations. Samples were subsequently cut out of the gel with a sterile blade and purified using the QIAquick® Gel Extraction Kit. The extraction was carried out according to the manufacturer's manual.

### 2.2.5 Sequencing

DNA samples were sequenced on an ABI 3730 sequencer (Applied Biosystems; Darmstadt), using the ABI Big Dye 3.1 sequencing protocol, by the core facility of the Max Planck Institute of Biochemistry (Martinsried).

## 2.3 Protein Isolation Methods

### 2.3.1 Protein Expression

All proteins were expressed in the *E. coli* Rosetta™ (DE3) strain which carries a plasmid coding for 6 additional eukaryotic tRNAs leading to enhanced protein expression.

A 10 ml overnight culture was used to inoculate 1 L of LB medium with antibiotics in a 3 L conical flask with chicanes. Cultures were incubated at 37 °C and 140 rpm until an optical density at 600 nm (OD<sub>600</sub>) of 0.5-0.6 was reached. Cultures were subsequently transferred to room temperature and induced with 1 mM IPTG as soon as the OD<sub>600</sub> reached 0.8-0.9. After overnight incubation at room temperature cells were harvested. Cell pellets were frozen at -80 °C.

### 2.3.2 Protein Extraction

Bacterially expressed proteins were extracted by sonication. For this purpose frozen bacterial pellets were thawed on ice and resuspended in the appropriate column binding buffer according to the affinity chromatography column to be used. Every 10 ml of cell suspension was sonicated four times for 2 minutes each time, at 70 % power level and 70 %/30 % pulse/pause interval, using a Sonoplus HD70 sonicator (Bandelin; Berlin). The sonicated cell suspension was centrifuged for 20 minutes at 19,000 rpm and 4 °C in an SS-34 rotor. The supernatant was additionally filtered using a Millex®-HA 0.45 µm sterile filter to completely remove cell debris and other insoluble components. The resulting protein solution was used for further purification.

### 2.3.3 Protein Purification

Expressed recombinant proteins can be purified by affinity chromatography. The method of purification depends on the expression plasmid and the hence expressed tag.

The principle of affinity chromatography is that expressed tagged proteins can specifically and reversibly interact via their affinity tag with ligands covalently attached to a column resin. After washing away unspecifically bound proteins, the desired protein can be eluted by adding free ligand or by a change of buffer conditions.

### 2.3.3.1 His-tag Affinity Chromatography

The His-tag is frequently used for the purification of recombinant proteins. The recombinant proteins produced in this thesis carried a tag consisting of 10 histidine residues. The imidazole groups of histidines can bind to Ni<sup>2+</sup> ions complexed with iminodiacetic acid or nitrilotriacetic acid bound to a column resin. Bound protein can be eluted by adding free imidazole.

All buffers used contained 1 mM aprotinin und 0.5 mM PMSF for protease inhibition. For His-tag chromatography, thawed cell pellets were resuspended in 4 ml of His-tag binding buffer per 100 ml of culture volume. The resulting protein solution after sonication was applied to an His•Bind® resin column. 250 µl of 50 % resin was used per 100 ml culture volume. The resin was settled into a Poly-Prep® chromatography column (0.8 x 4 cm), charged with 50 mM NiSO<sub>4</sub> and equilibrated in His-tag binding buffer before the protein solution was applied. Unspecifically bound proteins were subsequently removed by washing with 10 column bed volumes of His-tag binding buffer, 4 column bed volumes of His-tag wash buffer (60 mM imidazole), and 2 column bed volumes of His-tag wash buffer (200 mM imidazole). Purified protein was then eluted 2 times with 2 column bed volumes His-tag elution buffer each.

### 2.3.3.2 MBP-tag Affinity Chromatography

Recombinant proteins fused to a 40 kDa maltose binding protein (MBP) can be purified using a resin with immobilized amylose. The MBP binds to amylose and can be eluted by adding free maltose.

All buffers used contained 1 mM aprotinin und 0.5 mM PMSF for protease inhibition. For MBP-tag chromatography, thawed cell pellets were resuspended in 5 ml of amylose resin buffer per 100 ml of culture volume. The resulting protein solution after sonication was diluted 1/3 with amylose resin buffer and applied to an amylose resin column. 600 µl of amylose resin slurry was used per 100 ml culture volume. The resin was settled into a Poly-Prep® chromatography column (0.8 x 4 cm) and equilibrated in amylose resin buffer before the protein solution was applied. Unspecifically bound proteins were subsequently removed by washing with 3 column bed volumes of amylose resin column buffer. MBP-tagged proteins were eluted with 10 mM maltose in amylose resin column buffer in 4 elution fractions of 0.6 column bed volumes each.

### 2.3.4 Dialysis

After purification the ligands used for elution of protein had to be removed from the elution fractions. Furthermore protein had to be transferred into a buffer which would allow freezing and long-term storage without precipitation.

For this purpose all elution fractions were combined and the additional protease inhibitors 5µg/ml antipain, 0.5 µg/ml leupeptin and 0.7 µg/ml pepstatin were added. The protein solution was then filled into Spectra/Por® dialysis membranes (pore size: 3.5 kDa) which had been prepared by rinsing with 1 mM EDTA solution and water. Dialysis was performed three times against 100x the protein solution volume at 4 °C. The following dialysis buffer was used:

50 mM Tris/HCl (pH 8.0), 200 mM NaCl (for His-tagged Plk1 PBD: 400 mM), 1 mM EDTA, 1 mM DTT, 10 % glycerol, 0.1 % NP-40 substitute.

### 2.3.5 Protein Stocks

For long-term storage dialyzed protein was split into 50-100  $\mu\text{l}$  aliquots and snap-frozen in liquid nitrogen. Frozen aliquots were stored at  $-80\text{ }^{\circ}\text{C}$ .

## 2.4 Protein Biochemistry Methods

### 2.4.1 Determination of Protein Concentration

#### 2.4.1.1 Bradford Protein Assay

The measurement of protein concentration using the Bradford method (Bradford, 1976) is a colorimetric assay based on an absorbance shift of the dye Coomassie Brilliant Blue G-250 (CBB). When bound to protein, the red form of CBB (absorption maximum: 465 nm) is changed into the blue form (absorption maximum: 595 nm). The degree of absorption shift is dependent on the protein concentration.

In this case, the Bio-Rad Protein Assay dye solution was used. 200  $\mu\text{l}$  of a 1/5 dilution was added to 10  $\mu\text{l}$  protein sample and incubated for 15 minutes at room temperature. Absorption was subsequently measured at 595 nm and the concentration was determined by comparison with the absorption of a standard curve of  $\gamma$ -globulin (20-400  $\mu\text{g}/\text{ml}$ ).

#### 2.4.1.2 BCA Protein Assay

The measurement of protein concentration using the BCA protein assay (Smith *et al.*, 1985) is based on the reduction of copper ions from  $\text{Cu}^{2+}$  to  $\text{Cu}^{+}$  by peptide bonds in a temperature-dependent reaction.  $\text{Cu}^{+}$  ions get chelated by bicinchoninic acid (BCA) which causes a color change of the reaction sample from light green to purple. The amount of purple complex is proportional to protein concentration and can be detected at 562 nm.

In this case the BCA<sup>TM</sup> Protein Assay Kit was used according to the manufacturer's manual. Protein concentration was determined by comparison with the absorption of a standard curve of BSA (100-2000  $\mu\text{g}/\text{ml}$ ).

### 2.4.2 SDS Polyacrylamide Gel Electrophoresis (SDS-PAGE)

SDS polyacrylamide gels are used to separate proteins according to their molecular weight (Laemmli, 1970). The anionic detergent sodium dodecyl sulfate complexes proteins and gives all proteins a negative overall charge independent of amino acid composition and charges of side chains. The Laemmli buffer used contains  $\beta$ -mercaptoethanol, which reduces all inter- and intramolecular disulfide bridges. Furthermore, samples are boiled before electrophoresis at  $95\text{ }^{\circ}\text{C}$  for 10 minutes so that all secondary, tertiary and quaternary structures are removed. Movement of proteins in the gel is therefore dependent on molecular weight only.

The Atto Slab Electrophoresis Chamber System (Atto; Tokyo, JP) was used. Samples were run on two-layered gels consisting of stacking and resolving gel. The stacking gel contained 4 % acrylamide solution (in Tris/HCl, pH 6.8 and 0.4 % SDS), the resolving gel 7.5 – 12.5 % (in Tris/HCl, pH 8.8 and 0.4 % SDS). To start the polymerization reaction 0.125 % (v/v) TEMED and APS were added.

For sample preparation, Laemmli buffer was added to each protein sample, followed by

boiling for 10 minutes at 95 °C. Samples were loaded into the gel wells using a Microliter® syringe (Hamilton; Bonaduz, SUI). The Kaleidoscope™ protein marker was used as a molecular weight standard.

SDS-PAGE was performed at a constant current of 20 mA per gel. After electrophoresis gels were either stained with Coomassie solution or proteins were transferred to a nitrocellulose membrane (see 2.4.3).

For staining gels were washed for 10 minutes in Coomassie R-250 solution followed by destaining for several hours in 10 % methanol / 10 % acetic acid. For drying, gels were subsequently inserted air bubble-free between two wet layers of cellophane and left for 3 hours in a GelAir dryer (Bio-Rad; München).

### 2.4.3 Western Blot / Immunoblot

This method is used to specifically detect a protein within a cellular extract. First the protein sample is separated via SDS-PAGE, followed by transfer to a nitrocellulose membrane (Gershoni & Palade, 1983) where proteins can be probed by antibodies. Normally a two-step antibody detection system is used: a primary antibody binds to the antigen immobilized on the membrane, then a secondary antibody coupled to horseradish peroxidase (HRP) is used to detect the primary antibody. The enzymatic activity of the peroxidase can be used to visualize a protein band in a chemoluminescence reaction.

In this thesis after gel electrophoresis (see 2.4.2) proteins were transferred to a Protran® nitrocellulose transfer membrane in Transblot-SD buffer for 3h at 0.8 mA per cm<sup>2</sup> of membrane in a semidry-blotting system. The blot was set up in the following order: anode, 4 layers of Whatman paper, nitrocellulose membrane, polyacrylamide gel, another 4 layers of Whatman paper and cathode.

After proteins were transferred, the transfer was checked by staining the membrane with Ponceau S (2 % (w/v) in 30 % trichloroacetic acid) for 1 minute. This also allowed tagging of the marker bands on the membrane. Ponceau S was subsequently washed out with NET-gelatine.

To avoid unspecific binding of the primary antibody to nitrocellulose, the membrane was first blocked with NET-gelatine or 5% milk in TBST at 4 °C overnight. Next the membrane was incubated with primary antibody for 1 hour at room temperature, followed by three wash steps with NET-gelatine or TBST for 15 minutes each. Afterwards the membrane was incubated with the appropriate secondary antibody for 1 hour at room temperature followed by three further wash steps. Protein bands were detected using the Western Lightning™ Chemoluminescence Reagent Plus according to the manufacturer's manual.

If the membrane was to be reprobed, all bound antibodies were removed from the nitrocellulose by incubation in strip buffer for 1 hour at 50 °C. After intensive washing with NET-gelatine to remove all traces of β-mercaptoethanol, the membrane was probed again with another set of antibodies.

The following antibodies were used for immunoblotting: mouse anti-Myc (1:5,000), rabbit anti-Cdc25C (1:100), mouse anti-BubR1 (1:2,000), rabbit anti-Plk1 (1:1,000), and rabbit anti-actin (1:5,000), followed by incubation with a goat anti-mouse or a swine anti-rabbit HRP-conjugated secondary antibody (both 1:7,500).

## 2.5 Eukaryotic Cell Culture Methods

### 2.5.1 General Cell Culture Techniques

Cells were cultivated in HERAcell® 150 CO<sub>2</sub> incubators (Thermo Fisher; Schwerte) at 37 °C and 5 % CO<sub>2</sub> under humidified atmosphere. All working steps were carried out in sterile LaminAir hoods (Heraeus; Hanau and Holten; Allerod, DK).

Cells were kept in fresh medium and passaged constantly. For long-term storage, cells were transferred into cryo medium in CryoTube™ vials and after stepwise freezing stored at -196 °C in liquid nitrogen.

### 2.5.2 Transient Transfection of Mammalian Cells

Transient transfection of cells can be used to test the effects of ectopically overexpressed proteins in mammalian cells.

For this purpose cells were seeded in 6 well plates. After cell attachment plasmid transfections were carried out using the FuGENE® 6 reagent (Roche, Mannheim) according to the manufacturer's manual. 48 hours after transfection cells were either lysed (see 2.5.3) to check protein levels or used for immunofluorescence experiments (see 2.6.1).

### 2.5.3 Cell Lysis

For lysis cells were washed once with PBS, scraped off the culture plate into lysis buffer and shaken for 30 minutes at 250 rpm. Cell debris and DNA were removed by centrifuging for 20 minutes at 13,000 rpm. The supernatant was then transferred to a new tube and used for determination of concentration (BCA protein assay; see 2.4.1.2) and further analysis.

For long-term storage lysates were split in 100-500 µl aliquots and frozen in liquid nitrogen. Frozen aliquots were stored at -80 °C.

## 2.6 Cell Biology Methods

### 2.6.1 Immunofluorescence

Immunofluorescence techniques are used to visualize cellular organelles and structures or to show the subcellular localization and distribution of biomolecules within a cell. Visualization is achieved by fluorescence-labeling of cellular components with dyes or with antibodies conjugated to dyes.

In this thesis, HeLa cells were used for all immunofluorescence experiments. Cells were seeded in 12-well plates containing coverslips. The number of seeded cells was chosen so that the cell density at the timepoint of fixation was approximately 80 %. After 24 hours of incubation cells were arrested in G1/S phase by addition of 1 µg/ml aphidicolin for 14 hours. Cells were then released into aphidicolin-free medium. Depending on the experiment DMSO, 150 nM nocodazole or compounds were added to the medium at different time points. At various timepoints after the release, in most cases after 9 or 14 hours, cells were fixed. Transfected cells used for immunofluorescence were fixed 48 hours after transfection.

For fixation cells were first washed once with PBS and then fixed and permeabilized in methanol for 15 min at -20 °C. Afterwards cells were washed three times with PBS to dispose of all methanol.

Before antibody treatment cells were incubated for 60 min in blocking solution (1 % goat serum in PBST) to minimize background staining. All antibodies were diluted in blocking solution, and incubations were carried out for 1 hour at room temperature in a humidified chamber, followed by 3 washes with PBST. The following antibodies were used: mouse anti- $\gamma$ -tubulin (1:1,000) which was detected with Alexa Fluor® 546-conjugated goat anti-mouse (1:1,000), mouse anti- $\alpha$ -tubulin-FITC (1:500), rabbit anti-Plk1, NT (1:75; Upstate) and rabbit anti-Plk1 (1:75; Abcam) which were detected by Alexa Fluor® 488-conjugated goat anti-rabbit (1:1,000). DNA was stained with 2  $\mu$ g/ml DAPI.

Immunofluorescence microscopy was performed on an Axioplan 2 Imaging Microscope (Zeiss; Jena). All photos were taken on a DeltaVision® Microscope (Applied Precision; Issaquah, USA) at 100x magnification. Images were processed using a deconvolution algorithm of the softWoRx software (Applied Precision).

### 2.6.2 Determination of Mitotic Index and Mitotic Phases

To determine the percentage of mitotic cells, the number of cells undergoing mitosis was counted within a population of approximately 200 cells fixed on coverslips.

For determination of mitotic phase distribution approximately 50 mitotic cells were categorized into prophase, prometaphase, metaphase, and ana-/telophase. Cells with defects in metaphase form a subpopulation of metaphase cells.

All counting experiments were repeated three times.

### 2.6.3 Quantification of Plk1 Localization

The centrosomal/cytoplasmic ratio of Plk1 staining was determined by measuring the total intensity in a circular region of fixed diameter round the centrosome relative to the average intensity in three cytoplasmic regions of the same size. In each case 20 centrosomes were evaluated.

For quantification images were taken on the Axioplan 2 Imaging Microscope with identical exposure times and settings for recording. Fluorescence intensities were analyzed using the MetaVue™ software (Molecular Devices; Ismaning).

## 2.7 Fluorescence Polarization

The theory of fluorescence polarization (FP) was first described by Perrin in 1926. It is based on the observation that fluorescent molecules in solution, which are excited with polarized light, will also emit light in the same polarized plane if the molecule remains stationary during the excitation of the fluorophore. Since molecules in solution rotate and tumble during the excited state, light is emitted in planes different from the plane used for the initial excitation. The light used for excitation gets depolarized. The degree of depolarization is dependent on the rotational mobility of a fluorophore. Small molecules rotate relatively fast, causing a high degree of depolarization, while large molecules show only little mobility during the excited

state, leading to a minor impact on polarization. FP is calculated using the following formula ( $I_{\parallel}$ : fluorescence intensity measured parallel to applied light,  $I_{\perp}$ : fluorescence intensity measured perpendicular to applied light):

$$FP = \frac{I_{\parallel} - I_{\perp}}{I_{\parallel} + I_{\perp}}$$

A FP-based assay was used for screening in this thesis. Small fluorophore-labeled peptides causing a strong depolarization were used in assays with protein-binding domains. A protein-fluoropeptide complex, much bigger in size, caused a significantly smaller degree of depolarization. This system was used to test for molecules inhibiting the protein-fluoropeptide interaction, causing a decrease in FP. Figure 2.1 schematically depicts the used assay setup.

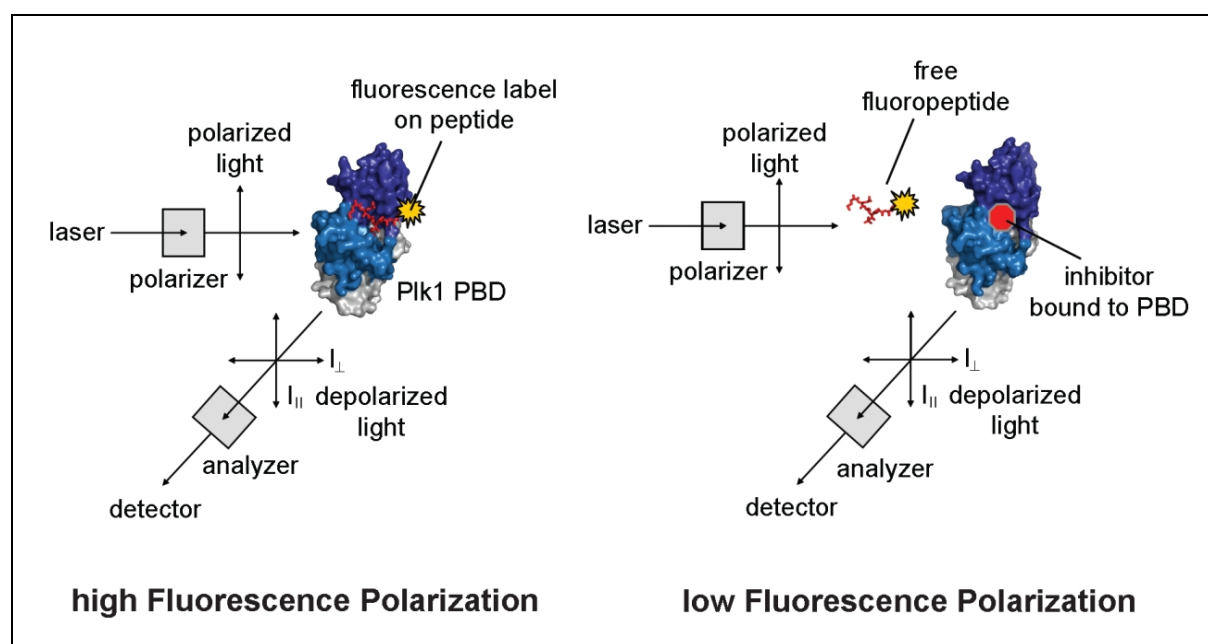


**Fig. 2.1: Scheme of the used fluorescence polarization assay.** The PBD-peptide complex rotates slowly, yielding a high FP signal. If binding is blocked by an inhibiting molecule, the free peptide rotates relatively fast, causing a high depolarization. The fluoropeptide is shown in red as sticks. The polo-boxes are shown in light and dark blue. PBD adapted from 1Q4K (see Fig. 1.3; Cheng *et al.*, 2003).

### 2.7.1 Binding Curves

Binding curves can be used to determine the dissociation constant ( $K_d$ -value) of a protein-protein interaction. The  $K_d$ -value is defined as the concentration of protein that will result in half-maximal binding. It is an important parameter to describe the binding affinity of two interaction partners. For the measurement of binding curves one binding partner is kept constant while the concentration of the other is steadily increased.

In this thesis several protein-protein interactions were investigated. The interaction was represented by binding of a fluorophore-labeled peptide derived from substrate studies or peptide screens to a protein-binding domain (see 2.1.11). Fusions of the peptides with fluorophores allowed the analysis of interactions via FP. 5-carboxyfluorescein (CF) was used as label for all peptides.

For binding curves 10 nM of fluoropeptide was added to increasing amounts of protein (0-2560 nM) in 10 mM Tris/HCl, pH 8.0 (for Stat1, Stat3, Stat5b, Lck: 10 mM HEPES, pH 7.5), 50 mM NaCl, 1 mM EDTA, 0.1 % Nonidet P-40, and 10 % DMSO. For Plk1 binding

studies various buffers were used (see 3.1.2.2). FP of a bound protein-peptide complex was measured in 384-well plates on an Ultra Evolution™ plate reader (Tecan; Crailsheim) using a G-factor of 0.998 (an intrinsic value used to correct for imperfections of the optical components of the measuring instrument; determined empirically). Corrected FP values were multiplied by 1000 and expressed in mP. Binding curve analysis and determination of the  $K_d$ -value was done with SigmaPlot (SPSS Science Software; Erkrath) using a “Hill Four Parameter” curve fit. Experiments were performed in triplicate.

## 2.7.2 Inhibition Curves

The  $IC_{50}$ -value of an inhibition curve is defined as half-maximal inhibitory concentration and gives information about the effectivity of an inhibitor.

In this thesis inhibitors (small molecules or peptides) were tested for their ability to disrupt the binding of proteins and the respective fluoropeptides which would lead to a decrease in FP. For this purpose constant amounts of protein and peptide were used with increasing amounts of inhibitor.

Proteins were used at the following final concentrations which correspond approximately to the  $K_d$ -values of the respective binding assays: Plk1: 45 nM, Plk2: 130 nM, Plk3: 1875 nM, Chk2: 240 nM, Pin1: 1000 nM, STAT1: 120 nM, STAT3: 160 nM, STAT5b: 110 nM; Lck: 40 nM. Unless stated otherwise, proteins were incubated at 22 °C with test compounds for 1 hr prior to addition of 10 nM fluorophore-labeled peptides. The final concentration of buffer components used was: 10 mM Tris, pH 8.0 (for Stat1, Stat3, Stat5b, Lck: 10 mM HEPES, pH 7.5), 50 mM NaCl, 1 mM EDTA, 0.1 % Nonidet P-40, and 10 % DMSO. FP was measured immediately afterwards as described above (see 2.7.1). Inhibition curves were fitted using the “Four Parameter Logistic” fit of SigmaPlot. Experiments were performed in triplicate.

## 2.7.3 Z'-Factor

In order to investigate the suitability of the FP assay for high-throughput screening, the Z'-factor was analyzed (Zhang *et al.*, 1999). This parameter correlates the individual variations between measurements in different wells containing identical assay components with the differences in the FP values of bound and free fluoropeptide-probe.

The Z'-factor was calculated using the following formula (SD: standard deviation, mP fluorescence polarization, bound: incubation of protein and peptide, free: incubation of protein, peptide and inhibitor):

$$Z' = 1 - \frac{(3SD_{bound} + 3SD_{free})}{(mP_{bound} - mP_{free})}$$

In the ideal case Z' equals 1, which means that well-to-well variations are negligible compared to the differences of the fluorescence polarization values of the probe in the free state and the state in which a fraction is bound to the protein. In the worst case, Z' approaches negative infinity, indicating that the differences of the fluorescence polarization values of the probe in the free state and the partially-bound state are negligible compared to the variations between wells containing the same assay components. An assay is considered to be well-suited to high-throughput screening if Z' is larger than 0.5.

In this thesis the Z'-factor was determined as follows: The "bound state" was represented by a mixture containing 10 nM of the peptide 5-CF-GPMQSpTPLNG with 45 nM of the Plk1 PBD. The "free state" contained the same components but was additionally incubated with 10  $\mu$ M of the unlabeled peptide MAGPMQSpTPLNGAKK which competes for binding to the Plk1 PBD. Four independent experiments were performed in which the FP of both the bound and free fluorescence-probe were analyzed in 192 wells each. Experiments were carried out in 10 mM Tris, pH 8.0, 50 mM NaCl, 1 mM EDTA, 1 mM DTT, 0.1% Nonidet P-40, and 10% DMSO.

### 2.7.4 High-Throughput Screen

The High-Throughput Screen (HTS) for inhibitors of the Plk1 PBD was carried out in a 384-well format on a Biomek® FX dual-pod screening system (Beckman Coulter; Krefeld). Protein and peptide solutions were transferred with a 96-multichannel pipetting head. Compound libraries were applied with a 384-pin HDR-tool (pin tool).

The following screening protocol based on FP was used: 20  $\mu$ l of Plk1 PBD (final concentration: 45 nM) was pipetted into 384-well plates. Compounds of chemically diverse libraries (22,461 small molecules in DMSO; see 2.1.2) were subsequently transferred. The pin tool settings for the transfers were:

Draw: -2.3 mm from liquid, pod speed 5 % when entering and exiting a well, pause for 5 seconds in liquid

Dispense: 0.7 mm from bottom, pod speed 5 % when entering and 30 % when exiting a well, 3 dips, pause for 5 seconds in liquid on last dip

These settings were determined to transfer a volume of approximately 45 nl. The number of transfers depended on the concentration of compounds in the different libraries and was adapted so that final compound concentrations of up to 60  $\mu$ M were used.

The mixture of protein and compounds was incubated for 1 hour at room temperature before 10  $\mu$ l of the peptide 5-CF-GPMQSpTPLNG (final concentration: 10 nM) was added. Each plate contained control wells with buffer only, peptide solution in buffer and a mixture of protein and peptide without compounds. The screening buffer used contained 10 mM Tris, pH 8.0, 50 mM NaCl, 1 mM EDTA, 1 mM DTT, 0.1% Nonidet P-40, and DMSO. The final DMSO concentration was 10%. Each compound was tested in duplicate.

FP values were measured on an Ultra Evolution™ plate reader as described above (see 2.7.1), using the Magellan™ software (Tecan; Crailsheim). Small molecules with inhibiting activity could be detected by a decrease in FP in comparison to the control wells.

## 3. Results

The serine/threonine kinase Plk1 is one of the key regulators of mitotic progression and it is overexpressed in many types of human cancers (Barr *et al.*, 2004; McInnes *et al.*, 2005; Strebhardt & Ullrich, 2006). Therefore a comprehensive knowledge of Plk1 functions is important for two reasons: for a better understanding of the cell cycle and its control, and for new strategies in cancer therapy.

The aim of this thesis was the identification of small-molecule inhibitors of the Plk1 PBD. With one exception (Gumireddy *et al.*, 2005), all currently described non-peptidic Plk1 inhibitors target the kinase domain (Stevenson *et al.*, 2002; Liu *et al.*, 2005; McInnes *et al.*, 2006; Peters *et al.*, 2006; Lansing *et al.*, 2007; Lenart *et al.*, 2007; Steegmaier *et al.*, 2007; Santamaria *et al.*, 2007). Therefore inhibitors of the Plk1 PBD would represent a valuable new Plk1 research tool, allowing the distinction between PBD-dependent and PBD-independent functions. Furthermore, they could be used as an alternative strategy to target Plk1 in human tumors.

### 3.1 Fluorescence Polarization Assay

High-throughput screening offers a fast approach for the identification of substances with inhibitory activity. It allows efficient testing of compound libraries containing large numbers of substances in a short period of time. However a suitable screening assay has to be used.

Inhibitors of the Plk1 PBD would block Plk1 from binding to its substrates. Therefore an assay was needed which allowed Plk1-substrate interactions to be monitored. As fluorescence polarization (FP) assays had already been successfully shown to be suitable for the analysis of protein-protein interactions in high-throughput screens (Nasir & Jolley, 1999; Schust *et al.*, 2004; Nikolovska-Coleska *et al.*, 2004; Du *et al.*, 2006; Saldanha *et al.*, 2006), it was decided to set up a Plk1-binding assay based on FP. In this assay Plk1-substrate interactions were to be represented by binding of fluorophore-labeled peptides to the PBD.

#### 3.1.1 Cloning, Expression and Purification of the Plk1 PBD

Since small-molecules inhibiting the PBD and *not* the kinase domain should be identified, the cDNA sequence coding for the PBD (aa 326-603) (Elia *et al.*, 2003b) only was cloned into the expression vector pET28a (see 2.1.9.1). After transformation, the PBD fused to a 10x His-tag

was expressed in *E. coli* Rosetta™ (DE3) and purified via His-tag affinity chromatography. After affinity chromatography, elution fractions were combined and dialyzed. Protein concentration was then determined. Several batches of PBD protein have been produced and the protein concentration of each batch was approximately 20-25  $\mu\text{M}$ . The isolated PBD was used for FP-based binding assays.

### 3.1.2 Establishment and Optimization of a FP-Based Binding Assay

A binding assay suitable for detecting inhibition has to fulfill two important requirements. Firstly, the resulting binding curve should show a steep gradient, which represents high binding affinity and guarantees high sensitivity for inhibition measurements. Secondly, the measurement window defined by minimal and maximal FP values should be as large as possible, so that experimental variations and standard deviations can easily be distinguished. In the following experiments different setups were tested to find optimal binding conditions.

#### 3.1.2.1 Application of Fluorophore-Labeled Peptides

The core consensus motif of the Plk1 PBD had originally been described as S-(pT/pS)-(P/X), and the peptide described to have the highest affinity for the Plk1 PBD was MAGPMQSpTPLNGAKK (Elia *et al.*, 2003a). Given the importance of the SpTP-motif for binding to the Plk1 PBD the following four 5-carboxyfluorescein (CF)-labeled peptides were designed on the basis of the optimal binding peptide:

5-CF-ASpTPLNGAKK  
GPMQSpTPL-K(5-CF)-NH<sub>2</sub>  
5-CF-MQSpTPLNG  
5-CF-GPMQSpTPLNG

Peptides differed in peptide length and proximity of the CF-label to the core consensus motif, respectively. Furthermore the effect of N-terminal or C-terminal location of the CF-label was tested. The fluorophore should be located as close as possible to the interaction site with the protein in order to avoid unnecessary degrees of rotational freedom. Figure 3.1 shows the binding curves for the different peptides.

Only weak binding was observed for 5-CF-ASpTPLNGAKK ( $K_d = 3.8 \pm 1.6 \mu\text{M}$ ). This result can be explained by two studies describing the crystal structure of the complex between the Plk1 PBD and peptides comprising its preferred binding motif, which revealed that not only the tripeptide SpTP, but the sequence motif MQSpTPL is bound by the Plk1 PBD (Elia *et al.*, 2003b; Cheng *et al.*, 2003).

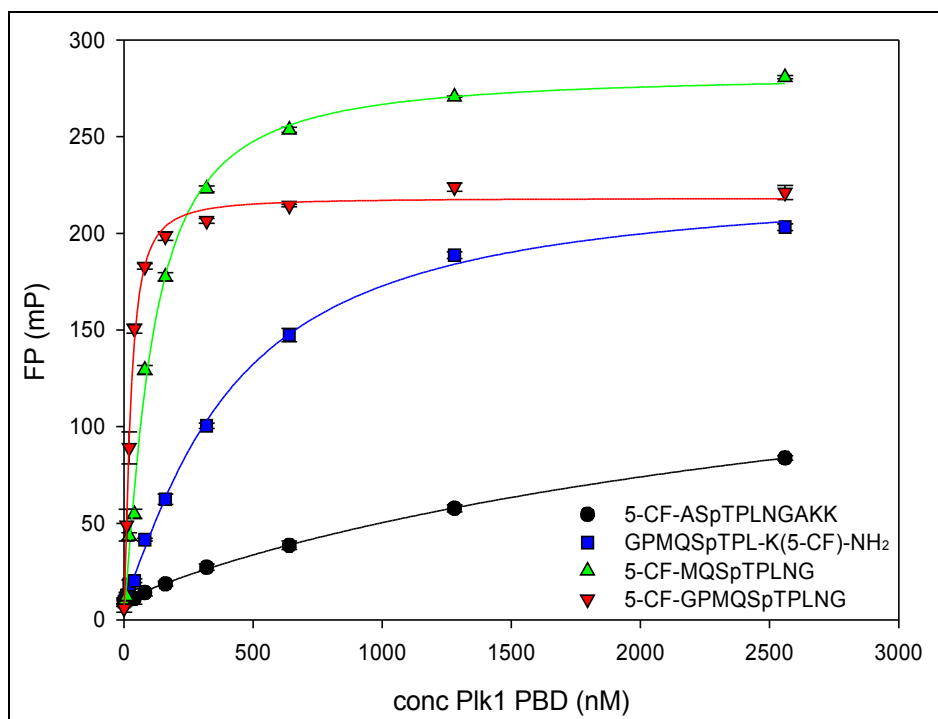


**Fig. 3.1: Comparison of four fluorophore-labeled peptides.** Binding curves of four peptides differing in peptide length and location of the fluorescence-label. Sequences indicating the location of 5-carboxy-fluorescein (5-CF)-label are given. Error bars represent standard deviations (SD).

Therefore, the fluoropeptides GPMQSpTPL-K(5-CF)-NH<sub>2</sub> and 5-CF-MQSpTPLNG were designed comprising the longer sequences. These two peptides were additionally used to compare the effect of N- and C-terminal location of the CF-label. Both probes contain two additional amino acids derived from the optimal binding peptide at their respective unmodified terminus to ensure that their ability to bind to the Plk1 PBD was not affected by positive or negative charges caused by protonation or deprotonation of the peptide termini. As expected, both probes showed improved affinity for the Plk1 PBD, whereas the affinity of the peptide GPMQSpTPL-K(5-CF)-NH<sub>2</sub> with the C-terminal label ( $K_d = 407 \pm 32$  nM) was not as high as for the peptide 5-CF-MQSpTPLNG with N-terminal CF ( $K_d = 107 \pm 10$  nM).

Since direct attachment of the bulky and hydrophobic fluorophore to the N-terminal methionine, the backbone of which is involved in binding to the protein, would certainly negatively affect the protein-peptide interaction, two additional amino acids derived from the optimal binding peptide were inserted between the fluorophore and the peptide sequence. Indeed, the resulting fluoropeptide 5-CF-GPMQSpTPLNG showed very high affinity for the Plk1 PBD ( $K_d = 26 \pm 2$  nM) and was used for all further studies.

### 3.1.2.2 Determination of Optimal Buffer Conditions

Various buffer components can influence protein-protein or protein-peptide interactions. The effect of NaCl and DMSO on the binding affinity of the fluoropeptide 5-CF-GPMQSpTPLNG towards the Plk1 PBD was therefore investigated.

#### NaCl

The crystal structure analysis of the complex between Plk1 and its binding motif revealed hydrogen bonds between the phosphothreonine of the peptide and histidine 538 and lysine 540 (Elia *et al.*, 2003b; Cheng *et al.*, 2003), both of which are known to be required for the function of the Plk1 PBD. As binding between 5-CF-GPMQSpTPLNG and the Plk1 PBD was mediated to a significant extent by recognition of the phosphothreonine residue of the probe, high concentrations of ions could interfere with binding. Therefore different concentrations of NaCl were tested (Fig. 3.2).

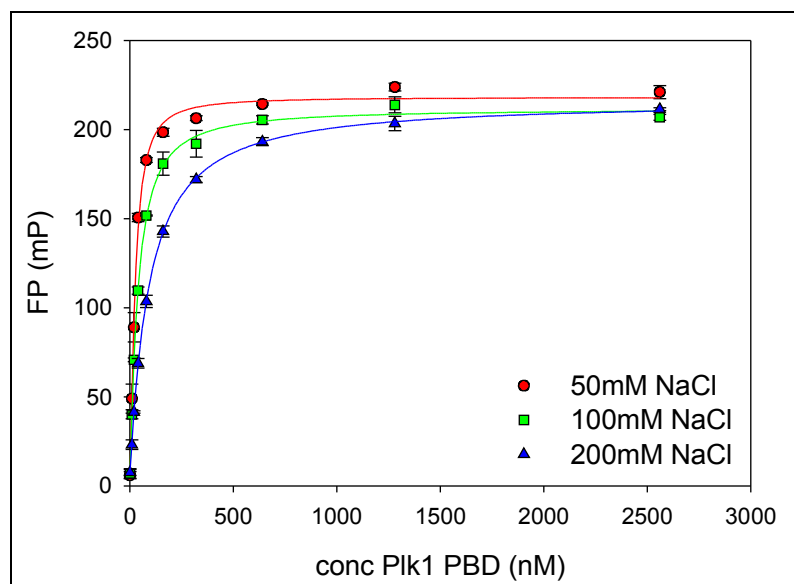


**Fig. 3.2: Effect of NaCl on binding.** Binding curves in presence of 50 mM, 100 mM and 200 mM NaCl. Error bars represent SD.

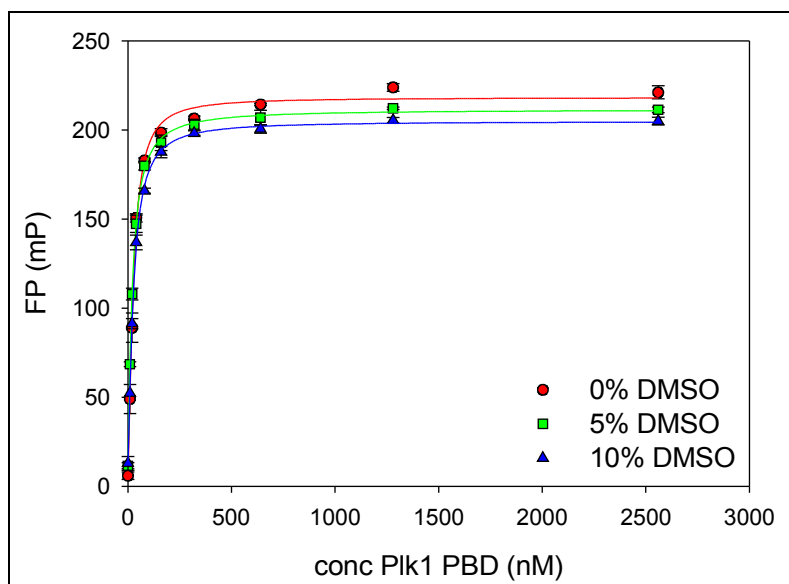
Binding was indeed weakened by increasing concentrations of NaCl (50 mM:  $K_d = 26 \pm 2$  nM; 100 mM:  $K_d = 39 \pm 2$  nM; 200 mM:  $K_d = 91 \pm 2$  nM). Thus, 50 mM NaCl was used for further experiments, because it resulted in the strongest binding affinity.

#### DMSO

DMSO is the most common solvent for chemical libraries, since the majority of compounds dissolve reasonably well in DMSO. Therefore, an assay to be used for the discovery of bioactive compounds must be stable in the presence of DMSO. In order to analyze the stability of the interaction between the probe 5-CF-GPMQSpTPLNG and the Plk1 PBD in the presence of DMSO, 5 % and 10 % of this co-solvent were added to the assay buffer (Fig. 3.3).

**Fig. 3.3: No dependency of binding affinity on DMSO concentration.**

Binding curves in absence and in presence of 5 % and 10 % DMSO. Error bars represent SD.



Despite a negligible decrease in window size, no significant change in the  $K_d$ -values was observed in the presence of DMSO (no DMSO:  $K_d = 26 \pm 2$  nM, 5 % DMSO:  $K_d = 21 \pm 1$  nM, 10 % DMSO:  $K_d = 26 \pm 1$  nM), indicating that the assay is compatible with up to 10 % DMSO.

### 3.1.2.3 Temporal Stability

High temporal stability of a binding assay allows the screening of large chemical libraries without imposing restrictions with regards to time. Binding between the probe 5-CF-GPMQSpTPLNG and the Plk1 PBD was stable over a course of 24 hours with a constant  $K_d$ -value of 25-27 nM, and thus displayed high temporal stability (Fig. 3.4).

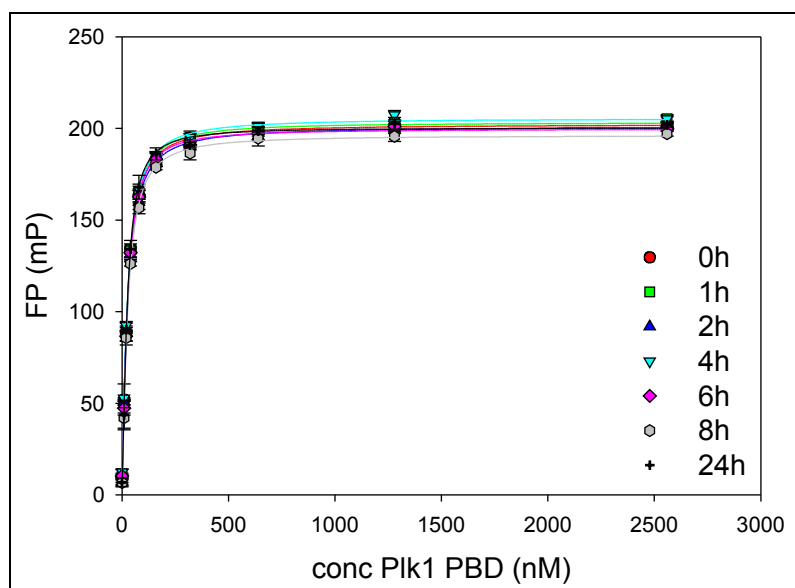


**Fig. 3.4: Temporal stability of the binding assay.** Binding curves showed stability for up to 24h. Error bars represent SD.

### 3.1.3 Test of Inhibition and Binding Studies

In order to test whether inhibition measurements are possible under the established assay conditions the inhibiting activity of the unlabeled peptide MAGPMQSpTPLNGAKK was analyzed in a competition study with the peptide 5-CF-GPMQSpTPLNG (Fig. 3.5). The Plk1 PBD was used at a final concentration of 45 nM providing an assay window larger than 100 mP.

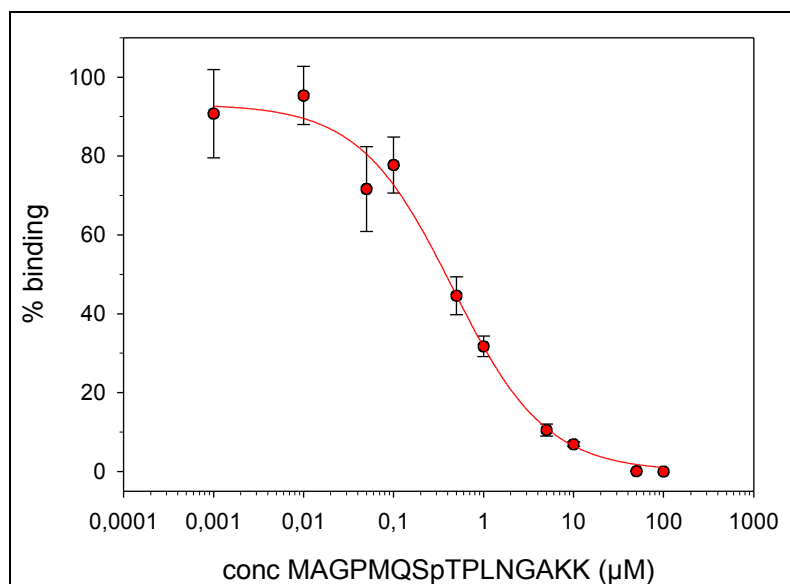


**Fig 3.5: Inhibition curve of MAGPMQSpTPLNGAKK.** The peptide inhibits PBD-fluoropeptide interaction. Error bars represent SD.

MAGPMQSpTPLNGAKK potently inhibited the Plk1 PBD-fluoropeptide interaction with an  $IC_{50}$  of  $0.39 \pm 0.11 \mu\text{M}$ , indicating that the assay is well-suited for inhibition measurements.

For further characterization of the interaction between 5-CF-GPMQSpTPLNG and the Plk1 PBD, competition analysis was performed with the following additional unlabeled peptides (Fig. 3.6):

MAGPMQSTPLNGAKK  
 Ac-ASpTPLNGAKK  
 Ac-ASpSPLNGAYKK  
 MAGPMQSDPLNGAKK  
 MAGPMQSEPLNGAKK  
 Ac-GHFDpTYLIRR (Chk2-binding)

The unphosphorylated peptide MAGPMQSTPLNGAKK displayed more than 200-fold weaker antagonistic activity ( $IC_{50} = 98.7 \pm 25.8 \mu\text{M}$ ) than the phosphorylated version MAGPMQSpTPLNGAKK ( $IC_{50} = 0.39 \pm 0.11 \mu\text{M}$ ). The peptide Ac-ASpTPLNGAKK ( $IC_{50} = 32.2 \pm 2.0 \mu\text{M}$ ), which lacks amino acids of the optimal binding motif N-terminal of the phosphothreonine, also showed a decrease in inhibitory activity. Consistent with the

previous observation that phosphothreonine provides significantly higher affinity for the Plk1 PBD than phosphoserine (Elia *et al.*, 2003a), the peptide Ac-ASpSPLNGAYKK was less active than Ac-ASpTPLNGAKK ( $19.2 \pm 12.1\%$  inhibition at  $100 \mu\text{M}$ ).

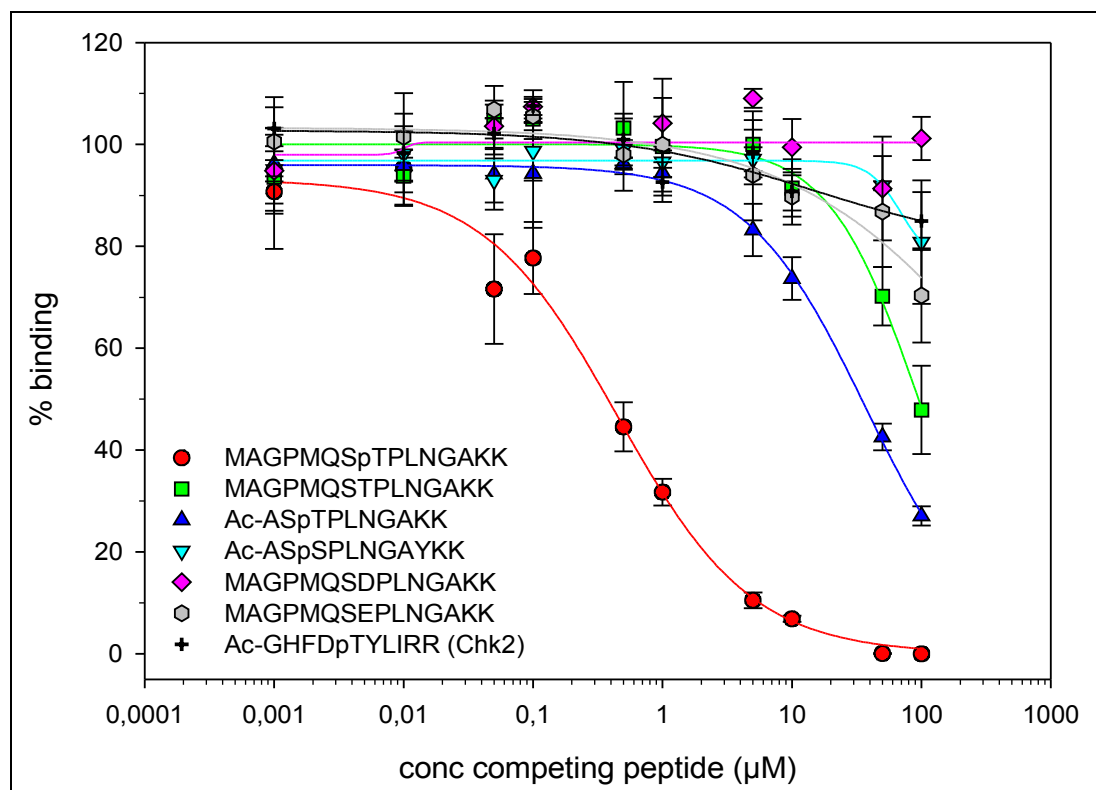


**Fig. 3.6: Binding studies with different competing peptides.** Inhibition curves of different unlabeled peptides competing with the probe 5-CF-GPMQSpTPLNG for binding to the Plk1 PBD. Error bars represent SD.

Substitution of phosphothreonine for aspartic or glutamic acid is frequently used to mimic constitutive phosphorylation of the threonine residue. In order to test whether the Plk1 PBD lends itself to this approach, the phosphothreonine residue within the optimal binding motif was substituted with aspartic or glutamic acid, but this led to a dramatic loss of activity ( $29.7 \pm 9.2\%$  inhibition at  $100 \mu\text{M}$  for glutamic acid, or no inhibition at all for aspartic acid).

To investigate the specificity of binding between 5-CF-GPMQSpTPLNG and the Plk1 PBD in more detail, we tested the effect of the peptide Ac-GHFDpTYLIRR described to bind to another phosphothreonine-binding domain, the forkhead-associated (FHA) domain of the kinase Chk2. This peptide showed minimal inhibition at the highest concentration tested ( $15.0 \pm 5.7\%$  inhibition at  $100 \mu\text{M}$ ), indicating specific recognition between the probe 5-CF-GPMQSpTPLNG and the Plk1 PBD.

### 3.1.4 Determination of the Z'-Factor

In order to investigate the suitability of the assay for high-throughput screening, the Z'-factor was analyzed (Zhang *et al.*, 1999). This parameter correlates the individual variations between measurements in different wells containing identical assay components with the differences in the fluorescence polarization values of the probe 5-CF-GPMQSpTPLNG in the absence and presence of the Plk1 PBD. An assay is considered to be well-suited to high-throughput screening if Z' is larger than 0.5.

To determine the Z'-factor of the FP assay used, we monitored the polarization of mixtures containing 5-CF-GPMQSpTPLNG (10 nM) and 45 nM Plk1 PBD. Since this concentration exceeds the  $K_d$ -value of  $26 \pm 2$  nM, the majority of the fluorescein-labeled peptide molecules are protein-bound ("bound state"). In another set of wells, the same assay components were additionally incubated with the inhibiting peptide MAGPMQSpTPLNGAKK (10  $\mu$ M), which displaced the fluorophore-labeled peptide molecules from the Plk1 PBD ("free state"). Z' was calculated as  $0.73 \pm 0.06$ , indicating that the assay is excellently suitable for high-throughput screening (Fig. 3.7).

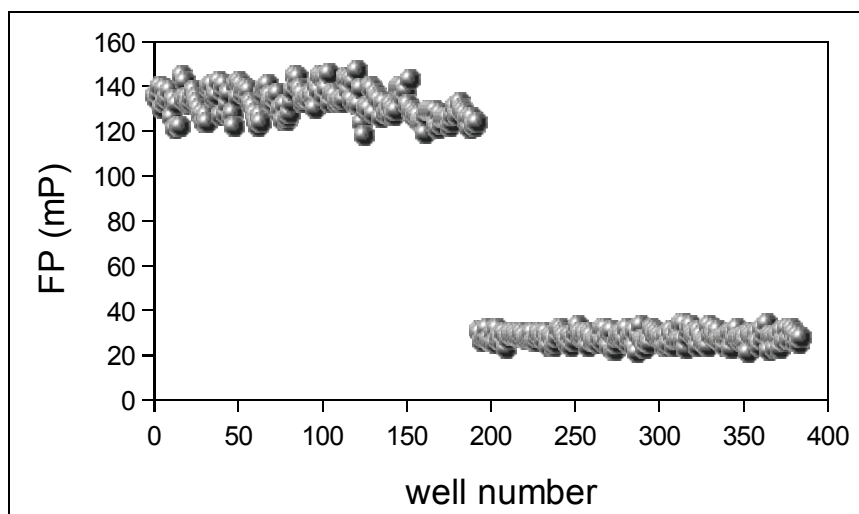


**Fig. 3.7 Graphical illustration of the determination of the Z'-factor.** Each dot represents the FP value of one well. There are 192 wells each with bound peptide and free peptide. The Z'-factor is determined according to the formula in 2.7.3 using the average values and the standard deviations for each state.

## 3.2 High-Throughput Screen

### 3.2.1 Screening Process

In this thesis, 22,461 compounds were tested for inhibitory activity towards binding of the Plk1 PBD to the probe 5-CF-GPMQSpTPLNG. The compounds were composed of a ChemDiv (CDI) library with 8,298 compounds, a Maybridge (MB) library, comprising 9,000 compounds, and 5,183 miscellaneous substances. The selected compounds covered a wide spectrum of chemical space ranging from natural products to semi-synthetic substances and *de novo* synthesized compounds. All compounds fulfilled Lipinski's "rule of 5" (Lipinski *et al.*, 2001), which describes the factors playing a role for cellular uptake of substances.

The screen was carried out on a Biomek® FX dual-pod screening system in 384-well plates. Compounds were transferred with a pin tool. All substances were screened at two different concentrations, 30  $\mu\text{M}$  and 60  $\mu\text{M}$ . Compounds were screened in duplicate.

After the screen, compounds were selected for further analysis according to their Plk1 PBD inhibiting activity, and the likelihood of specificity. The acquired screening data was compared with the results of two analogous screens previously performed by this group. The aim of these screens was the identification of inhibitors for the dimerization and DNA-binding of the transcription factor c-Myc/Max (Kiessling *et al.*, 2006) and for the SH2 domain of the transcription factor STAT3 (Schust *et al.*, 2006). In these screens, compounds were tested at 100  $\mu\text{M}$ .

As part of this thesis, the CDI and the MB libraries were additionally tested for inhibitors of the SH2 domain of the transcription factor STAT5b at 30  $\mu\text{M}$  and 60  $\mu\text{M}$ . An analogous FP-based assay as for the Plk1 PBD was set up, used for the detection of compounds with the ability to inhibit binding of the fluorophore-labeled peptide 5-CF-GpYLVLDKW, derived from the erythropoietin (EPO) receptor (Quelle *et al.*, 1996; May *et al.*, 1996) to the SH2 domain of STAT5b (aa 136-704) (Schust *et al.*, 2006) (see 4.3.3). For selection of hits, the results of the Plk1 PBD screen were also compared with the STAT5b screening data.

Only compounds inhibiting the Plk1 PBD in duplicate by more than 65 % at 60  $\mu\text{M}$  were selected, while not inhibiting c-Myc/Max and STAT3 by more than 50 % at 100  $\mu\text{M}$ , and STAT5b by more than 40 % at 60  $\mu\text{M}$ . Quantification showed strongly increased total fluorescence intensities for a number of compounds. These abnormal values were caused by intrinsic fluorescence of the test compounds. Such molecules were not analyzed further. Figure 3.8 visualizes the hit selection process using the data for the CDI library as example.

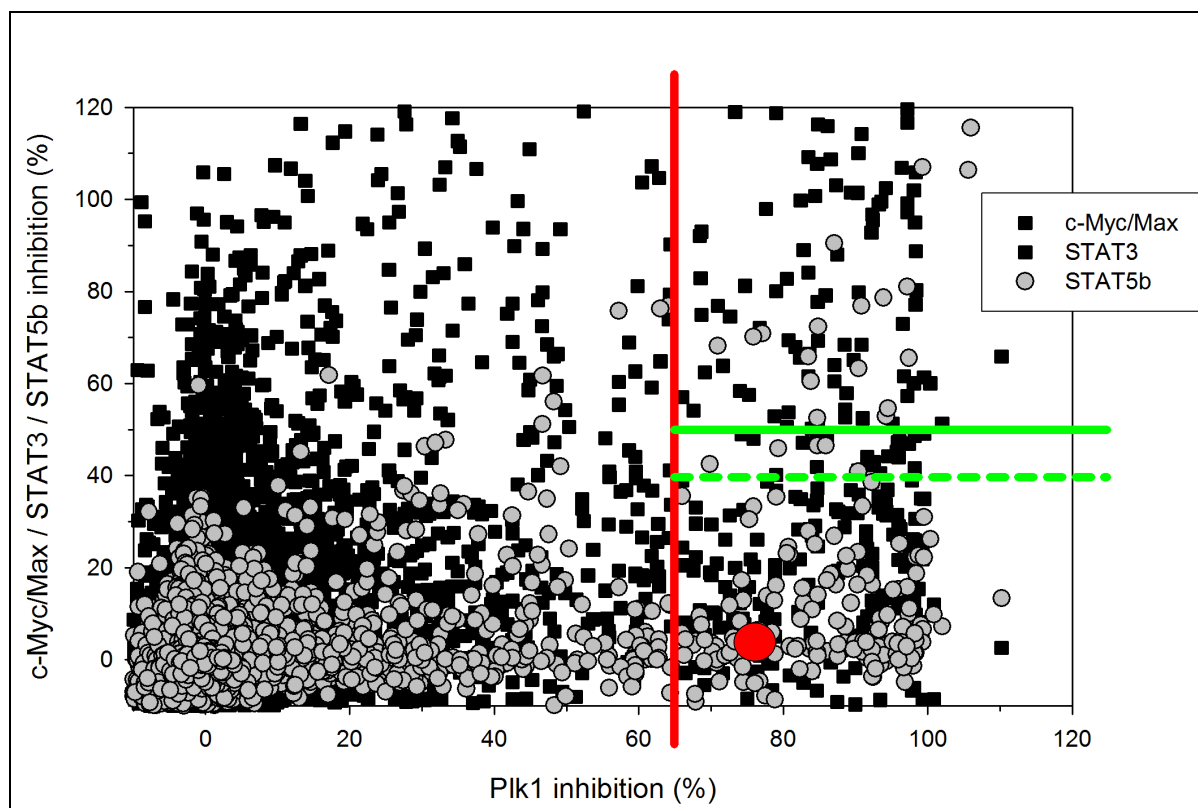


**Fig. 3.8: Compound selection, exemplified for the CDI library.** Each dot represents a single compound with Plk1 inhibition (60  $\mu$ M) plotted against c-Myc/Max, STAT3 (100  $\mu$ M each; black squares each) or STAT5b (60  $\mu$ M; gray circles) inhibition. The following compounds were taken into further analysis: All compounds right of the solid red line, all compounds symbolized by black squares below the solid green line, and additionally all compounds symbolized by gray circles below the dashed green line. The location of Poloxin (see 3.2.3) in the plot was very similar for all three comparisons and is symbolized by the large red dot.

Altogether approximately 1 % (223 compounds) of the 22,461 compounds were picked for further analysis.

### 3.2.2 Validation of Primary Screening Data

Since the pin tool only transfers volumes in the low nanoliter range using adhesion forces, the system is easily susceptible to errors. In order to sort out false positives, all compounds selected for further analysis were tested again by hand at 60  $\mu$ M. Only 94 of the selected 223 compounds (42 %) could be verified.

In the next step, first specificity controls were applied. In analogous assays, the inhibitory effect of the remaining molecules on c-Myc/Max, Jun/Jun, and C/EBP or STAT3 was tested manually at 60  $\mu$ M. Any compound inhibiting one of these proteins by more than 50 % was left out. Using these specificity controls 86 compounds remained.

After *in vitro* validation of selected compounds, their cellular effects were tested. Since Plk1 inhibition leads to an arrest of cells in mitosis (Spankuch-Schmitt *et al.*, 2002a; Yuan *et al.*,

2002; Stevenson *et al.*, 2002; Spankuch-Schmitt *et al.*, 2002b; Liu & Erikson, 2003; Liu *et al.*, 2005; Gumireddy *et al.*, 2005; McInnes *et al.*, 2006; Peters *et al.*, 2006; Lansing *et al.*, 2007; Lenart *et al.*, 2007; Steegmaier *et al.*, 2007; Santamaria *et al.*, 2007), all remaining compounds were tested for their ability to increase the mitotic index by at least 2-fold. Compounds were primarily used at 50  $\mu$ M. If this concentration turned out to be toxic to cells, substances were re-tested at 20  $\mu$ M. Most compounds did not show any effect on cells or displayed toxicity, so that only 19 compounds led to an increase of mitotic cells.

Compounds blocking cells in mitosis were subsequently analyzed for their ability to induce any of the mitotic arrest phenotypes that can be explained by Plk1 inhibition. However, only 2 compounds showed an appropriate phenotype. Most compounds either showed an increased mitotic index without any extraordinary phenotype, or seemed to interfere with tubulin-polymerization, causing a nocodazole-like phenotype (Fig. 3.9). Nocodazole is a spindle poison depolymerizing tubulin (Jordan *et al.*, 1992) (Fig. 3.9). Table 3.1 summarizes the validation of compounds.

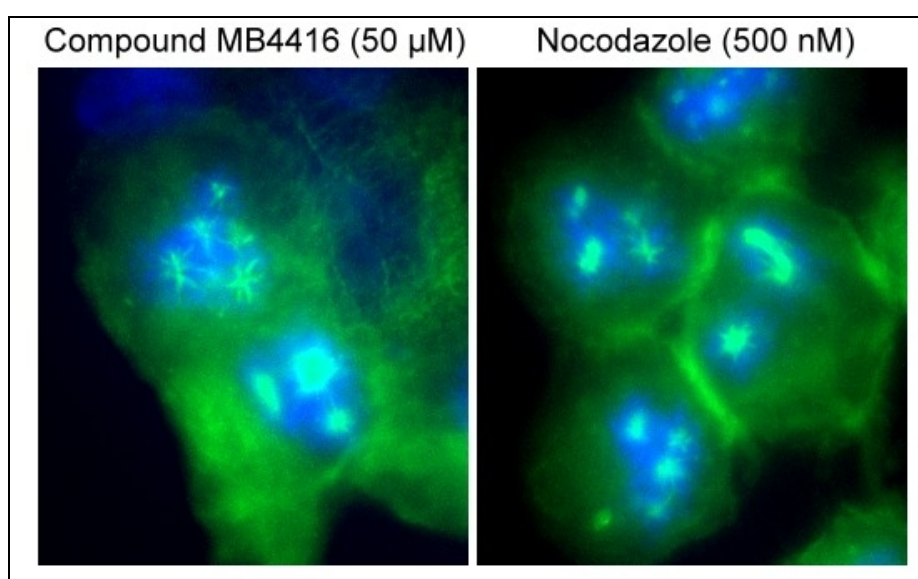


**Fig. 3.9: Example for an improper arrest phenotype.** MB compound 4416 is most likely depolymerizing spindles and by that causing a nocodazole-like phenotype. blue: DNA, green:  $\alpha$ -tubulin (spindels and cytoskeleton); magnification: 100x.

**Tab. 3.1: Summary of compound validation.**

Screened compounds	Compounds selected after screen	Compounds verified by hand	Compounds showing specificity	Compounds causing mitotic arrest	Compounds with correct phenotype
22,461	223	94	86	19	2

Of the 2 remaining compounds, the more effective compound was used for further analysis, while the other one will be evaluated in future studies.

### 3.2.3 Identification of Poloxin and Thymoquinone

The compound with the best specificity profile was named Poloxin (for *polo-box* domain *in*hibitor). Due to its diversity, the screening library did not contain analogues of Poloxin, from which preliminary structure-activity relationships might have been inferred.

Poloxin's core structure is represented by the natural product Thymoquinone. Thymoquinone is the bioactive constituent of the volatile oil of black seed (*Nigella sativa*), and is well-known for its anti-inflammatory and anti-oxidant activities (Gali-Muhtasib *et al.*, 2006). Moreover, numerous studies have demonstrated Thymoquinone's potent anti-neoplastic activity, which seems to be specific for cancer cells (Shoieb *et al.*, 2003; Rooney *et al.*, 2005; Kaseb *et al.*, 2007; Gali-Muhtasib *et al.*, 2008). However, direct molecular targets that could explain for its anti-neoplastic activity have not been reported to date.

Figure 3.10 shows the chemical structures of Poloxin and its core structure Thymoquinone.

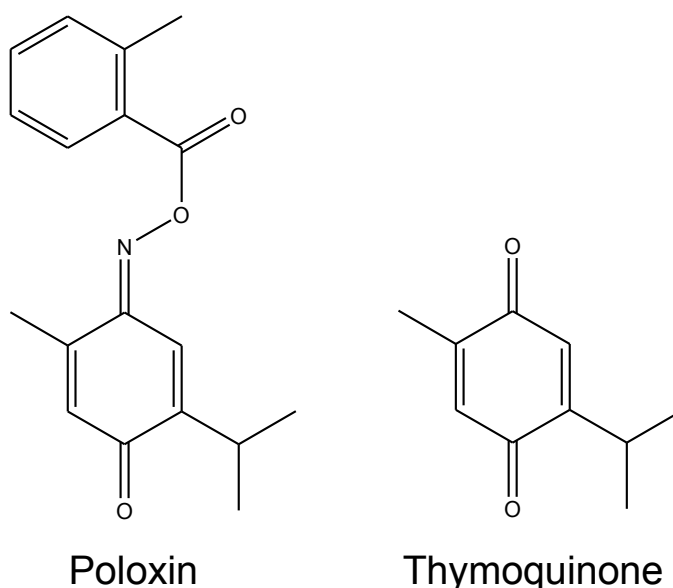
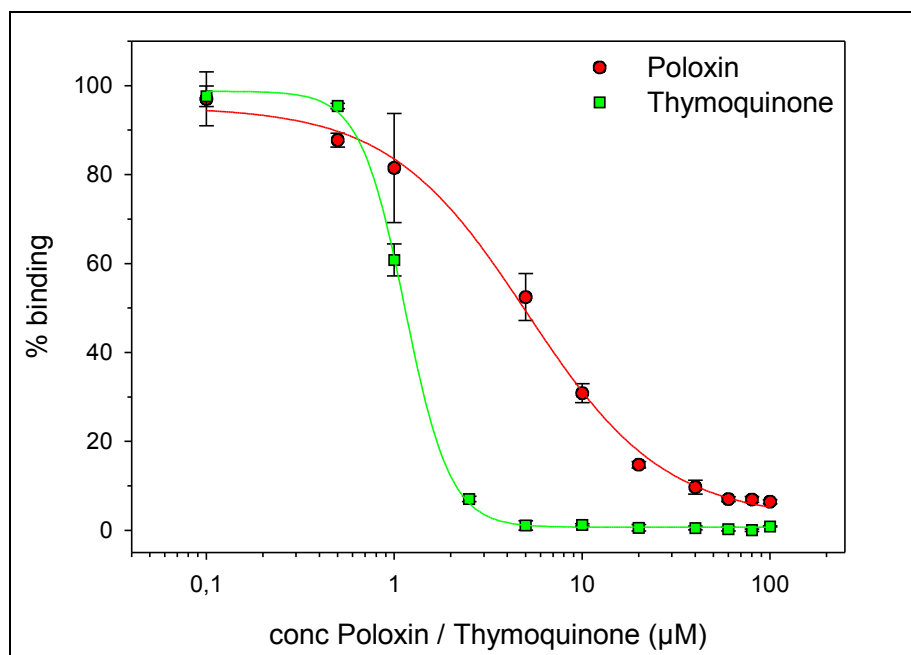


Fig. 3.10: Chemical structures of Poloxin and Thymoquinone.

In the screening and validation process, inhibition had been checked at single concentrations only. Full inhibition curves were next performed for these two compounds (Fig. 3.11). The Plk1 PBD was used at a final concentration of 45 nM.

Poloxin inhibited the Plk1 PBD with an apparent  $IC_{50}$  of  $4.8 \pm 1.3 \mu\text{M}$ . Thymoquinone was even four times more potent with an apparent  $IC_{50}$  of  $1.14 \pm 0.04 \mu\text{M}$ .



**Fig. 3.11: Inhibition curves of Poloxin and Thymoquinone.** Poloxin and Thymoquinone inhibit the Plk1 PBD. Error bars represent SD.

### 3.3 Specificity Profiles of Poloxin and Thymoquinone

Specificity and possible side effects are very important criteria for the evaluation of a small-molecule inhibitor.

The most stringent specificity controls for a compound inhibiting the Plk1 PBD would be the PBDs of the three other Plk family members, Plk2, Plk3, and Plk4. However, with regard to the differences in folding and formation of the polo-box binding cleft, the PBD of Plk4 is only distantly related (Barr *et al.*, 2004; Strebhardt & Ullrich, 2006). Furthermore there is no information on any Plk4 binding sequences available, which would be necessary for the design of fluorophore-labeled peptides for the use in FP assays. Thus the PBDs of Plk2 and Plk3 were used as the two most stringent specificity controls.

The PBD is part of the family of pS/pT-binding domains. Other pS/pT-binding domains are forkhead-associated (FHA) domains, WW domains (WW is derived from the presence of two signature tryptophane residues), and 14-3-3 proteins (Yaffe & Smerdon, 2004). A closely related family is formed by pY-binding domains, Src homology 2 (SH2) and PTB (phosphotyrosine-binding) domains are an example of this domain family.

For the acquisition of a comprehensive selectivity profile of Poloxin and Thymoquinone, it was attempted to monitor the inhibition of the PBDs of Plk2 and Plk3, of members of other pS/pT-binding domains, and of pY-binding in analogous FP-based binding assays. To this end

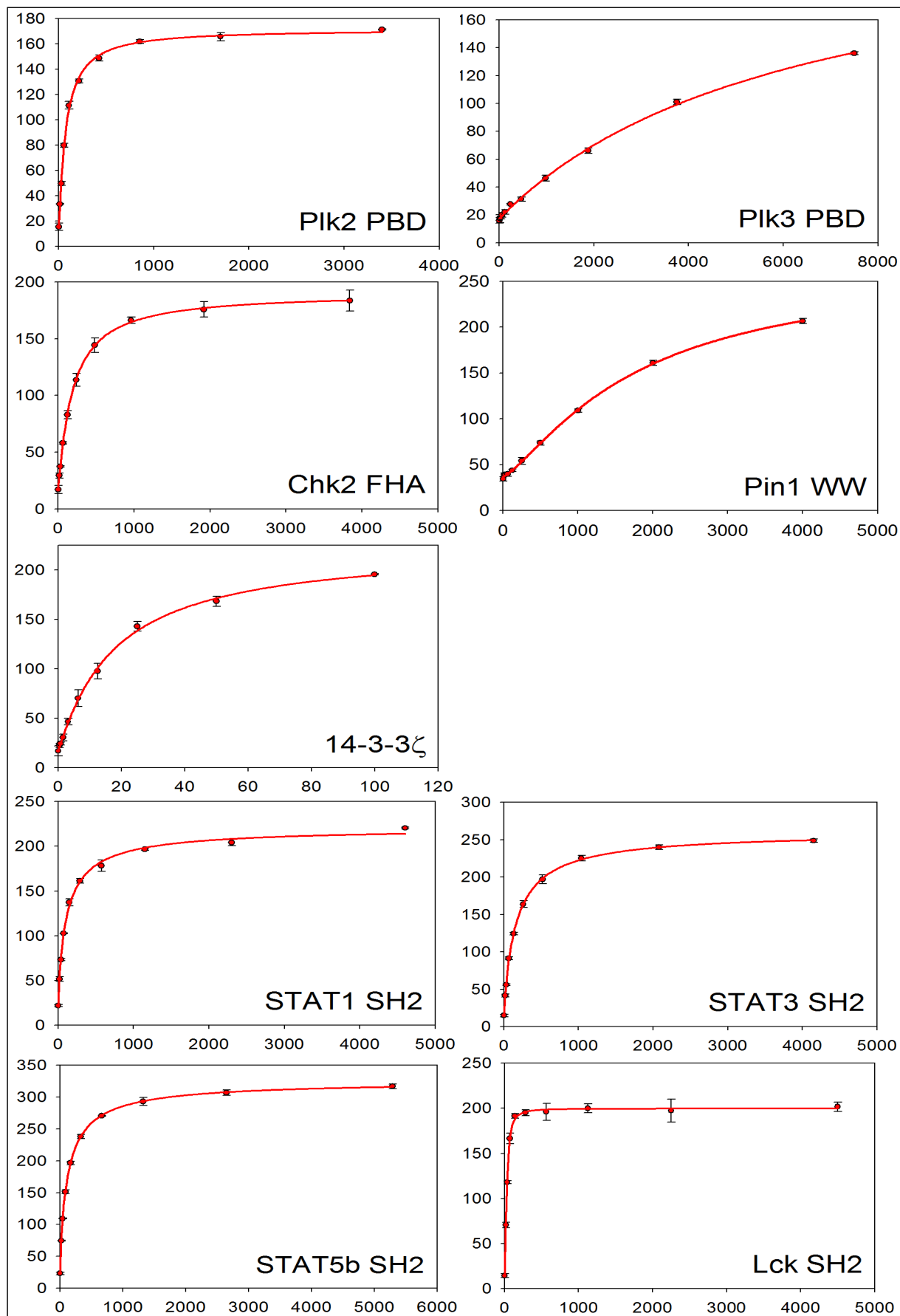


**Fig. 3.12: Binding curves for specificity controls.** Binding curves were recorded in analogous experiments as for Plk1 PBD. Y-axis: FP (mP), X-axis: conc protein (all: nM, except 14-3-3 $\zeta$ :  $\mu$ M). Error bars represent SD.

the cDNAs coding for the PBDs of Plk2 (aa 355-685; Elia *et al.*, 2003b) and Plk3 (aa 335-646; Elia *et al.*, 2003b), for the Chk2 FHA domain (aa 1-225; Durocher *et al.*, 2000) and for 14-3-3 $\zeta$  (Yaffe *et al.*, 1997b) were cloned into the pMAL-C (Plk2 and Plk3) or pET28a (Chk2 and 14-3-3 $\zeta$ ) expression vectors. After transformation, proteins were expressed in *E. coli* Rosetta™ (DE3) fused to a MPB-tag (pMAL-C) or 10x His-tag and purified via MBP-tag or His-tag affinity chromatography. The purified WW domain of Pin1 (aa 1-162; Yaffe *et al.*, 1997a) was provided by Martin Gräber (this group). The production of the SH2 domains of STAT1 (aa 135-712), STAT3 (aa 135-712), STAT5b (aa 136-704), and Lck (aa 121-226) has been described (Schust & Berg, 2004; Schust *et al.*, 2006).

As the first step, FP-based binding assays, analogous to the Plk1 PBD assay, were set up for these proteins. Figure 3.12 shows the binding curves resulting from the interaction between the proteins and fluorophore-labeled peptides.

The resulting binding curves gave the following  $K_d$ -values: Plk2 PBD:  $75 \pm 5$  nM, Plk3 PBD:  $6.2 \pm 1.6$   $\mu$ M, Chk2 FHA:  $189 \pm 6$  nM, Pin1 WW:  $1.8 \pm 0.1$   $\mu$ M, 14-3-3 $\zeta$ :  $17.8 \pm 1.8$   $\mu$ M, STAT1 SH2:  $111 \pm 11$  nM, STAT3 SH2:  $163 \pm 6$  nM, STAT5b SH2:  $119 \pm 2$  nM, Lck SH2:  $30 \pm 1$  nM. That means that all proteins except 14-3-3 $\zeta$  can be used for inhibition assays. For 14-3-3 $\zeta$  the  $K_d$ -value is too weak to guarantee a sensitive measurement of inhibitory activity.

Inhibition experiments were performed in an analogous manner to those for the Plk1 PBD (see 2.7.2). Proteins were used at the following final concentrations which correspond approximately to the  $K_d$ -values of the respective binding assays: Plk2: 130 nM, Plk3: 1875 nM, Chk2: 240 nM, Pin1: 1000 nM, STAT1: 120 nM, STAT3: 160 nM, STAT5b: 110 nM; Lck: 40 nM.

Poloxin's apparent  $IC_{50}$ -value for inhibition of the Plk1 PBD was  $4.8 \pm 1.3$   $\mu$ M. The  $IC_{50}$  values for the PBDs of Plk2 and Plk3 as the most stringent specificity controls were approximately 4-fold and 11-fold higher (Plk2 PBD:  $18.7 \pm 1.8$   $\mu$ M; Plk3 PBD:  $53.9 \pm 8.5$   $\mu$ M). The other protein-protein interaction domains were not significantly inhibited, so Poloxin appears to be highly specific (Fig. 3.13).

Thymoquinone inhibited the function of the Plk1 PBD even more potently than Poloxin with an apparent  $IC_{50}$  of  $1.14 \pm 0.04$   $\mu$ M, but displayed a less desirable specificity profile because it also affected the PBDs of Plk2 ( $1.90 \pm 0.10$   $\mu$ M) and Plk3 ( $22.4 \pm 0.8$   $\mu$ M), other subtypes of pS/pT-binding domains (Chk2 FHA:  $3.9 \pm 0.6$   $\mu$ M and Pin1 WW:  $20.4 \pm 0.9$   $\mu$ M), and the pY-binding SH2 domain of STAT3 ( $10.9 \pm 0.2$   $\mu$ M) (Fig. 3.14).

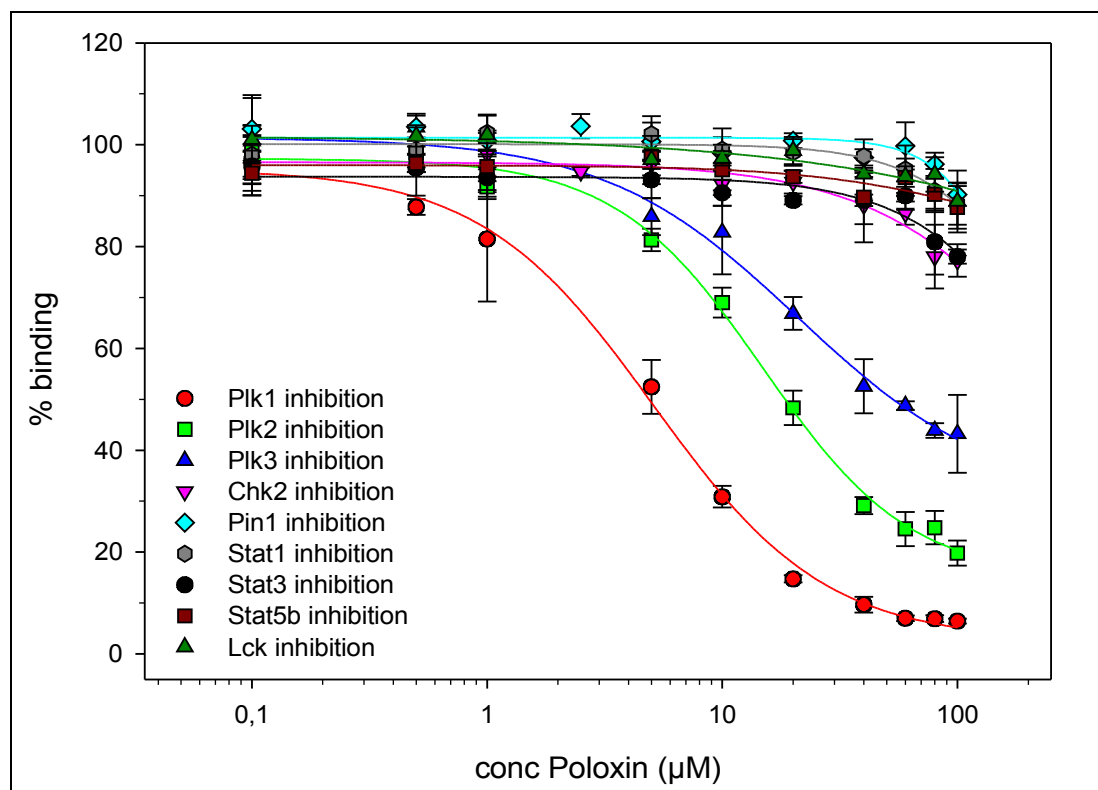


Fig. 3.13: Specificity profile for Poloxin. Error bars represent SD.

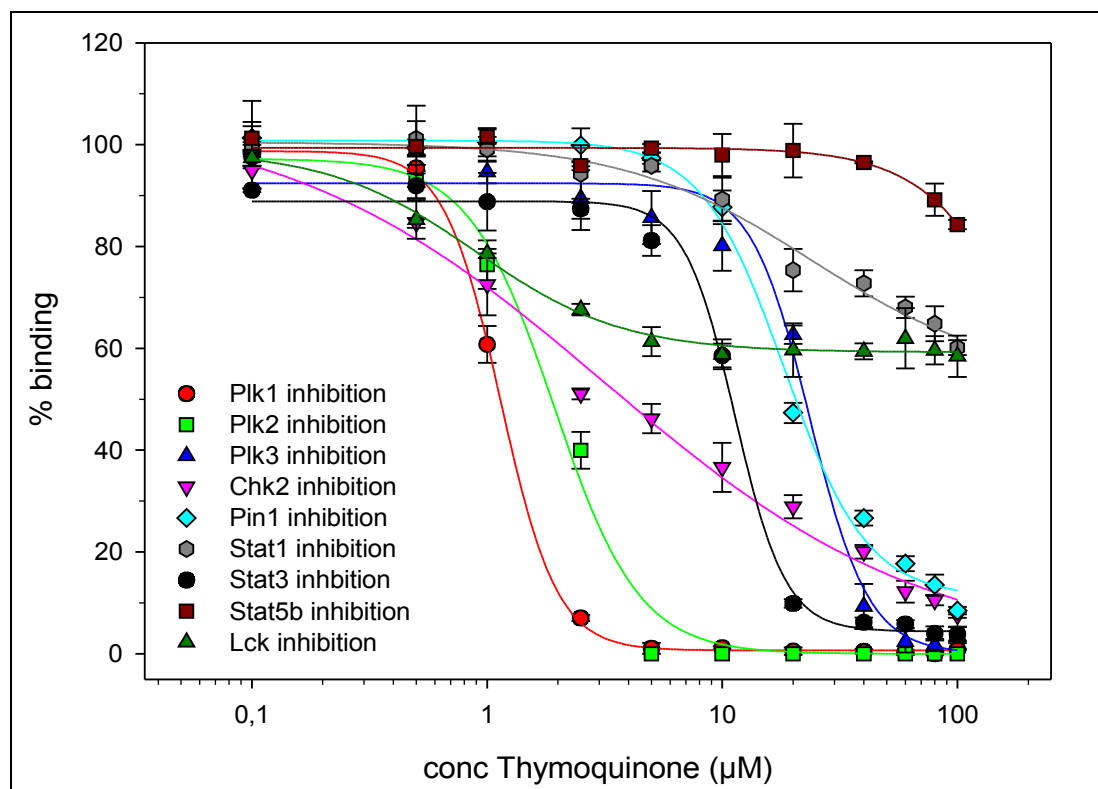


Fig. 3.14: Specificity profile for Thymoquinone. Error bars represent SD.

In summary, both Poloxin and Thymoquinone inhibit the Plk1 PBD. Poloxin shows a clear preference for the PBD family and displays the highest inhibitory activity against Plk1.

Thymoquinone inhibits Plk1 approximately 4-fold better than Poloxin, but also shows activity against several other protein-binding domains.

### 3.4 Cellular Assays

#### 3.4.1 Transfection of the Plk1 PBD

Before analyzing the cellular effects of Poloxin and Thymoquinone, an adequate positive control had to be found to indicate the consequences of *in vivo* Plk1 PBD inhibition.

For the study of Plk1 PBD inhibition, the differentiation between PBD-dependent (whereby phosphorylation by Plk1 requires pre-localization to substrates via the PBD) and PBD-independent (whereby Plk1 can phosphorylate substrates without specific pre-localization) functions is very important (Hanisch *et al.*, 2006). A PBD-specific inhibitor would block the PBD from binding to pS/pT-sequences on substrate proteins. The kinase domain would not be affected and could still perform all its functions. Therefore only PBD-specific functions would be inhibited (Fig. 3.15).

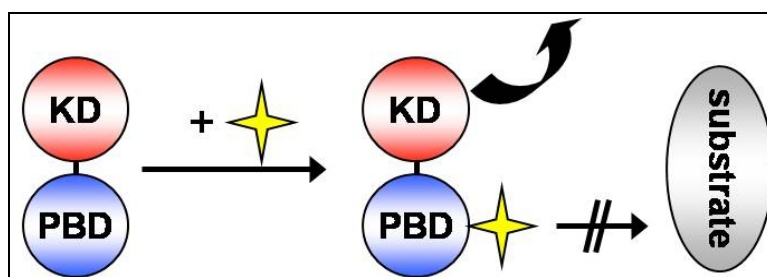


**Fig. 3.15: Scheme depicting the function of a PBD-specific inhibitor.** A PBD-specific inhibitor (yellow star) would block the PBD of endogenous Plk1 from binding to its substrates, the kinase domain (KD) could still carry out all PBD-independent phosphorylations (black curved arrow).

The application of siRNA (Spankuch-Schmitt *et al.*, 2002b; Liu & Erikson, 2003), one of the most common techniques for protein inhibition, is not appropriate in this situation because endogenous Plk1 would be completely eliminated. By this all Plk1 functions are inhibited. The same is true for using one of the described Plk1 kinase domain inhibitors (Stevenson *et al.*, 2002; Liu *et al.*, 2005; Gumireddy *et al.*, 2005; McInnes *et al.*, 2006; Peters *et al.*, 2006; Lansing *et al.*, 2007; Lenart *et al.*, 2007; Steegmaier *et al.*, 2007; Santamaria *et al.*, 2007). Endogenous Plk1 could still bind to its substrates, but all phosphorylations are blocked.

However, when ectopically expressing the PBD only, all cellular Plk1 binding sites would be blocked and binding of endogenous Plk1 is inhibited. The kinase domain would still be active. Since this state exactly resembles the situation, a PBD-specific inhibitor would cause, the

ectopic expression of the PBD was chosen as a positive control.

Figure 3.16 summarizes the modes of action of the different types of Plk1 inhibition.

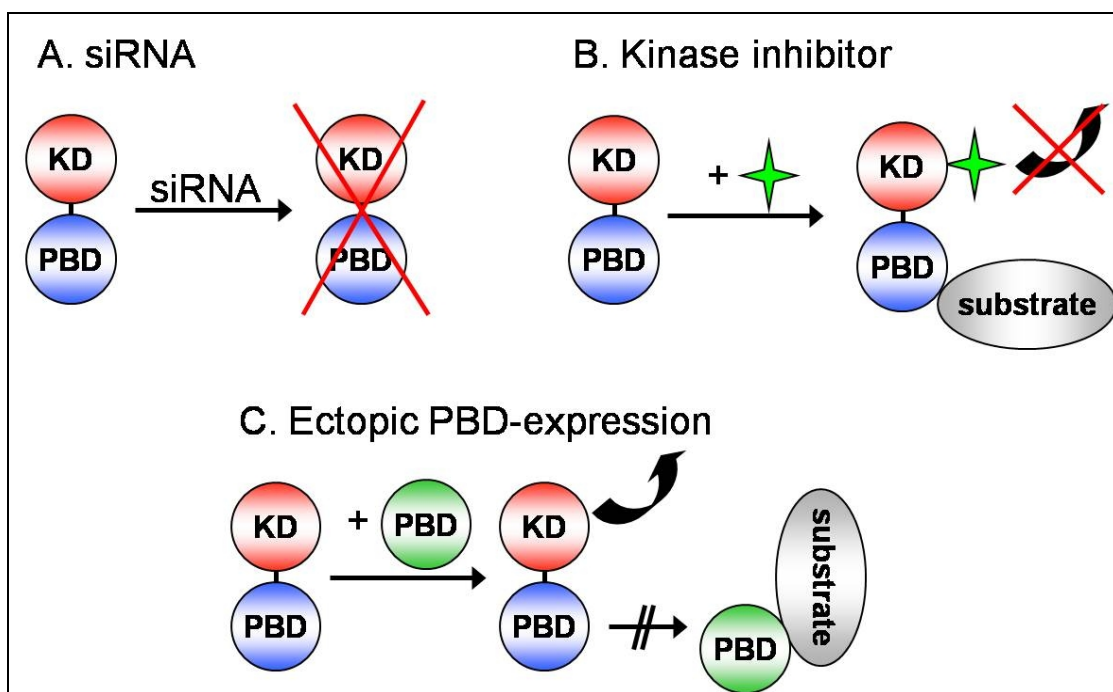
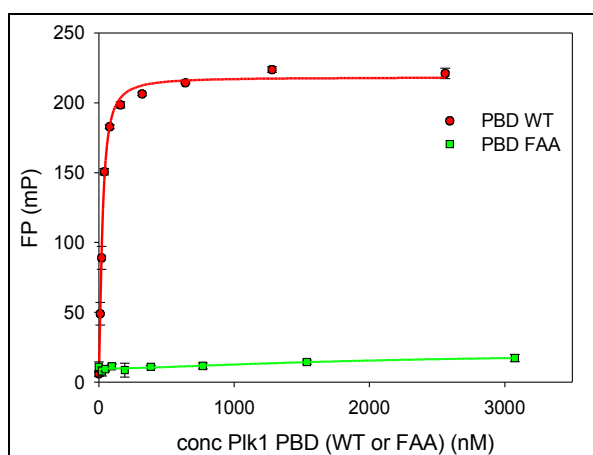


**Fig. 3.16: Scheme depicting the inhibition of Plk1 by siRNA, kinase inhibitors and ectopic PBD-expression.** A. siRNA and B. kinase inhibitors (green star) eliminate all Plk1 functions. C. Ectopically expressed PBD (green PBD) blocks PBD-dependent functions only. KD: kinase domain. Phosphorylation reactions are marked by black curved arrows.

The cDNA sequence coding for the Plk1 PBD (aa 326-603; PBD WT; Elia *et al.*, 2003a) was cloned into the vector pCS2-MT and transfected into HeLa cells. As a negative control, a PBD-triple mutant containing the amino acid exchanges W414F, H538A and K540A (PBD FAA) was cloned into the same vector and used in HeLa cells. The three amino acids W414, H538 and K540 contact the phosphogroup within the binding motif of substrates. The mutant form is not able to bind to Plk1 substrates any more (Hanisch *et al.*, 2006). To verify the inability of the mutant PBD version to bind to substrates, the PBD FAA was cloned analogously to the wildtype PBD (see 3.1.1) and tested in an FP binding assay. Figure 3.17 shows the binding inactivity of the triple-mutated PBD.

**Fig. 3.17: Binding curves of PBD WT and PBD FAA.** Error bars represent SD.



Transfection reactions were monitored via Western blotting (Fig 3.18).

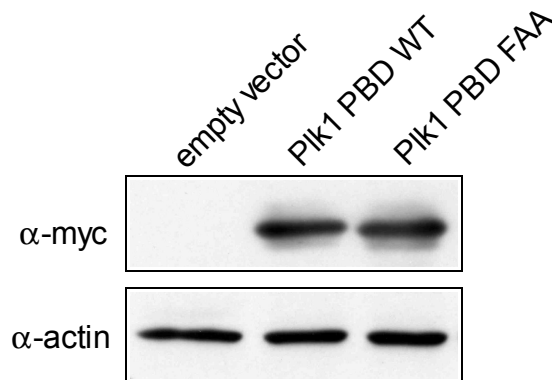


**Fig. 3.18: Western Blot monitoring PBD transfection.** HeLa cells were transfected with the empty vector, wildtype PBD (PBD WT) and a triple mutant form (PBD FAA). Cell lysates were probed for myc-tagged PBDs. Actin levels were used as loading control.

### 3.4.1.1 PBD-Expression Increases the Mitotic Index

48 hours after transfection the mitotic index of the different samples was determined. As previously shown in the literature (Hanisch *et al.*, 2006; Jiang *et al.*, 2006, Fink *et al.*, 2007), ectopic expression of the PBD led to an approximately 3-fold increase of mitotic cells ( $22.5 \pm 1.2$  % in comparison to  $6.7 \pm 0.7$  % in mock-transfected cells). Transfection with the mutated PBD led to no significant change of the mitotic index ( $10.0 \pm 1.0$  %) (Fig. 3.19).

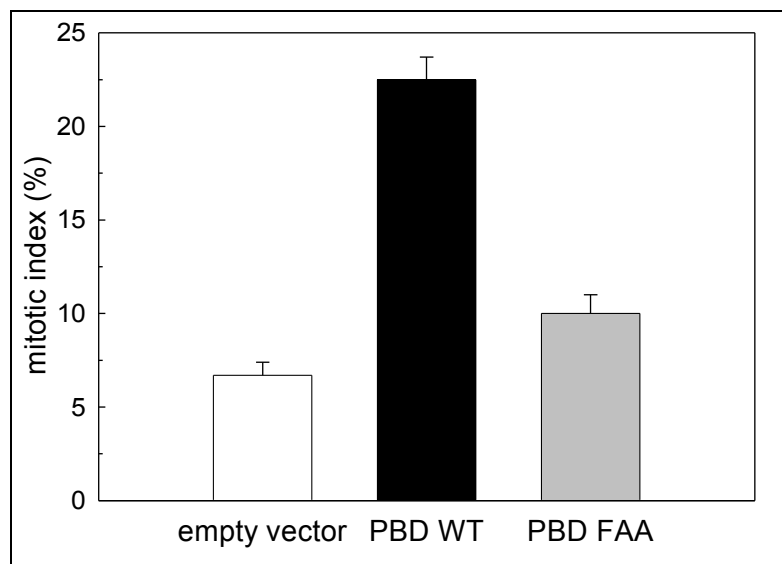


**Fig. 3.19: Mitotic indices for transfected HeLa cells.** Error bars represent SD.

### 3.4.1.2 PBD-Expression Causes a Prometaphase-Arrest

To elucidate the exact timepoint of the mitotic arrest, the distribution of mitotic cells over the different phases of mitosis was analyzed (Fig. 3.20).

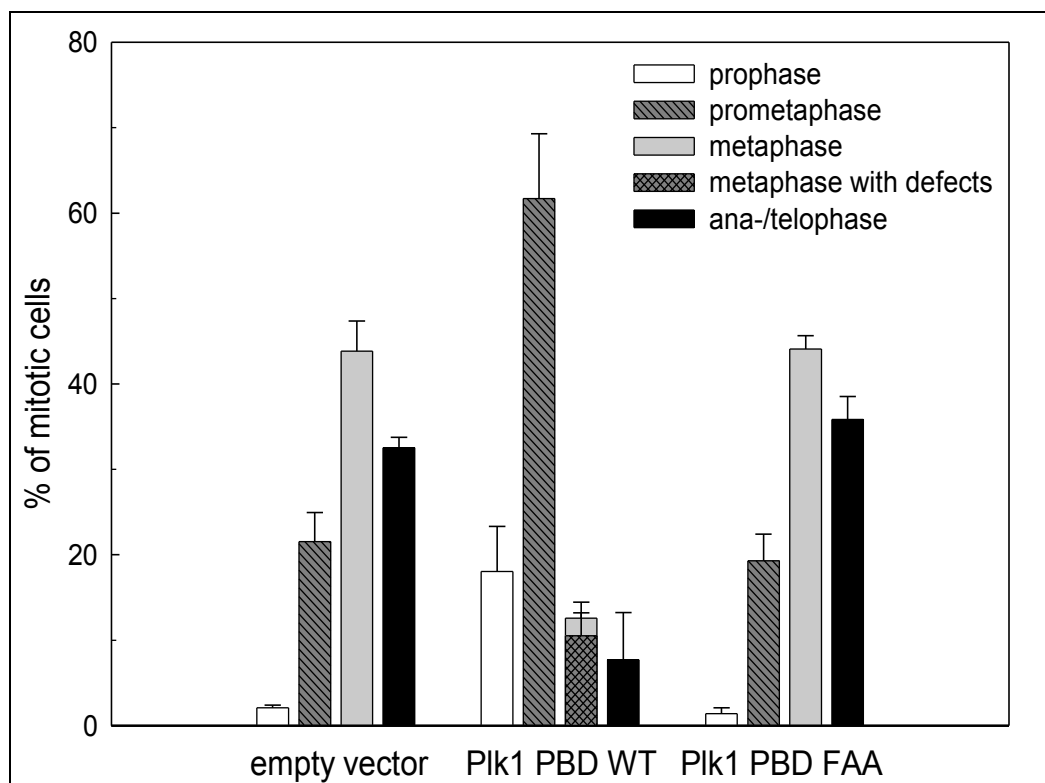


**Fig. 3.20: Mitotic phases for transfected HeLa cells.** “Metaphase with defects” describes a subpopulation of metaphase cells. Error bars represent SD.

Expression of the PBD caused a dramatic increase in prophase and prometaphase cells in comparison to cells transfected with empty vector, while the percentage of metaphase and ana-/telophase cells was significantly decreased. Furthermore approximately 80% of metaphase cells in PBD-transfected cells showed chromosome congression defects, a phenotype in which single or whole bundles of chromosomes are not properly congressed to the metaphase plate. Expression of the mutated PBD showed a similar phase profile to empty vector transfection (Tab. 3.2).

**Tab. 3.2: Quantification of phase distribution for transfected HeLa cells.**

	Prophase	Prometaphase	Metaphase	Metaphase with defects	Ana-/telophase
<b>Empty vector</b>	2.1 ± 0.3 %	21.5 ± 3.4 %	43.8 ± 3.5 %	-	32.5 ± 1.2 %
<b>Plk1 PBD WT</b>	18.0 ± 5.3 %	61.7 ± 7.6 %	12.6 ± 1.8 %	10.5 ± 2.7 %	7.7 ± 5.6 %
<b>Plk1 PBD FAA</b>	1.4 ± 0.7 %	19.3 ± 3.1 %	44.1 ± 1.6 %	-	35.9 ± 2.7 %

### 3.4.1.3 Phenotype of PBD-transfected Cells

No abnormalities were observed with respect to bipolar spindle formation and chromosome separation in empty vector and Plk1 PBD FAA transfection samples, as has been described

before (Hanisch *et al.*, 2006). However, most cells ectopically expressing the wildtype PBD were arrested in a prometaphase-state due to chromosome congression defects and clear metaphase plates were rarely observed (Fig. 3.21).

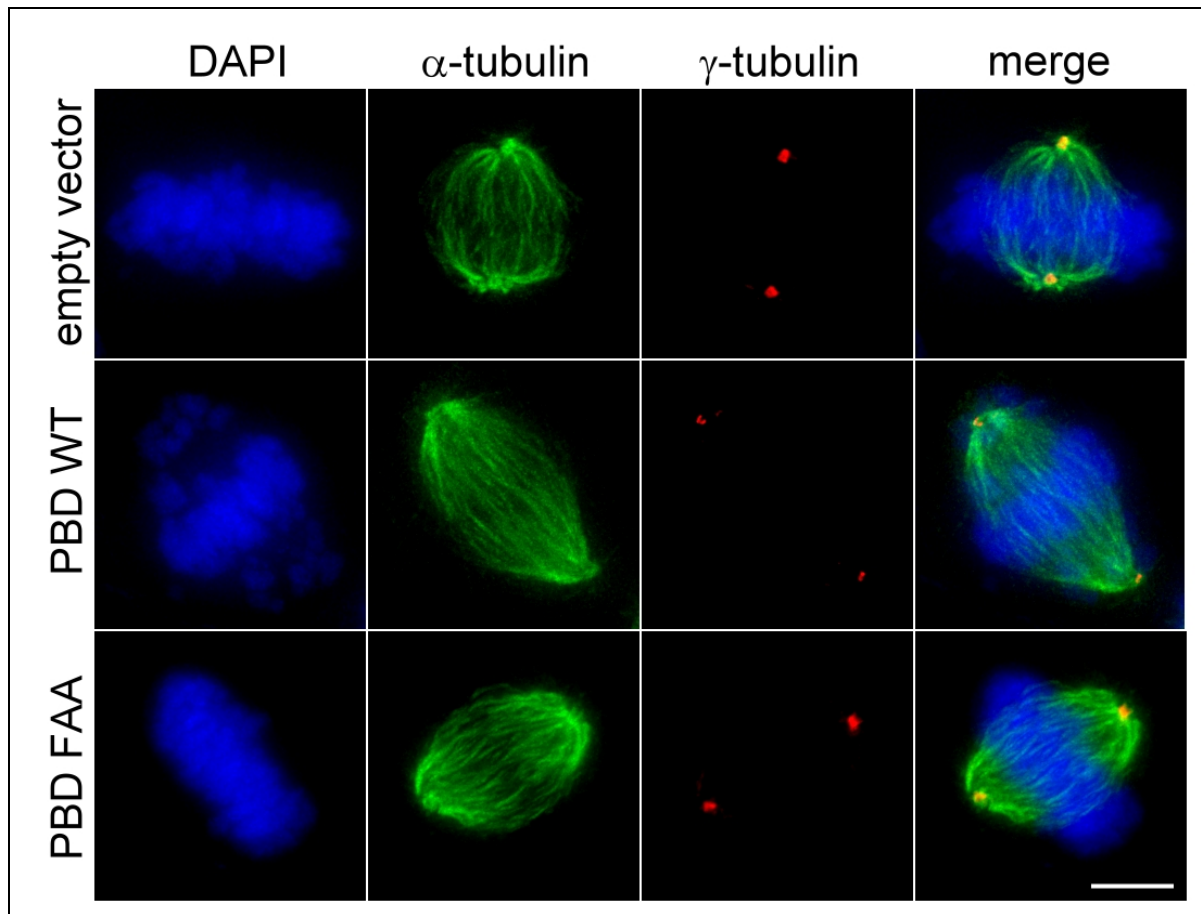


**Fig. 3.21: Phenotype caused by PBD-expression.** DAPI: DNA;  $\alpha$ -tubulin: spindles;  $\gamma$ -tubulin: centrosomes. Scale bar represents 5  $\mu$ m.

#### 3.4.1.4 Plk1 Localization in PBD-transfected Cells

During mitosis, Plk1 localizes to various cellular structures. In prometaphase and metaphase, Plk1 localizes to centrosomes and kinetochores (Barr *et al.*, 2004). Since ectopic expression of the PBD should mislocalize endogenous Plk1 from its natural binding sites, the intensity of Plk1-dependent staining on centrosomes was analyzed. The antibody used was raised against the N-terminus of Plk1, so that only endogenous Plk1, and not the transfected PBD is detected. Plk1 localized to centrosomes is clearly visible in empty vector and Plk1 PBD FAA samples by comparison with the colocalized  $\gamma$ -tubulin staining. PBD WT-transfected cells showed a reduction of Plk1-dependent staining on centrosomes. The antibody used displayed high background staining which accounts for the large number of green “dots” in the Plk1 staining (Fig. 3.22).

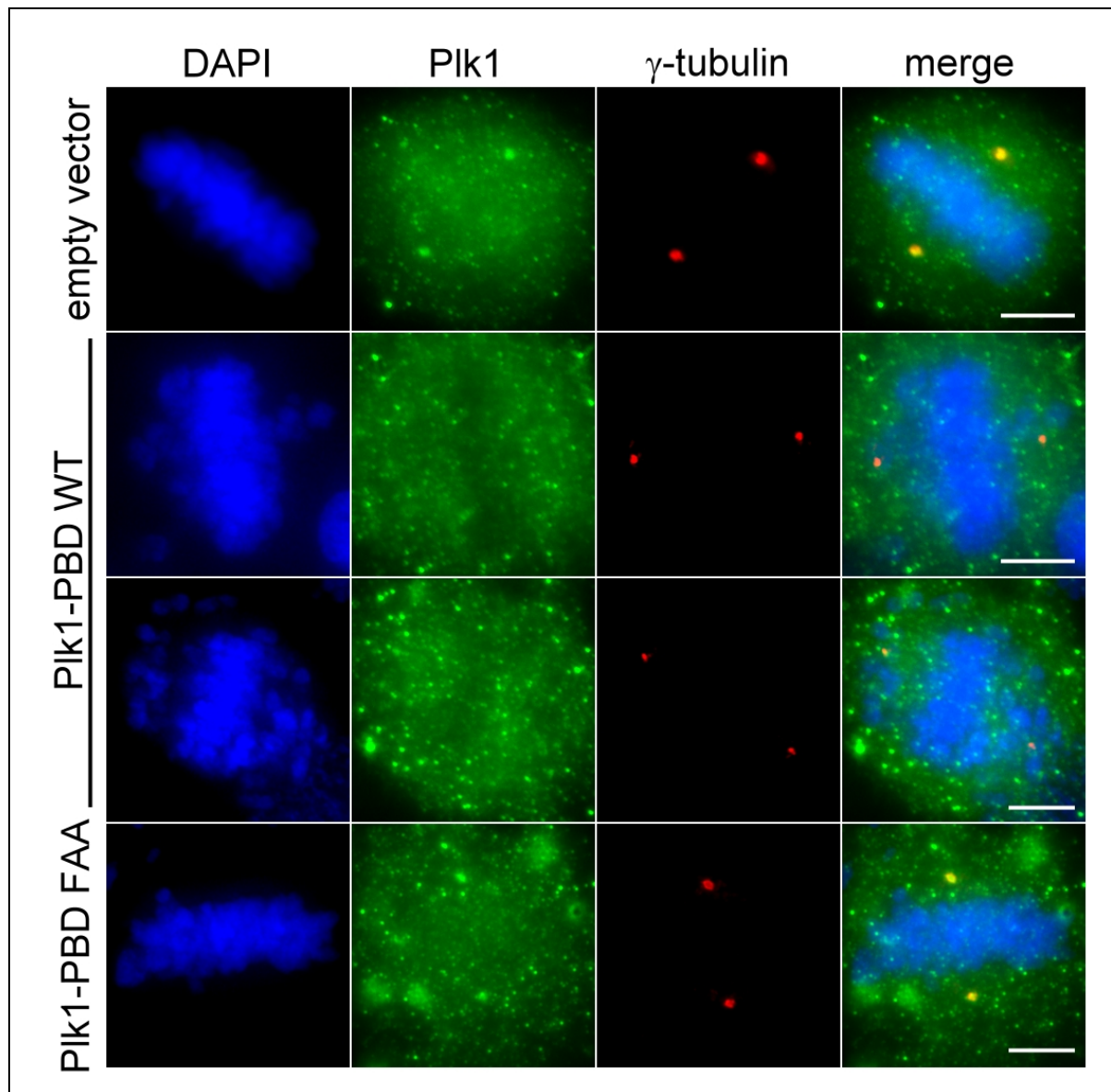


Fig. 3.22: Plk1 localization in PBD-transfected cells. DAPI: DNA;  $\gamma$ -tubulin: centrosomes. Scale bars represent 5  $\mu$ m.

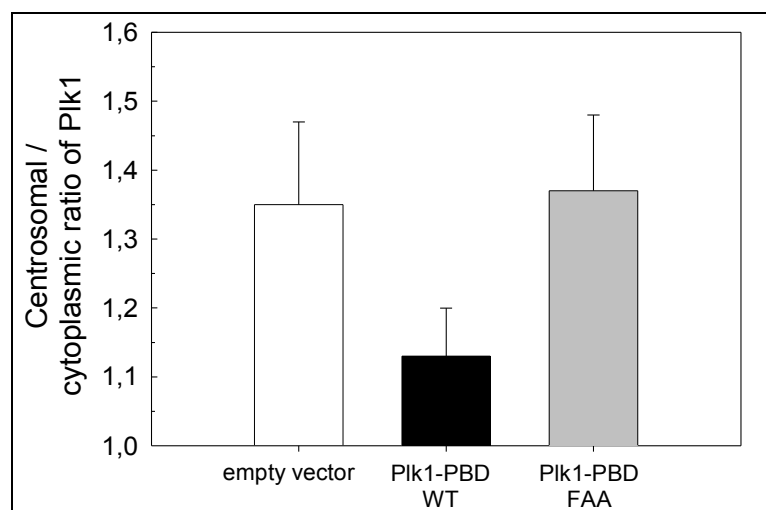


Fig. 3.23: Quantification of centrosomal Plk1 localization. Error bars represent SD.

Quantification of the centrosomal/cytoplasmic ratio of Plk1 staining showed a significant decrease with ectopic PBD-expression (empty vector:  $1.35 \pm 0.12$ ; Plk1 PBD WT:  $1.13 \pm 0.07$ ; Plk1 PBD FAA:  $1.37 \pm 0.11$ ) (Fig. 3.23).

### 3.4.2 Effects of Poloxin and Thymoquinone

#### 3.4.2.1 Determination of the Timepoint for Analysis of Effects

To investigate the cellular effects caused by Poloxin and Thymoquinone, an adequate timepoint for analysis had to be determined. Since the two compounds are expected to lead to a mitotic arrest, a timepoint should be chosen at which control cells have already left mitosis. To this end, cells were synchronized in G1/S phase with aphidicolin and then released into aphidicolin-free medium with 0.5 % DMSO. The course of mitosis was monitored by determination of the mitotic index at various timepoints (Tab. 3.3).

**Tab. 3.3: Course of mitosis after release from G1/S arrest.**

Time after release	5 h	6 h	7 h	8 h	9 h	10 h	11 h	12 h	13 h	14 h
Mitotic index	< 5%	< 5%	5-10%	10-20%	20-25%	20-25%	10%	< 5%	< 5%	< 5%

Most cells reached mitosis within 8-10 hours after release from G1/S arrest. After 12 hours virtually all cells had progressed through mitosis. Therefore a release of 14 hours was chosen, because by this timepoint a clear difference between control cells and mitotically arrested cells should be visible.

#### 3.4.2.2 Influence of Poloxin and Thymoquinone on the Mitotic Index

For the analysis of any effects of Poloxin and Thymoquinone on the mitotic index, cells were synchronized in G1/S phase by aphidicolin and then released into aphidicolin-free medium. Cells were fixed for analysis 14 hours later. Compounds were added at different timepoints after the release. Figure 3.24 depicts the experimental procedure.

In the first experiment cells were released into aphidicolin-free medium containing compounds. Both Poloxin and Thymoquinone caused a dose-dependent increase of the mitotic index of HeLa cells, as detected by visual inspection of cells under the microscope (Tab. 3.4 and Fig. 3.25).

Most HeLa control cells treated with DMSO reached mitosis 8-10 hours after release from aphidicolin-induced G1/S arrest. Protein levels of Plk1 are known to increase through G2-phase, peak in M-phase, and sharply decrease on exit from mitosis (Barr *et al.*, 2004;

Strebhardt & Ullrich, 2006).

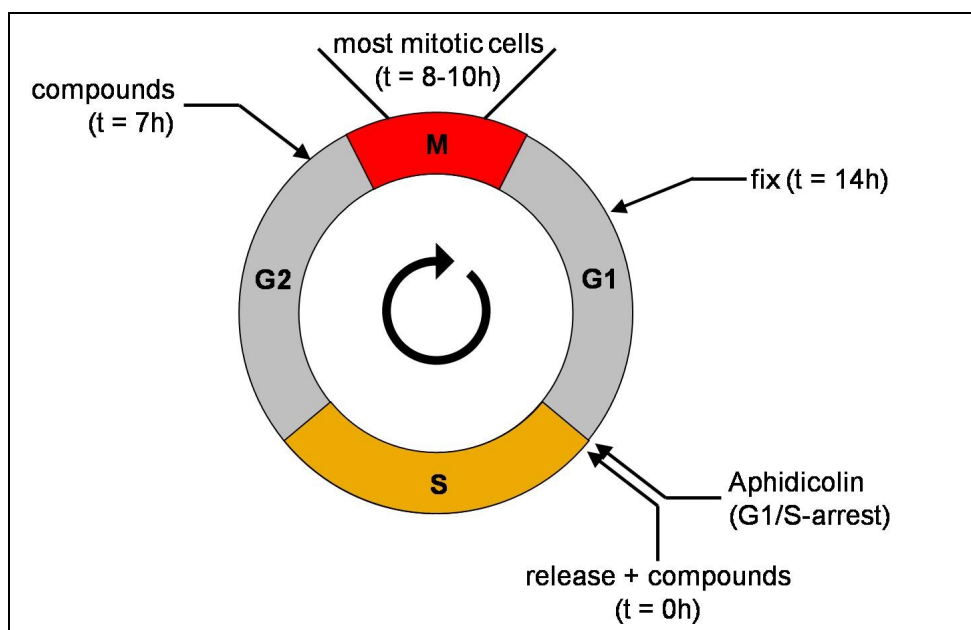


**Fig. 3.24:** Scheme depicting the experimental setup for detection of the mitotic index. Test of the effects of Poloxin and Thymoquinone on the mitotic index.

In order to rule out that the increase in the mitotic index observed 14 hours after release from G1/S arrest was caused by a delay in progression through S-phase, in which Plk1-levels are low, cells were released into inhibitor-free media for the first 7 hours, and treated with media containing the test compounds for the next 7 hours. Mitotic indices were not decreased under these experimental conditions, arguing against the possibility of off-target effects in S-phase as the cause of the mitotic arrest in HeLa cells. Rather, a slight increase in the mitotic indices was observed when the compounds were added 7 hours after G1/S-release, possibly because the later addition of the compounds limited the potential for their degradation or absorption by the components of the tissue culture media (Tab. 3.4 and Fig. 3.25).

**Tab. 3.4:** Mitotic indices caused by Poloxin and Thymoquinone. Compounds were added at given timepoints.

	0 h	7 h	0 h and 7 h
<b>DMSO</b>	4.7 ± 1.2 %	3.3 ± 0.8 %	3.3 ± 0.5 %
<b>Poloxin 5 µM</b>	5.4 ± 0.7 %	3.8 ± 0.6 %	4.9 ± 1.0 %
<b>Poloxin 10 µM</b>	6.5 ± 1.2 %	7.9 ± 0.5 %	11.5 ± 3.4 %
<b>Poloxin 25 µM</b>	15.0 ± 1.5 %	19.5 ± 5.2 %	25.8 ± 3.3 %
<b>Thymoquinone 5 µM</b>	4.6 ± 1.9 %	3.2 ± 1.0 %	4.0 ± 0.8 %
<b>Thymoquinone 10 µM</b>	4.8 ± 1.2 %	5.8 ± 0.6 %	7.2 ± 1.9 %
<b>Thymoquinone 25 µM</b>	8.9 ± 1.6 %	13.9 ± 3.6 %	11.6 ± 2.4 %

To ensure that all cells, including those entering mitosis earlier than 7 hours after G1/S-release, were exposed to the test compounds *before* mitotic entry, and that the cells were continuously exposed to approximately equal concentrations of intact test compounds, the inhibitors were added at the time of the G1/S-release, followed by an exchange of tissue culture media with media containing fresh compounds 7 hours later. Again, both compounds increased the mitotic index in a dose-dependent manner. Furthermore the strongest effects were seen with this mode of compound addition (Tab. 3.4 and Fig. 3.25). Therefore this experimental setup was used for all further experiments.

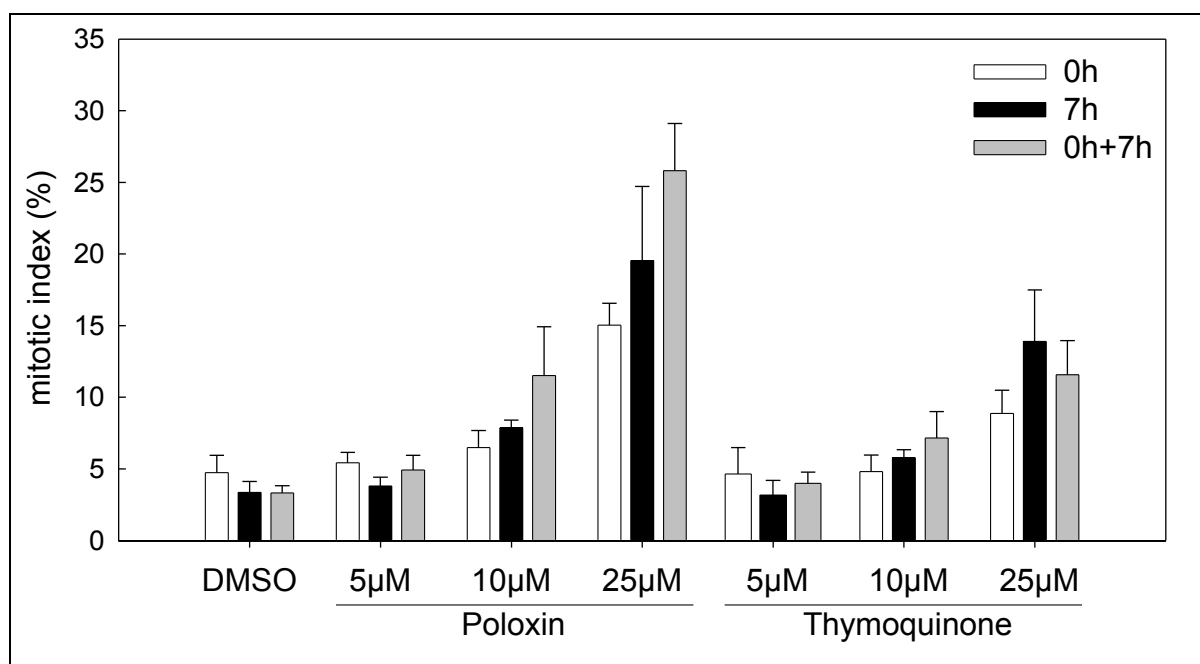


**Fig. 3.25: Mitotic indices caused by Poloxin and Thymoquinone.** Compounds were added at the given timepoints. Error bars represent SD.

Thus, even though Thymoquinone was about 4-5 times more active than Poloxin *in vitro*, the compounds' efficacy to induce mitotic arrest was comparable at a concentration of 10 µM, possibly because Thymoquinone's less selective mode of action decreased the effective concentration available for inhibiting the Plk1 PBD. At 25 µM, Thymoquinone displayed toxic side effects.

### 3.4.2.3 The Mitotic Marker Protein Phospho-Cdc25C

Another way to detect a mitotic arrest is the analysis of mitotic markers. The phosphatase Cdc25C is phosphorylated several times on entry into mitosis (Strausfeld *et al.*, 1994). This hyper-phosphorylation can be monitored via an upshifted band in a Western blot (Schmidt *et al.*, 2006). Lysates of cells treated with 25 µM of Poloxin in an analogous order as for the

determination of mitotic indices were probed for the presence of a shifted band. In this experiment, aphidicolin (blocks cells in G1/S phase) was used as a negative and nocodazole (blocks cells in mitosis) as a positive control (Fig. 3.26). Thymoquinone was not included in this test, because the toxic side effects at 25  $\mu\text{M}$  were not compatible with the assay setup for the Western blot analysis. Lysates of cells treated with 25  $\mu\text{M}$  of Poloxin show a shifted Cdc25C band, whereas no band is visible for DMSO treated control cells. This result also shows the mitotic arrest caused by Poloxin.

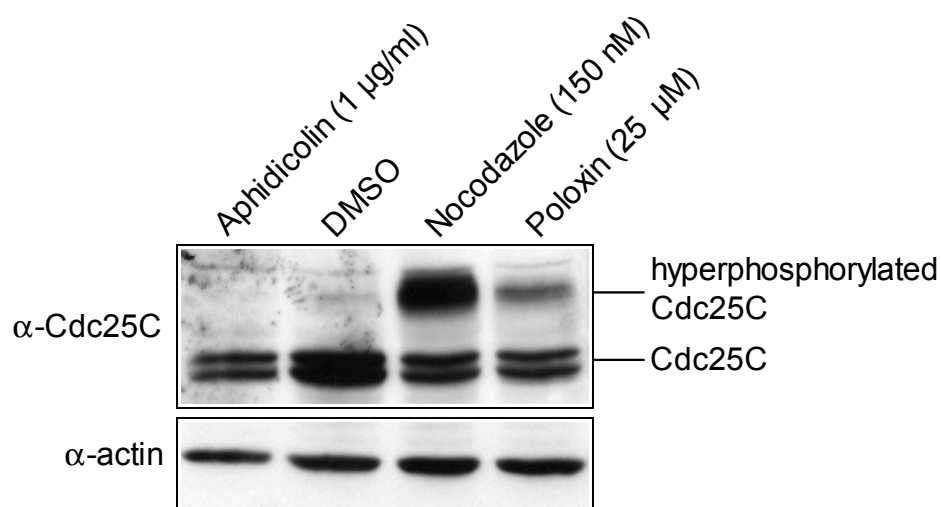


**Fig. 3.26: Cdc25C hyperphosphorylation as marker for mitotic arrest.** Mitotic Cdc25C is phosphorylated several times, resulting in an upshifted Cdc25C band. Actin levels were used as loading control.

#### 3.4.2.4 Phase-Distribution of Cells Arrested by Poloxin and Thymoquinone

Analysis of the mitotic phase distribution revealed a dose-dependent increase in cells arrested in prometaphase, and decrease in ana-/telophase cells in the presence of Poloxin and Thymoquinone. Amongst the cells that were arrested in a metaphase-like state, a dose-dependent increase of cells in which single or multiple chromosomes had failed to congress to the metaphase plate was visible. The percentage of metaphase cells with chromosome congression defects increased from 7% in the DMSO control to 12%, 21%, and 54% in the presence of 5  $\mu\text{M}$ , 10  $\mu\text{M}$ , and 25  $\mu\text{M}$  Poloxin, respectively. A lesser increase in the number of metaphase cells with chromosome congression defects was observed for Thymoquinone (9%, 16%, and 30% in the presence of 5  $\mu\text{M}$ , 10  $\mu\text{M}$ , and 25  $\mu\text{M}$  Thymoquinone), indicative of a lower degree of intracellular specificity as compared to Poloxin (Fig. 3.27 and Tab. 3.5).

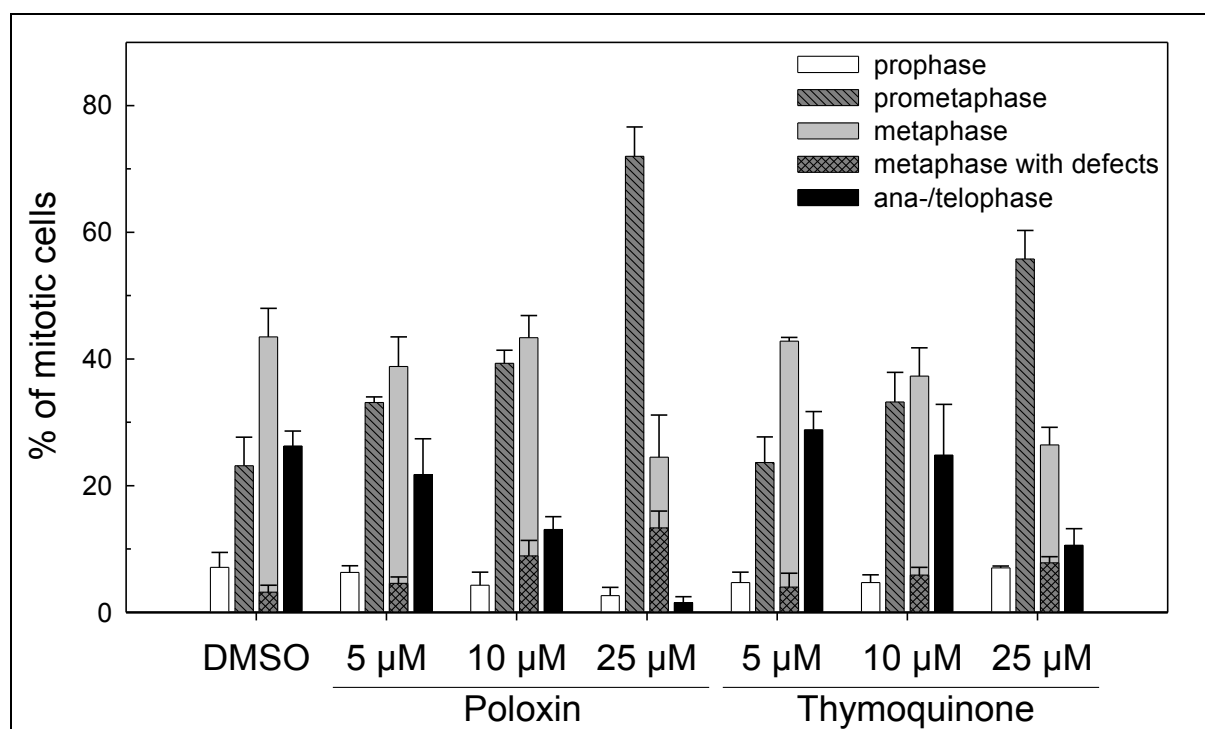


Fig. 3.27: Mitotic phases for HeLa cells treated with Poloxin and Thymoquinone. “Metaphase with defects” describes a subpopulation of metaphase cells. Error bars represent SD.

Tab. 3.5: Quantification of phase distribution for Poloxin and Thymoquinone treated HeLa cells.

	Prophase	Prometaphase	Metaphase	Metaphase with defects	Ana-/telophase
<b>DMSO</b>	7.1 ± 2.4 %	23.2 ± 4.5 %	43.5 ± 4.5 %	3.2 ± 1.1 %	26.3 ± 2.4 %
<b>Poloxin 5 μM</b>	6.3 ± 1.1 %	33.1 ± 0.9 %	38.8 ± 4.7 %	4.6 ± 1.0 %	21.7 ± 5.6 %
<b>Poloxin 10 μM</b>	4.3 ± 2.1 %	39.3 ± 2.0 %	43.3 ± 3.5 %	8.9 ± 2.4 %	13.1 ± 2.0 %
<b>Poloxin 25 μM</b>	2.6 ± 1.3 %	72.0 ± 4.6 %	24.5 ± 6.6 %	13.3 ± 2.7 %	1.5 ± 0.9 %
<b>Thymoquinone 5 μM</b>	4.7 ± 1.6 %	23.7 ± 4.0 %	42.8 ± 0.6 %	4.0 ± 2.2 %	28.8 ± 2.9 %
<b>Thymoquinone 10 μM</b>	4.7 ± 1.2 %	33.2 ± 4.7 %	37.3 ± 4.5 %	5.9 ± 1.2 %	24.8 ± 8.0 %
<b>Thymoquinone 25 μM</b>	7.0 ± 0.3 %	55.8 ± 4.5 %	26.4 ± 2.8 %	7.8 ± 1.0 %	10.6 ± 2.6 %

The similarity of the phenotypic effect exerted by Poloxin to that of PBD overexpression in a strongly dose-dependent manner suggests that Poloxin and Thymoquinone interfere with correct localization of Plk1 by targeting the Plk1 PBD as the dominant mode of action.

### 3.4.2.5 Phenotype Caused by Poloxin and Thymoquinone Treatment of Cells

As seen for overexpression of the PBD, Poloxin and Thymoquinone arrested cells in prometaphase due to chromosome congression defects and incorrectly formed metaphase plates (Fig 3.28).

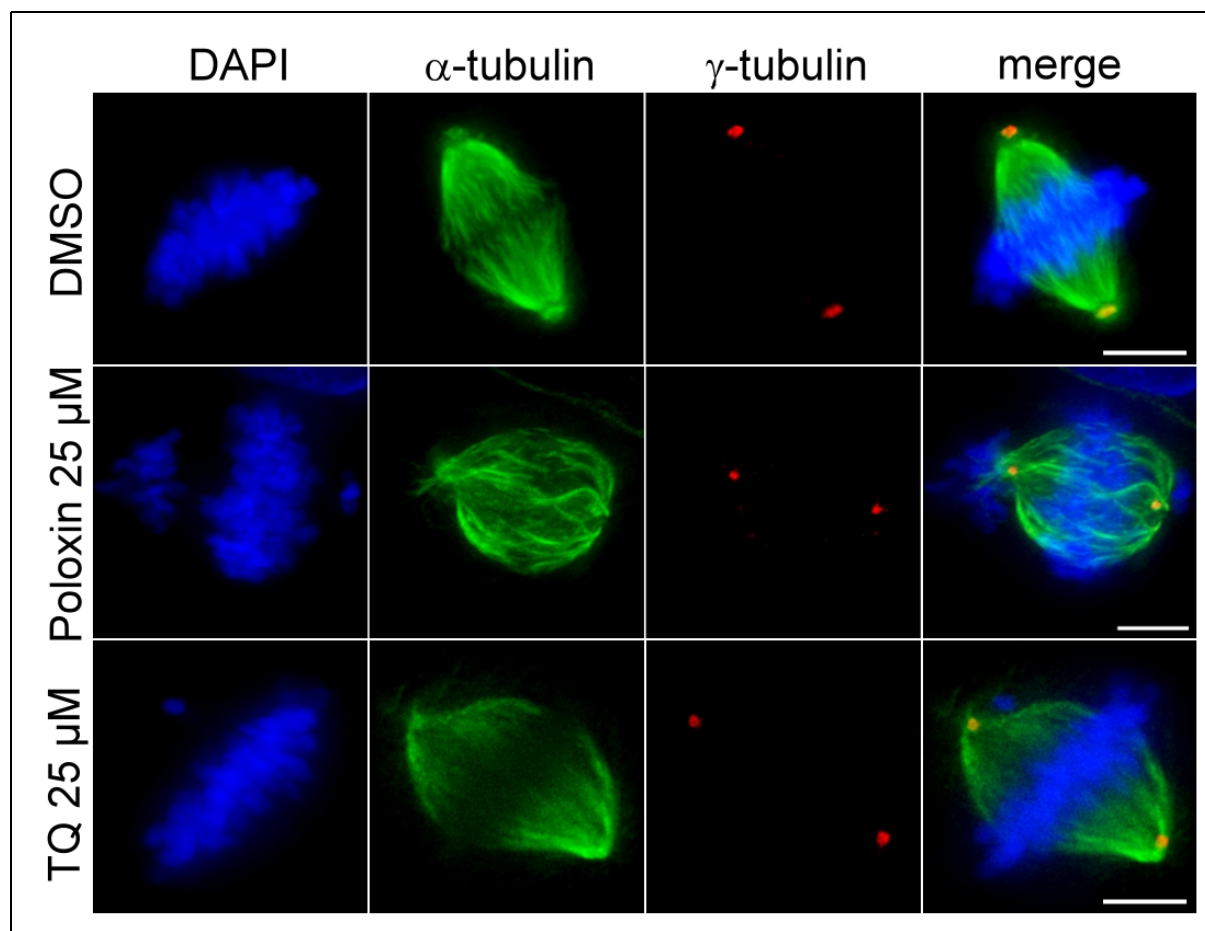
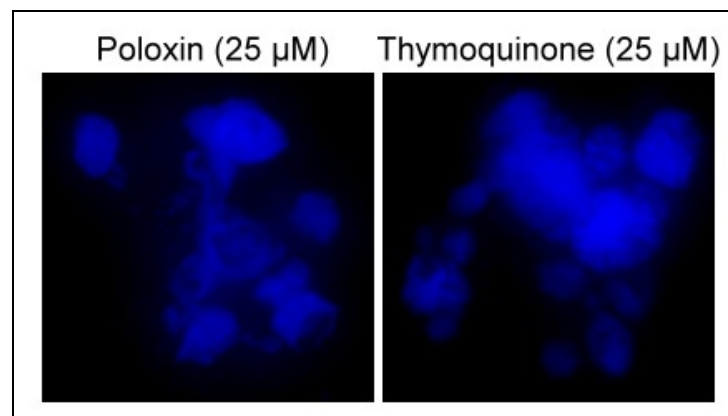


**Fig. 3.28: Phenotype caused by Poloxin and Thymoquinone.** DAPI: DNA;  $\alpha$ -tubulin: spindles;  $\gamma$ -tubulin: centrosomes. Scale bars represent 5  $\mu$ m.

### 3.4.2.6 Apoptosis

Inhibition of Plk1 functions by small-molecule inhibitors of its catalytic activity (Stevenson *et al.*, 2002; Liu *et al.*, 2005; Gumireddy *et al.*, 2005; McInnes *et al.*, 2006; Peters *et al.*, 2006; Lansing *et al.*, 2007; Lenart *et al.*, 2007; Steegmaier *et al.*, 2007; Santamaria *et al.*, 2007) or RNAi-mediated depletion (Spankuch-Schmitt *et al.*, 2002a; Liu & Erikson, 2003) induces apoptosis in cancer cells. In order to investigate whether inhibition of the intracellular Plk1 PBD by Poloxin and Thymoquinone is sufficient to cause apoptosis, cells were examined for



DNA fragmentation in immunofluorescence experiments. Indeed, cells with fragmented DNA could be detected (Fig. 3.29).

**Fig. 3.29: Apoptosis caused by Poloxin and Thymoquinone.**

Cells show DNA fragmentation, a sign of apoptosis. blue: DAPI-stained DNA; magnification: 100x.

A quantification of apoptotic cells was not possible due to the setup of the immunofluorescence experiments. During the process of sample preparation most apoptotic cells were washed off the coverslips.

### 3.4.2.7 Plk1 Localization in Poloxin and Thymoquinone Treated Cells

In order to verify that the mitotic arrest, the chromosome congression defects and apoptosis observed in the presence of the inhibitors were caused by incorrect distribution of endogenous Plk1, the localization of Plk1 was analyzed by immunofluorescence. In metaphase of DMSO treated control cells, Plk1 located to centrosomes and kinetochores. In contrast, in the presence of Thymoquinone and Poloxin, both centrosomal and kinetochores localization of Plk1 were significantly reduced (Fig 3.30).

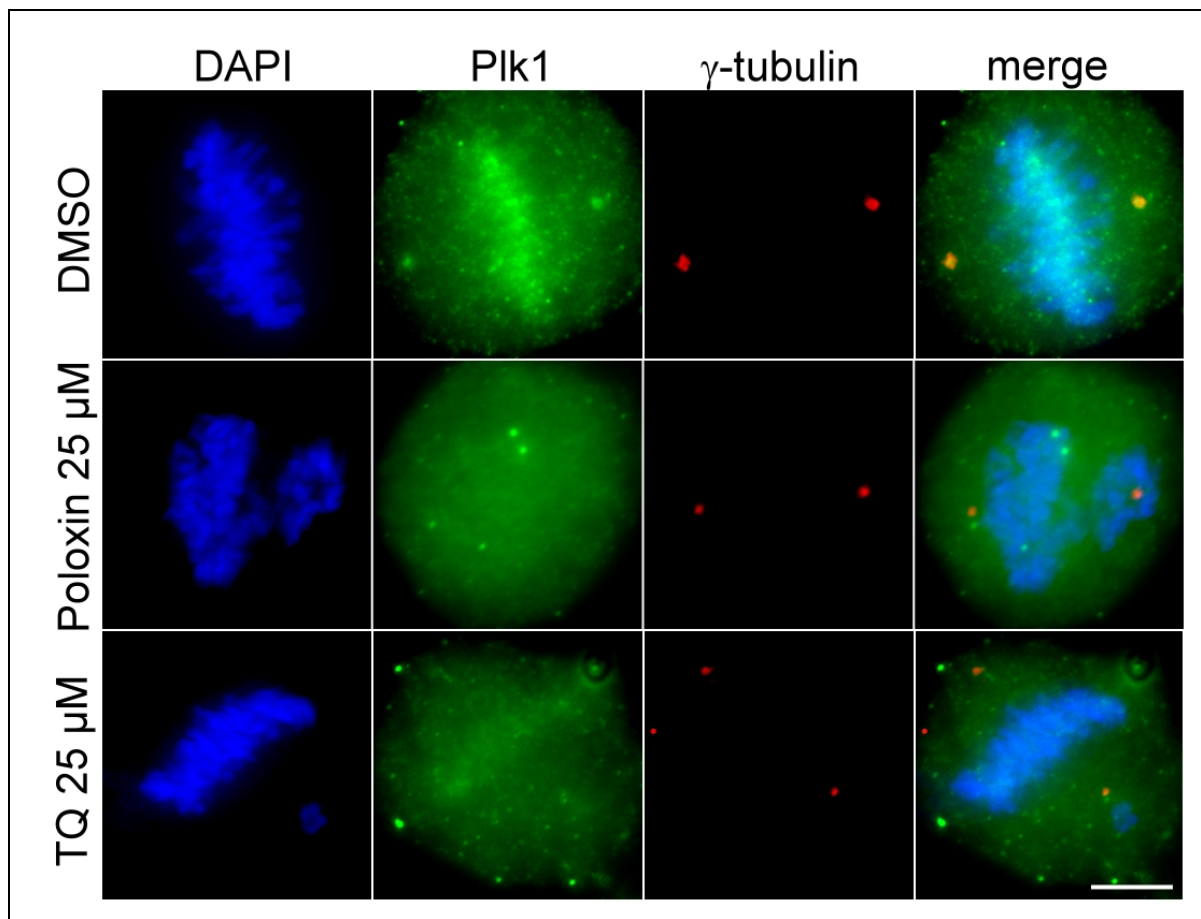


**Fig. 3.30: Plk1 localization in Poloxin and Thymoquinone treated metaphase cells.** DAPI: DNA;  $\gamma$ -tubulin: centrosomes. Scale bar represents 5  $\mu$ m.

Similarly, centrosomal localization of Plk1 in prometaphase was strongly reduced in the presence of Poloxin and Thymoquinone, but was not significantly affected in cells arrested in prometaphase by nocodazole treatment (Fig. 3.31). Nocodazole was used as a control in order

to rule out the possibility that Plk1 mislocalizes from its binding sites as consequence of any prolonged mitotic arrest.

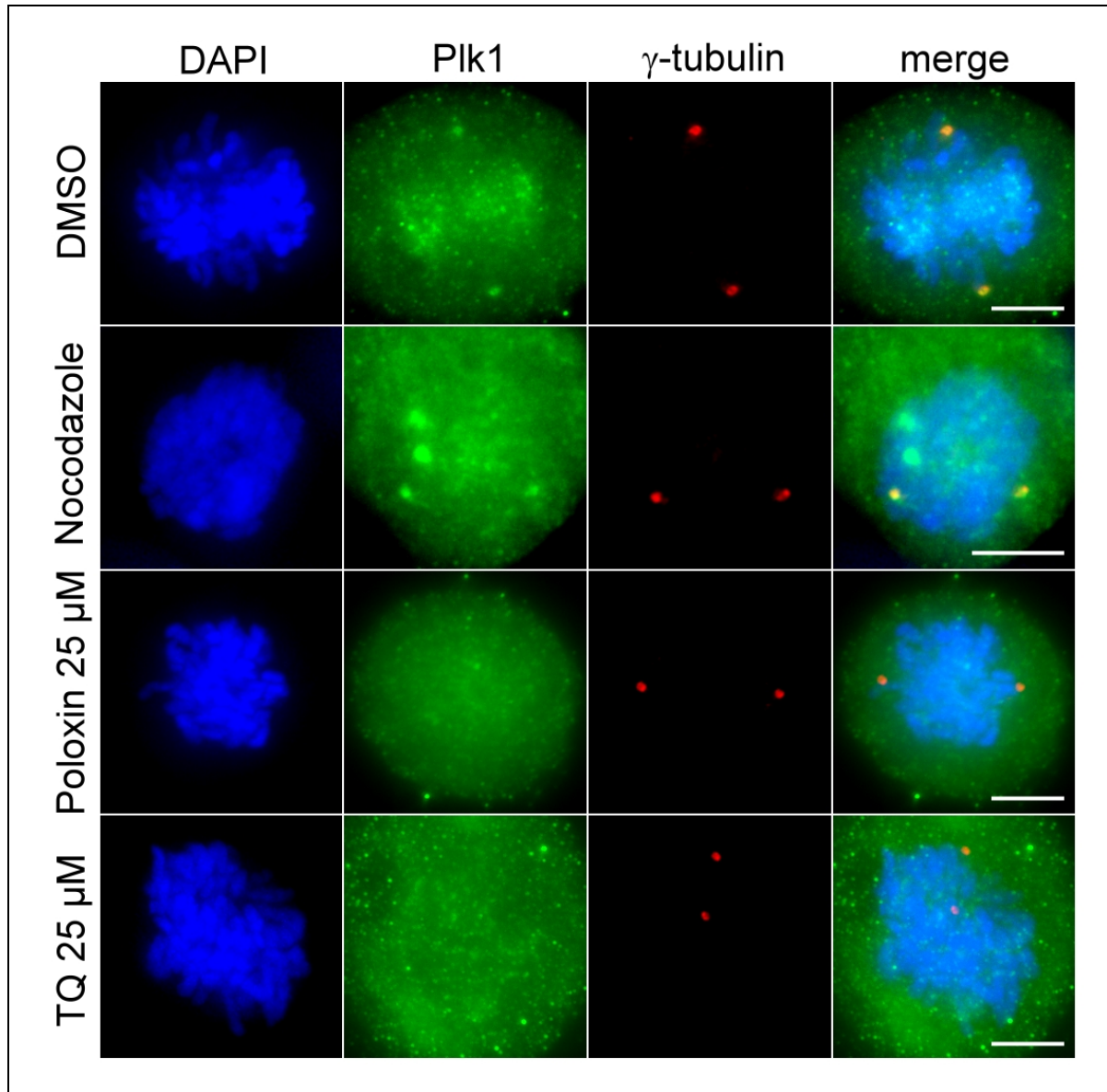


**Fig. 3.31: Plk1 localization in Poloxin, Thymoquinone, and nocodazole treated prometaphase cells.** DAPI: DNA;  $\gamma$ -tubulin: centrosomes. Scale bars represent 5  $\mu\text{m}$ .

Quantification of the centrosomal/cytoplasmic ratio of Plk1 in prometaphase- and metaphase-arrested cells revealed a highly significant decrease in the presence of Poloxin and Thymoquinone. As seen in all cell experiments before, the Poloxin showed higher cellular activity than Thymoquinone (DMSO:  $1.37 \pm 0.15$ ; Nocodazole:  $1.31 \pm 0.15$ ; Poloxin (25  $\mu\text{M}$ ):  $1.08 \pm 0.04$ ; Thymoquinone (25  $\mu\text{M}$ ):  $1.15 \pm 0.08$ ) (Fig. 3.32).

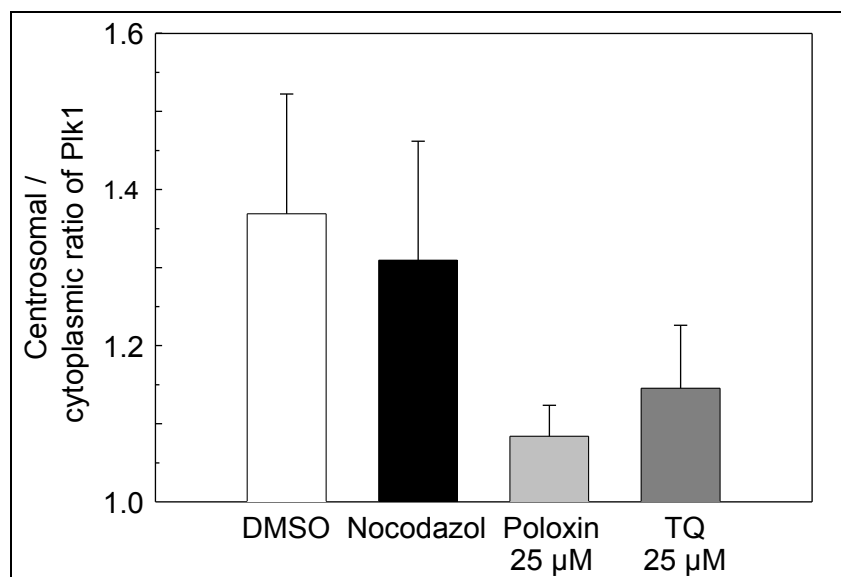


Fig. 3.32: Quantification of centrosomal Plk1 localization. Error bars represent SD.

#### 3.4.2.8 Phosphorylation of BubR1

Since Poloxin mislocalizes endogenous Plk1 from its cellular binding sites, the next step was to test whether a PBD-dependent phosphorylation signal decreases as a result of missing Plk1. For this purpose the phosphorylation of BubR1 by Plk1 was analyzed. BubR1 is a mitotic checkpoint kinase located on kinetochores, which is phosphorylated by Plk1 (Matsumura *et al.*, 2007). This phosphorylation strictly requires prior localization of Plk1 to kinetochores (Elowe *et al.*, 2007). The phosphorylation of BubR1 by Plk1 can be monitored via an upshifted BubR1 band in a Western Blot with cell lysates.

Different concentrations of Poloxin were added at 7 hours after release into medium containing 150 nM of nocodazole, just before most cells reached mitosis. Cells were lysed after 10 hours and tested in Western blots (Fig 3.33). Thymoquinone was left out of this experiment as it displayed toxicity at the concentrations used.

The Western Blot analysis showed a concentration-dependent reduction of phosphorylated BubR1 levels, while Plk1- and actin-levels remained unchanged. As Plk1 is only expressed in mitosis, the Plk1 level in asynchronous cells is reduced (Fig. 3.34). This shows that mislocalization of Plk1 by Poloxin leads to a consecutive reduction of PBD-dependent Plk1 activity.

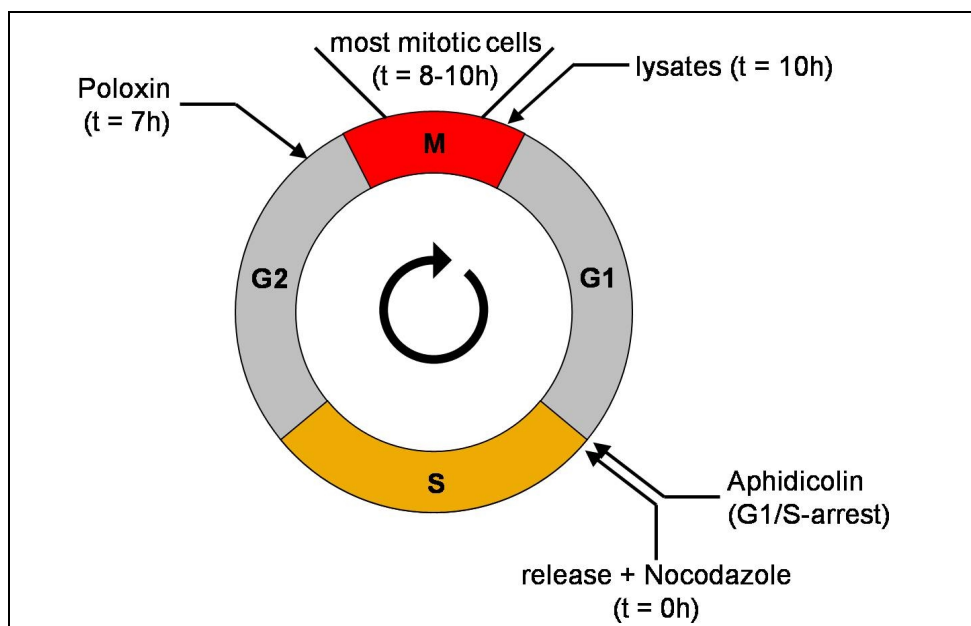


Fig. 3.33: Scheme depicting the experimental setup for the analysis of BubR1 phosphorylation.

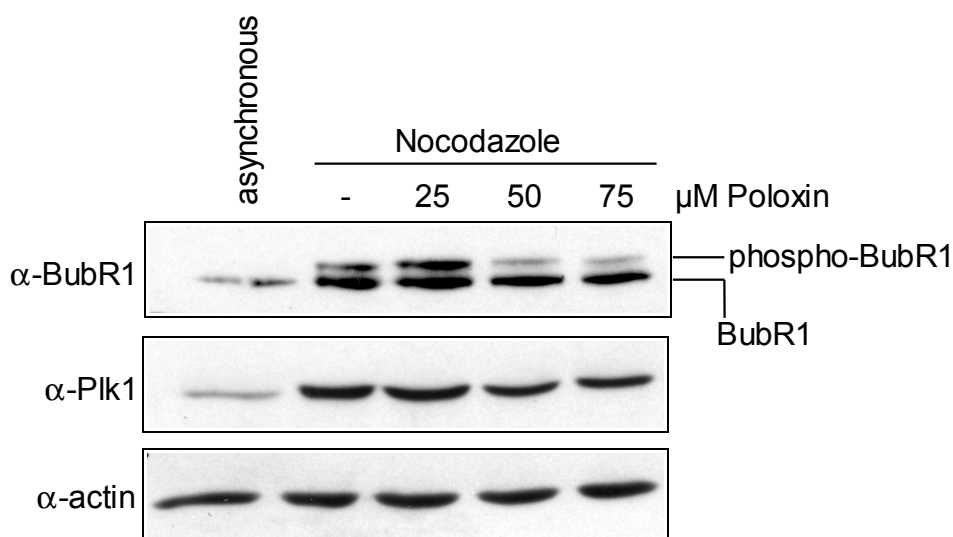
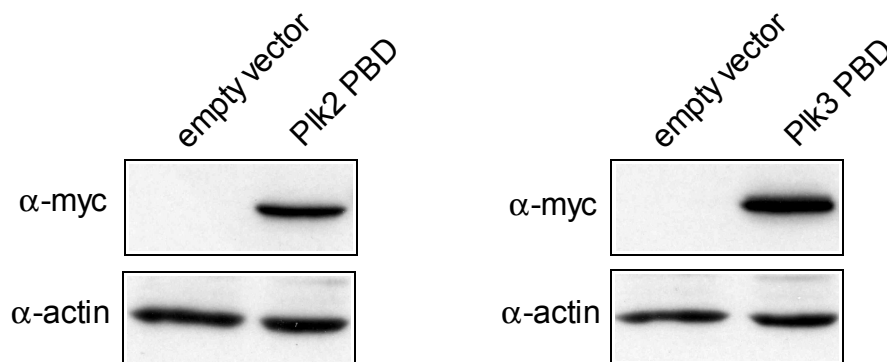


Fig. 3.34: Inhibition of PBD-dependent BubR1 phosphorylation. Dose-dependent reduction of phospho-BubR1 levels by Poloxin. Actin levels were used as loading control.

### 3.5 Inhibition of the Plk2 PBD and Plk3 PBD

Since the PBDs of Plk2 and Plk3 are partially inhibited *in vitro* by Poloxin and Thymoquinone, possible effects of an *in vivo* inhibition of these two proteins were investigated. For this purpose, analogous control experiments to the Plk1 PBD were performed. The cDNAs coding for the PBDs of Plk2 (aa 355-685) and Plk3 (aa 335-646) (Elia *et al.*, 2003b) were cloned into the transfection vector pCS2-MT and transfected into HeLa cells. Transfection reactions were monitored via Western blotting (Fig. 3.35).



**Fig. 3.35: Western Blot monitoring PBD transfection.** HeLa cells were transfected with the empty vector, Plk2 PBD and Plk3 PBD. Cell lysates were probed for myc-tagged PBDs. Actin levels were used as loading control.

The effects of ectopic expression of the Plk2 PBD and the Plk3 PBD in HeLa cells were analyzed. Unlike the Plk1 PBD, expression of the PBDs of Plk2 and Plk3 caused no increase in mitotic cells (Plk2:  $6.2 \pm 1.2$  % and Plk3:  $5.6 \pm 1.4$  %, in comparison to  $6.7 \pm 0.7$  % for the empty vector. (Fig. 3.36). The distribution over the different mitotic phases was similar to that of mock-transfected cells (Tab. 3.6 and Fig. 3.37). The results of overexpression of the Plk1 PBD (WT and FAA) have been added for comparison.

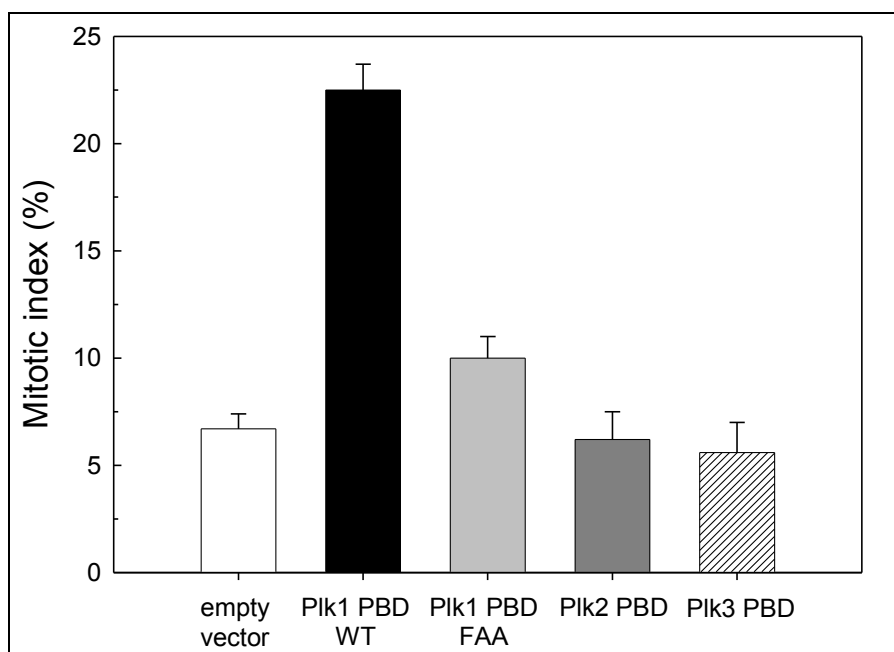


**Fig. 3.36: Mitotic indices for transfected HeLa cells.** Error bars represent SD.

**Tab. 3.6: Quantification of phase distribution for transfected HeLa cells.**

	Prophase	Prometaphase	Metaphase	Metaphase with defects	Ana-/telophase
<b>Empty vector</b>	$2.1 \pm 0.3$ %	$21.5 \pm 3.4$ %	$43.8 \pm 3.5$ %	-	$32.5 \pm 1.2$ %
<b>Plk2 PBD</b>	$3.4 \pm 2.4$ %	$12.8 \pm 4.0$ %	$46.0 \pm 6.3$ %	-	$37.8 \pm 2.4$ %
<b>Plk3 PBD</b>	$6.0 \pm 2.0$ %	$15.2 \pm 3.8$ %	$45.9 \pm 4.6$ %	-	$32.9 \pm 2.6$ %

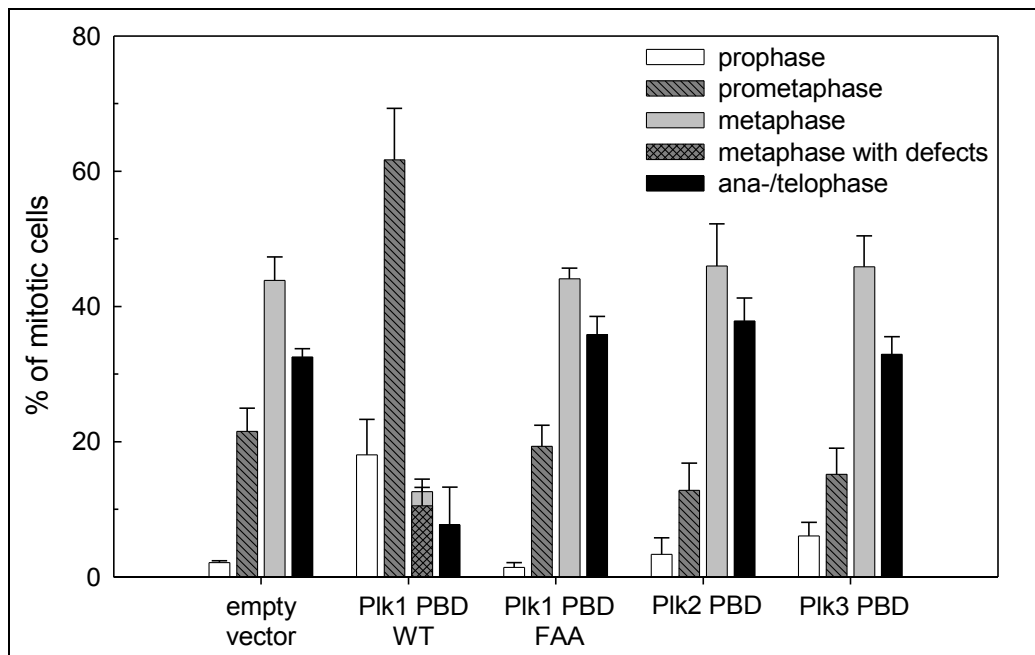


**Fig. 3.37: Mitotic phases for transfected HeLa cells.** “Metaphase with defects” describes a subpopulation of metaphase cells. Error bars represent SD.

Cells transfected with the PBDs of Plk2 and Plk3 showed a normal mitotic phenotype. No Chromosomes remained uncongressed and correct metaphase plates were formed (Fig. 3.38).

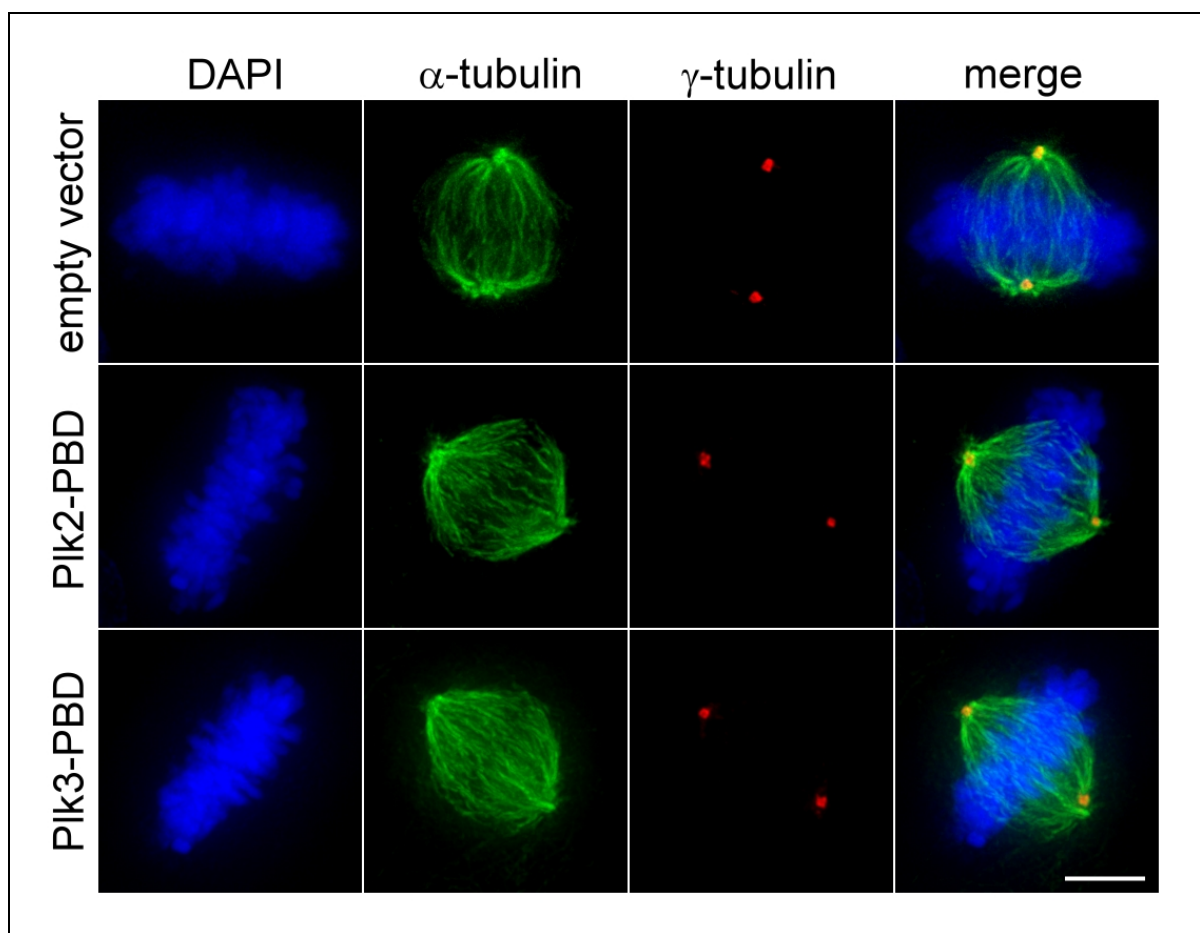


**Fig. 3.38: Phenotype caused by PBD-expression.** DAPI: DNA;  $\alpha$ -tubulin: spindles;  $\gamma$ -tubulin: centrosomes. Scale bar represents 5  $\mu$ m.

It seems that *in vivo* inhibition of Plk2 and Plk3 by ectopic expression of the PBDs of these two kinases has no obvious effect on HeLa cells. Therefore, one could argue that even if Poloxin and Thymoquinone inhibit the PBDs of Plk2 and Plk3 to some extent, it does not lead to any visible *in vivo* effects.

However, no definite conclusion is possible, as the expression levels of the PBDs of Plk2 and Plk3 may have been different from the one observed for Plk1. Furthermore, literature gives no clear results regarding the overexpression of the Plk3 PBD. It is reported to both cause no cellular effects (Hanisch *et al.*, 2006) and lead to cell cycle arrest with cytokinesis defects (Jiang *et al.*, 2006).

### 3.6 Inhibitory Mechanism of Poloxin and Thymoquinone

Time-dependency of a reaction is a strong criterion by which to distinguish between a covalent modification (time-dependent) and the formation of an equilibrium (time-independent). In order to investigate time-dependency of the inhibition caused by Poloxin and Thymoquinone, the Plk1 PBD was incubated for 20, 40 and 60 minutes before addition of 5-CF-GPMQSpTPLNG and subsequent measurement.

Inhibition of the Plk1 PBD by both Poloxin (apparent  $IC_{50}$ -values: 20min:  $16.6 \pm 2.5 \mu\text{M}$ , 40 min:  $10.1 \pm 0.3 \mu\text{M}$ , 60 min:  $4.8 \pm 1.3 \mu\text{M}$ ) and Thymoquinone (apparent  $IC_{50}$ -values: 20 min:  $2.59 \pm 0.51 \mu\text{M}$ , 40 min:  $1.67 \pm 0.26 \mu\text{M}$ , 60 min:  $1.14 \pm 0.04 \mu\text{M}$ ) was time-dependent (Fig. 3.39), opening the possibility that covalent protein modification may in part contribute to the inhibitor-protein interaction.

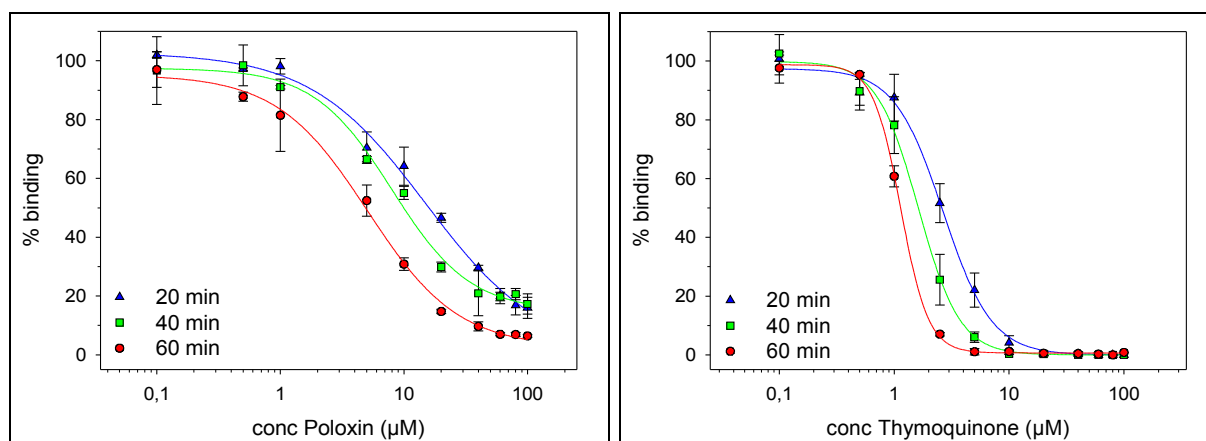


**Fig. 3.39: Time-dependency of Plk1 PBD inhibition by Poloxin and Thymoquinone.** Error bars represent SD.

## 4. Discussion

### 4.1 Validation of the Plk1 PBD as Target for Small-Molecule Inhibitors

The serine/threonine kinase Plk1 is one of the key enzymes of mitosis, being involved in all steps from G2/M-transition and mitotic entry to cytokinesis. Plk1 was shown to carry out crucial functions on many important mitotic cellular structures, like centrosomes, spindles or kinetochores. Furthermore, Plk1 activity has been indispensably linked with both DNA damage and the spindle checkpoint. For most of its functions, Plk1 has to bind to substrates with its protein-interaction domain, the PBD, followed by subsequent target phosphorylation (Barr *et al.*, 2004; van de Weerd & Medema, 2006).

Therefore, a key focus of mitotic research lies in a comprehensive elucidation of the cell cycle functions and mechanisms of Plk1. Inhibition is a valuable tool for exploring protein function. Currently, a number of small-molecule inhibitors of the enzymatic functions of Plk1 have been reported (Stevenson *et al.*, 2002; Liu *et al.*, 2005; Gumireddy *et al.*, 2005; McInnes *et al.*, 2006; Peters *et al.*, 2006; Lansing *et al.*, 2007; Lenart *et al.*, 2007; Steegmaier *et al.*, 2007; Santamaria *et al.*, 2007). With one exception (Gumireddy *et al.*, 2005), all these inhibitors are thought to compete for the ATP binding pocket. ATP competitors lead to an inhibition of the kinase domain, blocking all Plk1 functions. However, it has been shown that there are two kinds of Plk1 functions, PBD-dependent and PBD-independent functions (Hanisch *et al.*, 2006). Thus, a tool allowing differentiation between these two mechanisms of action would be needed for a more precise understanding of Plk1 activity. While kinase domain inhibitors block all Plk1 functions, an inhibitor specific for the PBD, blocking substrate binding of Plk1, would only interfere with the subset of Plk1 functions which are PBD-dependent. Information about this subset would help to clarify which functions require pre-localization of Plk1, and would give hints at functions that play a role on crucial mitotic structures, like centrosomes or kinetochores. PBD-specific inhibition can be achieved by ectopic expression of the PBD (Hanisch *et al.*, 2006). However, the transfection step required does not allow for an exact starting-point of inhibition, a prerequisite for all mitotic experiments. A small-molecule inhibitor of the PBD would be an ideal tool, since it guarantees tight temporal control of the inhibition.

Plk1 is overexpressed in a large variety of human tumors, causing increased cellular proliferation with aberrant spindles and multinucleated cells. Since it is regarded as an

adverse prognostic marker for tumor patients, Plk1 is widely considered to be a target for anti-cancer therapy (Eckerdt *et al.*, 2005, Strebhardt & Ullrich, 2006). Clinical trials with small-molecule inhibitors of Plk1 are ongoing (Gumireddy *et al.*, 2005; Steegmaier *et al.*, 2007).

Since the conserved nature of the ATP-binding pocket poses a serious hurdle for the development of mono-specific inhibitors, careful analysis of the compounds' activities on many kinases is necessary in order to select compounds which inhibit the right set of kinases. The difficulties associated with the specificities of ATP-competitive kinase inhibitors suggest the exploration of an alternative mode of Plk1 inhibition. The Plk1 PBD had been suggested as an ideal target for cancer therapy due to its unique nature which could facilitate the development of specific agents targeting its function (Strebhardt & Ullrich, 2006).

Nevertheless, small-molecule inhibitors which could validate the Plk1 PBD as meaningful target for small molecules had not been reported at the onset of this thesis. Therefore, it was the goal of my project to explore the feasibility of inhibiting the Plk1 PBD by small molecules.

## 4.2 Assay Development

### 4.2.1 A Homogeneous Assay Based on Fluorescence Polarization

The assay principle of fluorescence polarization (Owicki, 2000) was chosen for the primary screen, as this assay type is ideally suited for the identification of small-molecule inhibitors of binding between components of biological systems, such as inhibitors of DNA-protein interactions (Rishi *et al.*, 2005; Kiessling *et al.*, 2006), or peptide-protein interactions (Coleman *et al.*, 2005; Schust & Berg, 2004; Schust *et al.*, 2006). Recently, the scope of fluorescence polarization assays was expanded to test inhibitors of a protein-aptamer interaction (Hafner *et al.*, 2006).

The initial goal was to devise an assay based on fluorescence polarization (FP) which would allow for the analysis of the effect of test compounds on the function of the Plk1 PBD. To this end, peptides derived from the known binding motifs of the Plk1 PBD (Elia *et al.*, 2003a) were labeled with 5-carboxyfluorescein. Since their molecular weight is relatively low compared to the molecular weight of the protein, they rotate quite fast in the unbound state in solution. Because of this high mobility, applied linear polarized light is subject to strong depolarization. Upon binding of a probe to the Plk1 PBD, the rotation of the fluorophore, as

part of the protein-peptide complex, is strongly reduced. In turn, the measured FP is much higher. This system allowed the detection of substances with inhibitory activity for binding of the PBD to the fluoropeptide or substrates, respectively. PBD inhibitors would cause a dissociation of the probe from the PBD, resulting in a concentration-dependent decrease in measured FP.

A binding assay suitable for detecting inhibition has to fulfill two important requirements. First, the resulting binding curve should show a steep gradient, which represents high binding affinity and guarantees high sensitivity for inhibition measurements. Second, the measurement window defined by minimal and maximal FP values should be as large as possible, so that experimental variations and standard deviations can easily be distinguished. Therefore, different set-ups were tested to find optimal binding conditions.

The probe 5-CF-GPMQSpTPLNG ( $K_d = 26 \pm 2$  nM) produced a superior binding curve in comparison to the other probes 5-CF-ASpTPLNGAKK ( $K_d = 3.8 \pm 1.6$   $\mu$ M), GPMQSpTPLK(5-CF)-NH<sub>2</sub> ( $K_d = 407 \pm 32$  nM), and 5-CF-MQSpTPLNG ( $K_d = 107 \pm 10$  nM) (Fig. 3.1). This result indicates that peptide-binding to the PBD not only depends on the existence of the core phosphomotif S-(pS/pT)-(P/X), but also on the sequence in immediate vicinity to the phosphogroup. Additionally, placing the fluorophore on the C-terminal side of the peptide interfered with peptide binding, probably by steric hindrance. The probe 5-CF-GPMQSpTPLNG covers enough amino acids of the optimal PBD-binding sequence to guarantee high-affinity binding, and its size is still small enough, to result in a large measurement window. Additionally, the fluorophore-label is kept away from the phosphomotif far enough, so that no steric hindrance occurs.

An increase in the concentration of NaCl in the assay buffer from 50 nM ( $K_d = 26 \pm 2$  nM), to 100 nM ( $K_d = 39 \pm 2$  nM) and 200 nM ( $K_d = 91 \pm 2$  nM) led to a gradual weakening of binding affinity (Fig. 3.2). Probably, the increase in free ions interferes with the interactions of the PBD with the charged O-atoms of the peptide's phosphate group. Therefore, 50 mM NaCl was used for all further assays.

DMSO is one of the most common solvents for chemical substances. Since all libraries used were dissolved in DMSO, the screening assay had to show stability in the presence of DMSO. Testing of various DMSO concentrations (0 %, 5 %, and 10 %) showed that the  $K_d$ -value was stable at approximately 26 nM (Fig. 3.3), indicating that the assay is suitable for use with the libraries at hand. 10 % DMSO were used for the final screening buffer, ensuring compound

solubility.

Since the screening process, required temporal stability of the assay over a course of 1-2 hours, the stability of the assay was analyzed with regard to time. The binding assay showed high temporal stability for 24 hours with a constant  $K_d$ -value of approximately 25-27 nM (Fig. 3.4), setting no strict limitations on the duration of the screening process.

#### 4.2.2 Assay Controls and Z'-factor

Subsequently, the suitability of the assay for the detection of substances with PBD-specific activities needed to be investigated. As positive control for a compound with high affinity for the Plk1 PBD, the peptide MAGPMQSpTPLNGAKK was used. This was described as the optimal binding sequence for the Plk1 PBD (Elia *et al.*, 2003a). In comparison to the fluoropeptide, this unlabeled peptide comprised several additional residues on both termini, thought to be involved in contacting the PBD. High affinity for binding of the PBD was therefore expected, leading to dissociation of the fluorescence probe and a decrease in the FP-value. Indeed, dose-dependent inhibition of fluoropeptide-binding to the PBD by the probe MAGPMQSpTPLNGAKK was observed ( $IC_{50} = 0.39 \pm 0.11 \mu\text{M}$ ) (Fig. 3.5).

To rule out that the inhibition observed was due to unspecific binding effects in the presence of high concentrations of competitor, a negative control was also tested. To this end, the unlabeled probe Ac-GHFDpTYLIRR was applied. Its sequence was derived from the binding motif described for FHA domains (Durocher *et al.*, 2000). In binding experiments carried out in this thesis, the CF-labeled version of this peptide was shown to effectively bind the FHA domain of Chk2 (aa 1-225) ( $K_d = 189 \pm 6 \text{ nM}$ ; Fig. 3.12). When tested as a competitor for PBD binding together with the probe 5-CF-GPMQSpTPLNG, only very low activity was observed ( $15.0 \pm 5.7 \%$  inhibition at  $100 \mu\text{M}$ ) (Fig. 3.6), indicating that only molecules with PBD-binding affinity can cause dissociation of the fluoropeptide.

Another important determinant to evaluate the suitability of an assay for high-throughput screening, is the Z'-factor (Zhang *et al.*, 1999) (see 2.7.3). An assay is considered to be well-suited for high-throughput screening if Z' is larger than 0.5. The Z'-factor determined for the established assay, using the peptide MAGPMQSpTPLNGAKK as inhibitor was  $0.73 \pm 0.06$  (Fig. 3.7), indicating that this assay is suitable for high-throughput screens. The competitor peptide MAGPMQSpTPLNGAKK was used at a final concentration of  $10 \mu\text{M}$ , equal to approximately 90 % inhibition of fluoropeptide-binding to the PBD. The Z'-factor could have been further enhanced by using higher concentrations of competitor, leading to a broader

measurement range.

### 4.2.3 Binding Studies

In order to investigate to what extent certain features of the PBD-binding motif contribute to the observed affinity for the PBD, various peptide probes were tested in equivalent inhibition setups, as described for MAGPMQSpTPLNGAKK above (Fig. 3.6). The higher the binding affinity for the PBD, the stronger the effect on dissociation of the fluoropeptide 5-CF-GPMQSpTPLNG, and the higher the influence of a particular feature.

First, two relatively short peptides, Ac-ASpTPLNGAKK and Ac-ASpSPLNGAYKK were used for testing the influence of the core phosphomotif. Although described to bind to the motif S-(pS/pT)-(P/X), the PBD showed a clear preference for the phosphothreonine ( $IC_{50} = 32.2 \pm 2.0 \mu\text{M}$ ). The corresponding phosphoserine motif displayed only very weak affinity for the Plk1 PBD ( $19.2 \pm 12.1 \%$  inhibition at  $100 \mu\text{M}$ ) compared to the optimal peptide MAGPMQSpTPLNGAKK, similar to the negative control Ac-GHFDpTYLIRR.

A more than 200-fold weaker antagonistic activity ( $IC_{50} = 98.7 \pm 25.8 \mu\text{M}$ ) was observed for the unphosphorylated peptide MAGPMQSTPLNGAKK. However, inhibition was still significantly higher than observed for Ac-GHFDpTYLIRR, indicating that not only the core phosphomotif, but also the surrounding amino acids contribute to the PBD-binding affinity.

Substitution of phosphothreonine by aspartic or glutamic acid is frequently used to mimic phosphorylation of a threonine residue and to convert phosphopeptide sequences into more drug-like non-phosphorylated sequences, since the aspartic or glutamic acid side-chain presents a negatively charged group at approximately the same distance from the amino acid's chiral center as phosphothreonine. However, replacement of the phosphothreonine residue within the optimal binding motif with aspartic and glutamic acid lead to a dramatic loss in binding activity (glutamic acid:  $29.7 \pm 9.2 \%$  inhibition at  $100 \mu\text{M}$ ; aspartic acid: no inhibition at  $100 \mu\text{M}$ ). This result shows that the PBD is not applicable for this drug-discovery approach.

## 4.3 Evaluation of the High-Throughput Screen

### 4.3.1 Comparison of Different Screening Techniques

The frequent lack of lead structures for small-molecule inhibitors of protein-protein interactions can be overcome by high-throughput screening of large compound libraries. Chemical diversity in these libraries ensures a broad coverage of chemical space to increase the likelihood of identifying privileged substructures for interference with protein-protein interactions (Berg, 2003). There are three main screening approaches: *in vitro* screening, cell-based screening and virtual (*in silico*) screening.

*In vitro* screens present a rapid and economical method for the analysis of large numbers of compounds compiled into chemically diverse libraries. In this kind of screen, biochemical assays are used for the identification of inhibitors. One great advantage is that these assays, in contrast to cell-based assays, can be tailored to exactly address particular protein functions. In cellular screenings, the effects of substances always have to be evaluated in consideration of the global implications for the whole cell. Unfortunately, *in vitro* screening data give no hint of a compound's cellular activity. However, if the screened compounds have already been preselected according to Lipinski's "rule of 5" (Lipinski *et al.*, 2001), screening hits should provide a good starting point with regard to cellular uptake.

Cell-based screening of chemical libraries has the advantage of immediate information on cell permeability and toxicity of a compound. In the case of *in vitro* or *in silico* screenings, these have to be tested in separate *in vivo* assays after the primary screen.

Like the *in vitro* approach, *in silico* screening is a very fast and economic technique. However, detailed knowledge about the protein-protein interaction site, possible compound binding sites or preferred binding orientations of compounds is required. The unknown plasticity of such interaction sites often makes *in silico* screening complicated to analyze (Jones & Thornton, 1996).

In this thesis, a fluorescence polarization based *in vitro* assay was used for the detection of inhibitors of protein-protein interactions. In general, fluorescence polarization represents an ideally-suited method for high-throughput screening, which is emphasized by the increasing number of publications describing FP-based assays for inhibitor screening (Schust & Berg, 2004; Nikolovska-Coleska *et al.*, 2004; Du *et al.*, 2006; Saldanha *et al.*, 2006; Müller *et al.*, 2008b). In the reaction mixtures used for FP-based assays, equilibria are formed very rapidly, keeping incubation times relatively short. Reactions can be carried out in a miniaturized

format, for example in 384-well plates, requiring only minimal volumes. This makes FP a time- and material-saving method. Furthermore, FP is very sensitive. However, FP techniques are vulnerable to substances with intrinsic fluorescence. This can result in very high total fluorescence intensity values, rendering such compounds incompatible with the determination of inhibitory activity. This problem can be overcome by the application of different fluorophore-labels. In this thesis, 5-carboxyfluorescein (excitation wavelength: 485 nm; emission wavelength: 535 nm) was used. If a tested substance shows intrinsic fluorescence at a wavelength close to 535 nm, it can be re-tested with another fluorophore, for example Texas Red (excitation wavelength: 590 nm; emission wavelength: 635 nm).

### 4.3.2 Analysis and Processing of Screening Data

The high-throughput screen performed in this thesis involved testing of 22,461 compounds for inhibitory activity on the Plk1 PBD. The screen was performed at 30  $\mu$ M and 60  $\mu$ M. These relatively high concentrations were chosen to ensure that no potential candidate was missed out. The screening buffer contained a final concentration of 10 % DMSO, in general guaranteeing solubility for most tested small molecules.

Screening data for the 22,461 chemical substances were analyzed in consideration of several criteria to select the compounds for further analysis. In order to rule out any false-positive screening hits, all compounds were screened in duplicate, and only substances showing comparable results in both data sets were evaluated further. Compounds with intrinsic fluorescence, detectable due to their dramatically increased total fluorescence intensities, could not be correctly evaluated in the screening setup and were left out for further analysis. The most important selection criteria, however, were the initial specificity controls. The acquired screening data was compared with the results of two analogous screens previously performed in this group. The aim of these screens was the identification of inhibitors for the dimerization and DNA-binding of the transcription factor c-Myc/Max and for the SH2 domain of the transcription factor STAT3 (Kiessling *et al.*, 2006; Schust *et al.*, 2006). The data for the CDI and MB libraries were additionally checked against screening results for inhibitors of the SH2 domain of the transcription factor STAT5b, an analogous screen which was performed as part of this thesis (see 4.3.3). Only compounds inhibiting the Plk1 PBD at 60  $\mu$ M above 65 %, c-Myc/Max and STAT3 at 100  $\mu$ M below 50 %, and STAT5b at 60  $\mu$ M below 40 % were used for further analysis (Fig. 3.8). The selection threshold for c-Myc/Max seems relatively high, but in the inhibitor screens for these two proteins, compounds were

used at 100  $\mu$ M. Application of these criteria led to the selection of 223 compounds for further testing, which equals approximately 1 % of the 22,461 library molecules.

Empirical determination showed that the pin tool of the Biomek® FX screening system, used for transferring the compound libraries into the assay solution, transfers only very small volumes in the low nanoliter range, driven by adhesion forces. Thus, this setup is very sensitive to transfer errors. To sort out false positive screening hits, detected because of inaccuracies of the automated transfer step, all compounds selected for further analysis were re-tested by hand. Only 94 of the selected 223 compounds (42 %) could be validated as positive hits. This relatively small yield confirms the susceptibility of the transfer method to errors. A different method, for example the application of a high-precision pipetting head, allowing exact transfers of low microliter volumes, might present a more stable and reproducible approach.

For these reasons, the remaining compounds were tested again by hand in assays with the specificity controls c-Myc/Max, STAT3, or STAT5. Jun/Jun and C/EBP were included as additional controls. 86 of the 94 molecules still showed specific inhibition of Plk1, emphasizing the relevance of the applied specificity criteria for primary hit selection. Additionally, this result points out the good comparability of different screens performed with the same libraries.

After *in vitro* validation, remaining compounds were further validated in the cellular context. As it has been uniformly shown that Plk1 inhibition leads to an arrest of cells in mitosis (Spankuch-Schmitt *et al.*, 2002a; Yuan *et al.*, 2002; Stevenson *et al.*, 2002; Spankuch-Schmitt *et al.*, 2002b; Liu & Erikson, 2003; Liu *et al.*, 2005; Gumireddy *et al.*, 2005; McInnes *et al.*, 2006; Peters *et al.*, 2006; Lansing *et al.*, 2007; Lenart *et al.*, 2007; Steegmaier *et al.*, 2007; Santamaria *et al.*, 2007), all remaining compounds were tested for their ability to increase the mitotic index. As expected, cell permeability and cellular activity turned out to be the toughest exclusion criterion. Only 19 compounds led to a relatively significant increase of mitotic cells. Despite fulfilling Lipinski's "rule of 5" (Lipinski *et al.*, 2001), apparently most molecules simply were not taken up by cells. If they were able to cross the cell membrane, they either did not show any cellular effects, or could have been degraded. Many compounds also displayed toxicity.

The last step in the validation process was the test whether the compounds causing a mitotic arrest display a phenotype consistent with Plk1 inhibition. Since there are hundreds of

proteins involved in regulation of the cell cycle and inhibition of any of these could lead to a block in mitosis, the chances are relatively high that a compound might arrest cells in mitosis by effects other than inhibition of the Plk1 PBD. Indeed, only 2 compounds showed a Plk1-specific inhibition phenotype, while most compounds did not show any particular phenotype at all or turned out to act as spindle poisons, interfering with tubulin polymerization (Fig. 3.9).

In summary, two compounds from the libraries were identified as potential inhibitors of the Plk1 PBD, yielding a final hit rate of 0.009 %. Although this rate might seem quite low, considering the chemical diversity of the used libraries and the lack of information about structural compound classes, which preferably bind to the PBD, this represent a realistic result. The more effective of the two compounds was named Poloxin (for *polo*-box domain *in*hibitor). The second identified compound will be evaluated in further studies. The natural product Thymoquinone represents Poloxin's core structure and was included for all further assays.

### 4.3.3 Screening for Inhibitors of STAT5b

As part of this thesis, the libraries from ChemDiv (8,298 compounds) and Maybridge (9,000 compounds) were tested for inhibitors of the SH2 domain of STAT5b in a parallel screen. This latent transcription factor has been recognized as a therapeutic target for many human tumors (Levy & Darnell, 2002). Screening was performed with an analogous FP-based assay to that used for the Plk1 PBD, which was used to detect compounds with the ability to inhibit binding of the fluorophore-labeled peptide 5-CF-GpYLVLDKW, derived from the erythropoietin (EPO) receptor (Quelle *et al.*, 1996; May *et al.*, 1996), to the SH2 domain of STAT5b (aa 136-704) (Schust *et al.*, 2006; Müller *et al.*, 2008b).

This particular protein-peptide interaction appears to be very hard to inhibit. Screening of the 17,298 compounds of the indicated libraries generated only one hit, showing specificity with respect to Plk1 PBD screen. The identified compound was a chromone-derived acyl hydrazone and disrupted the interaction between STAT5b and its binding peptide with an apparent IC<sub>50</sub> of 47 ± 17 µM. This compound was further validated by other members of this group, Judith Müller and Bianca Sperl, leading to the publication of the first nonpeptidic small-molecule inhibitor of the STAT5b SH2 domain (Müller *et al.*, 2008a).

## 4.4 Poloxin and Thymoquinone

Poloxin, the most specific PBD-inhibiting compound detected in the screen, and its core structure Thymoquinone, the bioactive component of the volatile oil of black seed (*Nigella sativa*) were further validated in various *in vitro* and *in vivo* assays.

### 4.4.1 *In vitro* Characterization and Specificity Profiles

During the screening and validation process, the compounds had been tested at a two concentrations only. For a complete analysis of inhibitory activity, entire inhibition curves were first recorded for Poloxin and Thymoquinone (Fig. 3.11). Poloxin showed inhibition of the Plk1 PBD in the low micromolar range (apparent  $IC_{50} = 4.8 \pm 1.3 \mu M$ ), clearly confirming the activity observed in the screen. Thymoquinone was even four times more potent with an apparent  $IC_{50}$  of  $1.14 \pm 0.04 \mu M$ . One possible explanation for Thymoquinone's higher inhibitory activity could be that because of its smaller molecular size and the lack of bulky side chains, it can target a potential binding site on the PBD more effectively.

In general, specificity towards a certain target protein is a very important criterion rating the effectiveness and the applicability of a small-molecule inhibitor. Only highly-specific inhibitory compounds can be used to clearly analyze functions of proteins, especially in the cellular context. For disease treatment, specific inhibitors are desirable in order to minimize unintentional or even harmful side-effects.

Poloxin and Thymoquinone inhibit peptide- or substrate-binding to the Plk1 PBD. The PBD is part of the domain family of pS/pT-binding domains. The best specificity controls are therefore represented by other pS/pT-binding domain family members, with the PBDs of Plk2 and Plk3 being the most stringent controls. The PBD of Plk4 is the most distant member of the family of PBDs, comprising only one polo-box. Because of the differences in folding, the Plk4 PBD is the least important specificity control within the family of PBDs. Nonetheless, it was attempted to set up a binding assay for the recombinant PBD of Plk4 (aa 638-970) (Habedanck *et al.*, 2005). However, since there is no information on binding sequences available, and none of the other Plk's binding peptides showed any affinity towards Plk4, the setup of an equivalent binding assay failed. Other family members with pS/pT-binding domains are FHA domains, WW domains, and 14-3-3 proteins (Yaffe & Smerdon, 2004). A closely related family is formed by pY-binding domains, for example SH2-domains. For a comprehensive specificity profile, the PBDs of Plk2 and Plk3, and representatives from all the

other domain families were included (FHA: Chk2; WW: Pin1; SH2: STAT1, STAT3, STAT5b, Lck). The setup of an inhibition assay for 14-3-3 proteins failed due to the weak affinity of the published binding-peptide (Yaffe *et al.*, 1997b).

In analogous FP assays to that used for the Plk1 PBD, Poloxin showed an excellent specificity profile. It selectively targeted the PBD family only, with a significant preference for the Plk1 PBD (apparent IC<sub>50</sub>s: Plk1: 4.8 ± 1.3 μM; Plk2: 18.7 ± 1.8 μM; Plk3: 53.9 ± 8.5 μM) (Fig. 3.13). Despite its more potent inhibition of the Plk1 PBD, Thymoquinone inhibited the PBDs of Plk2 and Plk3 and several other of the specificity controls (apparent IC<sub>50</sub>s: Plk1: 1.14 ± 0.04 μM; Plk2: 1.90 ± 0.10 μM; Plk3: 22.4 ± 0.8 μM; Chk2: 3.9 ± 0.6 μM; Pin1: 20.4 ± 0.9 μM; STAT3: 10.9 ± 0.2 μM) (Fig. 3.14). The same features of Thymoquinone that facilitate Plk1 inhibition probably cause the side effects observed on several other protein-binding domains. It seems that the oxime and the toluoyl group of Poloxin cause a decrease in Plk1 inhibition in comparison to Thymoquinone, accompanied by a potent enhancement in specificity.

It was attempted to validate the inhibitory activities of Poloxin and Thymoquinone in further, fluorescence-independent *in vitro* assays. Various pulldown assays were used to test, whether both compounds can interfere with binding of the PBD to immobilized Cdc25C, a natural Plk1 target involved in the onset of mitosis (Nigg, 2001), or to an immobilized peptide comprising the optimal PBD binding sequence. To this end, recombinant GST- oder MBP-tagged Cdc25C was immobilized on GST sepharose or amylose resin, respectively. Cdc25C had been prephosphorylated with Cdk1/Cyclin B to create the docking site for the PBD. The optimal PBD-binding peptide, carrying a cysteine residue on a linker, was coupled to iodoacetamide beads. However, no matter what immobilization methods were used, all three beads turned out to allow too much unspecific binding, resulting in assays to instable and variable to allow for testing of small molecules.

#### 4.4.2 Cellular Activities

Since Plk1 is one of the key regulators and promoters of mitosis, inhibition of Plk1 has been uniformly described to cause a mitotic arrest (Spankuch-Schmitt *et al.*, 2002a; Spankuch-Schmitt *et al.*, 2002b; Liu & Erikson, 2003; Yuan *et al.*, 2002; Stevenson *et al.*, 2002; Liu *et al.*, 2005; Gumireddy *et al.*, 2005; McInnes *et al.*, 2006; Peters *et al.*, 2006; Lansing *et al.*, 2007; Lenart *et al.*, 2007; Steegmaier *et al.*, 2007; Santamaria *et al.*, 2007).

Ectopic expression of the Plk1 PBD, an ideal positive control for small-molecule inhibitors of

the PBD, also arrested HeLa cells in prometaphase. The arrest phenotype showed chromosome congression defects, caused by mislocalization of endogenous Plk1 (Fig. 3.19-3.23; Hanisch *et al.*, 2006). Poloxin and Thymoquinone also caused a prometaphase arrest (Fig. 3.25-3.27). In cooperation with Klaus Strebhardt's group from the University of Frankfurt, this arrest was further demonstrated by a clear increase of the mitotic markers Cyclin B1 and phosphohistone H3 in Western blots, and an increase of the G2/M peak in FACS (fluorescence-activated cell sorting) analysis. Poloxin and Thymoquinone also faithfully recapitulated the chromosome congression phenotype and mislocalization of Plk1 (Fig. 3.28, 3.30 and 3.31), a clear indication that both compounds inhibit Plk1 by blocking PBD-mediated protein-protein interactions *in vivo*.

Chromosome congression defects describe a phenotype in which single or whole bundles of chromosomes are not properly congressed to the metaphase plate. It has been shown that Plk1 inhibition may lead to destabilized microtubule-kinetochore interactions, not creating enough tension across sister kinetochores (van Vugt *et al.*, 2004a; Sumara *et al.*, 2004). Therefore, one possible explanation for the occurrence of these defects could be that mislocalization of endogenous Plk1 by Poloxin or Thymoquinone may also cause instable microtubule-kinetochore attachments and a lack of tension, not allowing spindle forces to congress chromosomes to the metaphase plate. One reason for the decreased spindle-kinetochore interactions could in turn be the absence of Plk1-mediated phosphorylations on key kinetochore proteins, for example BubR1 (Elowe *et al.*, 2007). A clear dose-dependent decrease of BubR1 phosphorylation was shown for Poloxin (Fig. 3.34).

It was repeatedly shown that a prolonged mitotic arrest, caused by inhibition of Plk1 functions (Spankuch-Schmitt *et al.*, 2002a; Spankuch-Schmitt *et al.*, 2002b; Liu & Erikson, 2003; Yuan *et al.*, 2002; Stevenson *et al.*, 2002; Liu *et al.*, 2005; Gumireddy *et al.*, 2005; McInnes *et al.*, 2006; Peters *et al.*, 2006; Lansing *et al.*, 2007; Lenart *et al.*, 2007; Steegmaier *et al.*, 2007; Santamaria *et al.*, 2007) induces apoptosis in cancer cells. The applications of both Poloxin and Thymoquinone lead to the occurrence of apoptotic cells, identifiable by DNA fragmentation in immunofluorescence experiments (Fig. 3.29). The group of Klaus Strebhardt at the University of Frankfurt was able to quantify the emergence of apoptosis, showing a clear dose-dependent increase of apoptotic cells caused by Poloxin and Thymoquinone. At 25  $\mu$ M, first toxic side effects of Thymoquinone were observed.

In summary, both Poloxin and Thymoquinone showed clear signs of *in vivo* inhibition of the Plk1 PBD. Although showing a more potent Plk1 inhibition *in vitro*, Thymoquinone's

effectivity on the increase of the mitotic index, the percentage of cells with chromosome congression defects or the mislocalization of endogenous Plk1 from chromosomes was always less potent than for Poloxin. This observation suggests that due to various side activities, the effectivity of Plk1 inhibition of Thymoquinone is reduced in comparison to Poloxin. This notion is backed by the results of the specificity studies.

#### 4.4.3 Binding Mechanism

In general, there are two possibilities for a small-molecule inhibitor to interact with its target protein: covalent modification or non-covalent binding, mediated by ionic bonds, hydrophobic interactions or van-der-Waals forces, for example. When interacting with a target protein, there are several possible mechanisms for the inhibitory activity of a small molecule: An interaction site could simply be blocked by an inhibiting compound, a mechanism used for the inhibition of protein kinases with ATP-competitors, for example (Kothe *et al.*, 2007b). Another possibility for blocking protein-protein interactions would be binding of a small molecule followed by subsequent changes in a protein's conformation in an allosteric manner (DeDecker, 2000) or partial unfolding.

Both Poloxin and Thymoquinone showed a time-dependent inhibition of the Plk1 PBD in the fluorescence polarization assay (Fig. 3.39). Time-dependency of inhibition reactions normally implies that the underlying mechanisms involves covalent modification of the inhibition target. In consideration of the structure of Poloxin, two possible chemical modifications would be Michael addition or condensation.

Supporting evidence for covalent modification of Plk1 by Poloxin could arise from experimental approaches which involve incubation of the protein with Poloxin, subsequent tryptic/chymotryptic digest, and identification of peptides by mass spectrometry. However, attempts to identify a nucleophilic amino acid modified by Poloxin, remained inconclusive. It is conceivable that an amino acid which might have been modified by Poloxin was part of the protein sequence which was not detected in the mass spectrometric analysis. Alternatively, protein modification via Michael addition of a nucleophilic amino acid side chain to one of the activated double bonds of Poloxin, or condensation of Poloxin's carbonyl group with a lysine side chain, could have been lost during sample preparation due to the reversible nature of these chemical reactions. Structural data would help to clarify the protein-inhibitor interactions.

## 4.5 Relevance of the Identified Plk1 Inhibitors

To my knowledge, Poloxin and Thymoquinone represent the first described inhibitors of the Plk1 PBD, opening up the possibility for a completely new approach to Plk1 inhibition. This has significant implications for both Plk1 research, since PBD-specific inhibitors allow a fast and precise differentiation of PBD-dependent and PBD-independent functions, and for cancer therapy, providing an alternative strategy to kinase domain inhibitors for targeting Plk1 in cancer cells.

Despite Thymoquinone's well-documented anti-neoplastic effects, clinical trials which could validate the benefit of Thymoquinone or derivatives for cancer patients have not been initiated. The lack of information about the molecular targets underlying Thymoquinone's anti-cancer activity poses a serious hurdle to drug development. Such knowledge would facilitate medicinal chemistry efforts aimed at improving the compound's pharmacological properties to the level required for drugs, and also the pre-selection of patients which are likely to respond in clinical trials (Corson *et al.*, 2007). Thus, the discovery of the Plk1 PBD, and also of the STAT3 SH2 domain as molecular targets of Thymoquinone not only suggests a rational explanation for this natural product's anti-neoplastic effects (Gali-Muhtasib *et al.*, 2006), but also provides a strong argument for the development of Thymoquinone-derivatives as anti-cancer drugs. Moreover, the data acquired in this thesis add Thymoquinone to the very short list of natural products known to inhibit a protein-protein interaction. Nevertheless, it is to be expected that Thymoquinone has additional molecular targets related to its anti-cancer activities that were not uncovered in this study.

Poloxin, a synthetic derivative of Thymoquinone, displays a superior specificity profile *in vitro* and in cells. In addition, Poloxin offers the means of targeting the PBD on fast timescales, which should open the door for examining the function of the PBD in the context of cell-division dynamics. Finally, the specificity profiles of agents targeting the unique PBD like Poloxin are potentially more straightforward to analyze and manage than those of ATP-competitive kinase inhibitors.

## 4.6 Outlook

There are several questions left to be addressed in future studies. For example, it would be very interesting to find out precisely what chemical groups are responsible for the enhancement of specificity on the transition from Thymoquinone to Poloxin. For this purpose,

specificity profiles of stepwise intermediate substances such as the oxime, the *O*-acetylated oxime or the *O*-benzoylated oxime could be determined. Such a study can also be easily extended for the determination of structure-activity relationships (SAR). For example, different quinone core structures can be tested, or differently substituted phenyl rings, or whole new substituents. Determination of the binding mechanism of Poloxin by structural approaches would also facilitate understanding of Poloxin's inhibitory activity and would greatly enhance the design of more potent Poloxin derivatives.

For a clear confirmation of Poloxin's potential anti-tumor activity, its pro-apoptotic effects have to be validated in various other cancer cell lines from different tissues and different tumor types. If Poloxin should show a broad anti-tumor activity, it could be tested in xenograft mouse models. This would indicate that PBD-specific inhibitors have the potential to be used as anti-cancer therapeutics. Additionally, Poloxin or any future derivatives could be used together with already existing Plk1 kinase domain inhibitors, allowing a more complete inhibition of Plk1 in cancer cells.

## 5. Summary

The serine/threonine kinase Polo-like kinase 1 (Plk1) is a key regulator of multiple stages of mitosis. It is overexpressed in many types of human cancers and has been implicated as an adverse prognostic marker for tumor patients. Inhibition of Plk1 activity in certain cancer cells leads to apoptosis, thus validating Plk1 as a target for anti-cancer therapy. As Plk1 activity is indispensable for progression through mitosis, inhibition of Plk1 by cell-permeable inhibitors could provide novel insights into the cell cycle, and forms the basis for new anti-cancer therapeutics. Small-molecule inhibitors of Plk1 usually target the enzyme's conserved ATP-binding site.

This thesis provides proof-of-principle that Plk1 can alternatively be targeted by small molecules which inhibit the function of the polo-box domain (PBD) of Plk1, which is required for correct intracellular localization of Plk1. Two small molecules, the natural product Thymoquinone and a synthetic derivative named Poloxin, have been identified as the first known inhibitors of the PBD. Their activities and specificities have been validated *in vitro* and *in vivo*.

First, an assay based on fluorescence polarization was developed, which allowed the rapid detection of potential small-molecule inhibitors of the Plk1 PBD in a high-throughput screen. Testing of chemical diverse libraries comprising 22,461 compounds led to the identification of Poloxin. The core structure of Poloxin is represented by the natural product Thymoquinone, the bioactive constituent of the volatile oil of black seed (*Nigella sativa*), which is well-known for its anti-inflammatory and anti-neoplastic activities. Both compounds inhibited the functions of the Plk1 PBD *in vitro* in the low micromolar concentration range. Poloxin inhibited the functions of Plk1 PBD in a highly specific manner. Despite a more potent Plk1 inhibition, Thymoquinone showed a less selective specificity profile. *In vivo*, both compounds arrested cancer cells in mitosis with chromosome congression defects, consistent with mislocalization of endogenous Plk1.

In summary, these data provide the first molecular explanation for the anti-cancer activity of the natural product Thymoquinone, and make it one of the very few natural products known to inhibit a protein-protein interaction. Poloxin's more selective activity against the PBD should make it an excellent tool for analyzing the role of the PBD in mammalian cells, and has implications for the future design of anti-cancer drugs.

## 6. Abbreviation Index

The following list shows frequently used abbreviations. For additional abbreviations of chemical substances and reagents see 2.1.1.

aa	Amino acids
Ac	Acetyl
APC/C	Anaphase-promoting complex/cyclosome
ASO	Antisense oligonucleotide
ATP	Adenosine triphosphate
BCA	Bicinchoninic acid
cDNA	Complementary DNA
CDI library	ChemDiv library
CDK	Cyclin-dependent kinase
(5-)CF	(5-)Carboxyfluorescein
DNA	Deoxyribonucleic acid
EDTA	Ethylene diamine tetraacetic acid
EGFR	Epidermal growth factor receptor
Fig.	Figure
FHA domain	Forkhead-associated domain
FNK	FGF-inducible kinase
FP	Fluorescence polarization
$\gamma$ -TuRC	$\gamma$ -tubulin ring complex
HRP	Horseradish peroxidase
HTS	High-throughput screen
IC <sub>50</sub>	Half-maximal (50 %) inhibitory concentration
K <sub>D</sub>	Dissociation constant
LB	Luria-Bertani broth
MB library	Maybridge library
MBP	Maltose binding protein
mRNA	Messenger RNA
OD <sub>600</sub>	Optical density at 600 nm
PDB	Protein Data Bank
PBD	Polo-box domain
PCR	Polymerase chain reaction
Plk	Polo-like kinase
PRK	Proliferation-related kinase
RNA	Ribonucleic acid
RNAi	RNA interference
SD	Standard deviation(s)
SDS-PAGE	Sodium dodecyl sulfate-polyacrylamide gel electrophoresis
siRNA	Small interfering RNA
SH2 domain	Src-homology 2 domain
SNK	Serum-inducible kinase
STAT	Signal transducer and activator of transcription
Tab.	Table
T <sub>M</sub>	Melting temperature of a primer
tRNA	Transfer RNA

Amino acids were described by their one or three letter code. Phosphorylated amino acids were referred to as pX (X: one letter code).

## 7. Bibliography

- Abrieu, A., Brassac, T., Galas, S., Fisher, D., Labbe, J. C., and Doree, M. (1998). The Polo-like kinase Plx1 is a component of the MPF amplification loop at the G2/M-phase transition of the cell cycle in *Xenopus* eggs. *J Cell Sci* *111* (Pt 12), 1751-1757.
- Ahonen, L. J., Kallio, M. J., Daum, J. R., Bolton, M., Manke, I. A., Yaffe, M. B., Stukenberg, P. T., and Gorbsky, G. J. (2005). Polo-like kinase 1 creates the tension-sensing 3F3/2 phosphoepitope and modulates the association of spindle-checkpoint proteins at kinetochores. *Curr Biol* *15*, 1078-1089.
- Anderson, M., Ng, S. S., Marchesi, V., MacIver, F. H., Stevens, F. E., Riddell, T., Glover, D. M., Hagan, I. M., and McNerny, C. J. (2002). Plx1(+) regulates gene transcription at the M-G(1) interval during the fission yeast mitotic cell cycle. *Embo J* *21*, 5745-5755.
- Ando, K., Ozaki, T., Yamamoto, H., Furuya, K., Hosoda, M., Hayashi, S., Fukuzawa, M., and Nakagawara, A. (2004). Polo-like kinase 1 (Plk1) inhibits p53 function by physical interaction and phosphorylation. *J Biol Chem* *279*, 25549-25561.
- Aumailley, M., Gurrath, M., Muller, G., Calvete, J., Timpl, R., and Kessler, H. (1991). Arg-Gly-Asp constrained within cyclic pentapeptides. Strong and selective inhibitors of cell adhesion to vitronectin and laminin fragment P1. *FEBS Lett* *291*, 50-54.
- Bahassi el, M., Conn, C. W., Myer, D. L., Hennigan, R. F., McGowan, C. H., Sanchez, Y., and Stambrook, P. J. (2002). Mammalian Polo-like kinase 3 (Plk3) is a multifunctional protein involved in stress response pathways. *Oncogene* *21*, 6633-6640.
- Bandeiras, T. M., Hillig, R. C., Matias, P. M., Eberspaecher, U., Fanghanel, J., Thomaz, M., Miranda, S., Crusius, K., Putter, V., Amstutz, P., *et al.* (2008). Structure of wild-type Plk-1 kinase domain in complex with a selective DARPIn. *Acta Crystallogr D Biol Crystallogr* *64*, 339-353.
- Barr, F. A., Sillje, H. H., and Nigg, E. A. (2004). Polo-like kinases and the orchestration of cell division. *Nat Rev Mol Cell Biol* *5*, 429-440.
- Berg, T. (2003). Modulation of protein-protein interactions with small organic molecules. *Angew Chem Int Ed Engl* *42*, 2462-2481.
- Bogan, A. A., and Thorn, K. S. (1998). Anatomy of hot spots in protein interfaces. *J Mol Biol* *280*, 1-9.
- Bottger, V., Bottger, A., Howard, S. F., Picksley, S. M., Chene, P., Garcia-Echeverria, C., Hochkeppel, H. K., and Lane, D. P. (1996). Identification of novel mdm2 binding peptides by phage display. *Oncogene* *13*, 2141-2147.
- Bradford, M. M. (1976). A rapid and sensitive method for the quantitation of microgram quantities of protein utilizing the principle of protein-dye binding. *Anal Biochem* *72*, 248-254.

- Burns, T. F., Fei, P., Scata, K. A., Dicker, D. T., and El-Deiry, W. S. (2003). Silencing of the novel p53 target gene Snk/Plk2 leads to mitotic catastrophe in paclitaxel (taxol)-exposed cells. *Mol Cell Biol* 23, 5556-5571.
- Casenghi, M., Meraldi, P., Weinhart, U., Duncan, P. I., Korner, R., and Nigg, E. A. (2003). Polo-like kinase 1 regulates Nlp, a centrosome protein involved in microtubule nucleation. *Dev Cell* 5, 113-125.
- Casenghi, M., Barr, F. A., and Nigg, E. A. (2005). Phosphorylation of Nlp by Plk1 negatively regulates its dynein-dynactin-dependent targeting to the centrosome. *J Cell Sci* 118, 5101-5108.
- Chase, D., Serafinas, C., Ashcroft, N., Kosinski, M., Longo, D., Ferris, D. K., and Golden, A. (2000a). The polo-like kinase PLK-1 is required for nuclear envelope breakdown and the completion of meiosis in *Caenorhabditis elegans*. *Genesis* 26, 26-41.
- Chase, D., Golden, A., Heidecker, G., and Ferris, D. K. (2000b). *Caenorhabditis elegans* contains a third polo-like kinase gene. *DNA Seq* 11, 327-334.
- Cheng, K. Y., Lowe, E. D., Sinclair, J., Nigg, E. A., and Johnson, L. N. (2003). The crystal structure of the human polo-like kinase-1 polo box domain and its phospho-peptide complex. *Embo J* 22, 5757-5768.
- Clackson, T., and Wells, J. A. (1995). A hot spot of binding energy in a hormone-receptor interface. *Science* 267, 383-386.
- Clay, F. J., McEwen, S. J., Bertoncello, I., Wilks, A. F., and Dunn, A. R. (1993). Identification and cloning of a protein kinase-encoding mouse gene, Plk, related to the polo gene of *Drosophila*. *Proc Natl Acad Sci U S A* 90, 4882-4886.
- Coleman, D. R. t., Ren, Z., Mandal, P. K., Cameron, A. G., Dyer, G. A., Muranjan, S., Campbell, M., Chen, X., and McMurray, J. S. (2005). Investigation of the binding determinants of phosphopeptides targeted to the SRC homology 2 domain of the signal transducer and activator of transcription 3. Development of a high-affinity peptide inhibitor. *J Med Chem* 48, 6661-6670.
- Corson, T. W., and Crews, C. M. (2007). Molecular understanding and modern application of traditional medicines: triumphs and trials. *Cell* 130, 769-774.
- Davis-Ward, R., Mook, R. A., Jr., Neeb, M. J., and Salovich, J. M. (2004). Preparation of pyrimidine derivatives as Polo-like kinases inhibitors for treatment of cancers. World Patent WO 2004074244
- de Carcer, G., de Castro, I. P., and Malumbres, M. (2007). Targeting cell cycle kinases for cancer therapy. *Curr Med Chem* 14, 969-985.
- Dechantsreiter, M. A., Planker, E., Matha, B., Lohof, E., Holzemann, G., Jonczyk, A., Goodman, S. L., and Kessler, H. (1999). N-Methylated cyclic RGD peptides as highly active and selective alpha(V)beta(3) integrin antagonists. *J Med Chem* 42, 3033-3040.

- DeDecker, B. S. (2000). Allosteric drugs: thinking outside the active-site box. *Chem Biol* 7, R103-107.
- DeLuca, J. G., Moree, B., Hickey, J. M., Kilmartin, J. V., and Salmon, E. D. (2002). hNuf2 inhibition blocks stable kinetochore-microtubule attachment and induces mitotic cell death in HeLa cells. *J Cell Biol* 159, 549-555.
- Descombes, P., and Nigg, E. A. (1998). The polo-like kinase Plx1 is required for M phase exit and destruction of mitotic regulators in *Xenopus* egg extracts. *Embo J* 17, 1328-1335.
- Donaldson, M. M., Tavares, A. A., Hagan, I. M., Nigg, E. A., and Glover, D. M. (2001). The mitotic roles of Polo-like kinase. *J Cell Sci* 114, 2357-2358.
- Du, Y., Masters, S. C., Khuri, F. R., and Fu, H. (2006). Monitoring 14-3-3 protein interactions with a homogeneous fluorescence polarization assay. *J Biomol Screen* 11, 269-276.
- Duncan, P. I., Pollet, N., Niehrs, C., and Nigg, E. A. (2001). Cloning and characterization of Plx2 and Plx3, two additional Polo-like kinases from *Xenopus laevis*. *Exp Cell Res* 270, 78-87.
- Durocher, D., Taylor, I. A., Sarbassova, D., Haire, L. F., Westcott, S. L., Jackson, S. P., Smerdon, S. J., and Yaffe, M. B. (2000). The molecular basis of FHA domain:phosphopeptide binding specificity and implications for phospho-dependent signaling mechanisms. *Mol Cell* 6, 1169-1182.
- Eckerdt, F., Yuan, J., and Strebhardt, K. (2005). Polo-like kinases and oncogenesis. *Oncogene* 24, 267-276.
- Elia, A. E., Cantley, L. C., and Yaffe, M. B. (2003a). Proteomic screen finds pSer/pThr binding domain localizing Plk1 to mitotic substrates. *Science* 299, 1228-1231.
- Elia, A. E., Rellos, P., Haire, L. F., Chao, J. W., Ivins, F. J., Hoepker, K., Mohammad, D., Cantley, L. C., Smerdon, S. J., and Yaffe, M. B. (2003b). The molecular basis for phosphodependent substrate targeting and regulation of Plks by the Polo-box domain. *Cell* 115, 83-95.
- Ellinger-Ziegelbauer, H., Karasuyama, H., Yamada, E., Tsujikawa, K., Todokoro, K., and Nishida, E. (2000). Ste20-like kinase (SLK), a regulatory kinase for polo-like kinase (Plk) during the G2/M transition in somatic cells. *Genes Cells* 5, 491-498.
- Elowe, S., Hummer, S., Uldschmid, A., Li, X., and Nigg, E. A. (2007). Tension-sensitive Plk1 phosphorylation on BubR1 regulates the stability of kinetochore microtubule interactions. *Genes Dev* 21, 2205-2219.
- Engels, W. R. (1993). Contributing software to the internet: the Amplify program. *Trends Biochem Sci* 18, 448-450.

- Fang, G., Yu, H., and Kirschner, M. W. (1998). The checkpoint protein MAD2 and the mitotic regulator CDC20 form a ternary complex with the anaphase-promoting complex to control anaphase initiation. *Genes Dev* *12*, 1871-1883.
- Ferrara, N., Hillan, K. J., Gerber, H. P., and Novotny, W. (2004). Discovery and development of bevacizumab, an anti-VEGF antibody for treating cancer. *Nat Rev Drug Discov* *3*, 391-400.
- Fink, J., Sanders, K., Rippl, A., Finkernagel, S., Beckers, T. L., and Schmidt, M. (2007). Cell type-dependent effects of Polo-like kinase 1 inhibition compared with targeted polo box interference in cancer cell lines. *Mol Cancer Ther* *6*, 3189-3197.
- Fode, C., Motro, B., Yousefi, S., Heffernan, M., and Dennis, J. W. (1994). Sak, a murine protein-serine/threonine kinase that is related to the *Drosophila* polo kinase and involved in cell proliferation. *Proc Natl Acad Sci U S A* *91*, 6388-6392.
- Fode, C., Binkert, C., and Dennis, J. W. (1996). Constitutive expression of murine Sak-a suppresses cell growth and induces multinucleation. *Mol Cell Biol* *16*, 4665-4672.
- Gali-Muhtasib, H., Roessner, A., and Schneider-Stock, R. (2006). Thymoquinone: a promising anti-cancer drug from natural sources. *Int J Biochem Cell Biol* *38*, 1249-1253.
- Gali-Muhtasib, H., Ocker, M., Kuester, D., Krueger, S., El-Hajj, Z., Diestel, A., Evert, M., El-Najjar, N., Peters, B., Jurjus, A., *et al.* (2008). Thymoquinone reduces mouse colon tumor cell invasion and inhibits tumor growth in murine colon cancer models. *J Cell Mol Med* *12*, 330-342.
- Gavin, A. C., Bosche, M., Krause, R., Grandi, P., Marzioch, M., Bauer, A., Schultz, J., Rick, J. M., Michon, A. M., Cruciat, C. M., *et al.* (2002). Functional organization of the yeast proteome by systematic analysis of protein complexes. *Nature* *415*, 141-147.
- Gershoni, J. M., and Palade, G. E. (1983). Protein blotting: principles and applications. *Anal Biochem* *131*, 1-15.
- Goldberg, R. M. (2005). Cetuximab. *Nat Rev Drug Discov Suppl*, S10-11.
- Golsteyn, R. M., Schultz, S. J., Bartek, J., Ziemiecki, A., Ried, T., and Nigg, E. A. (1994). Cell cycle analysis and chromosomal localization of human Plk1, a putative homologue of the mitotic kinases *Drosophila* polo and *Saccharomyces cerevisiae* Cdc5. *J Cell Sci* *107 (Pt 6)*, 1509-1517.
- Golsteyn, R. M., Mundt, K. E., Fry, A. M., and Nigg, E. A. (1995). Cell cycle regulation of the activity and subcellular localization of Plk1, a human protein kinase implicated in mitotic spindle function. *J Cell Biol* *129*, 1617-1628.
- Guan, R., Tapang, P., Levenson, J. D., Albert, D., Giranda, V. L., and Luo, Y. (2005). Small interfering RNA-mediated Polo-like kinase 1 depletion preferentially reduces the survival of p53-defective, oncogenic transformed cells and inhibits tumor growth in animals. *Cancer Res* *65*, 2698-2704.

- Guenard, D., Gueritte-Voegelein, F., Dubois, J., and Potier, P. (1993). Structure-activity relationships of Taxol and Taxotere analogues. *J Natl Cancer Inst Monogr*, 79-82.
- Gumireddy, K., Reddy, M. V., Cosenza, S. C., Boominathan, R., Baker, S. J., Papathi, N., Jiang, J., Holland, J., and Reddy, E. P. (2005). ON01910, a non-ATP-competitive small molecule inhibitor of Plk1, is a potent anticancer agent. *Cancer Cell* 7, 275-286.
- Habedanck, R., Stierhof, Y. D., Wilkinson, C. J., and Nigg, E. A. (2005). The Polo kinase Plk4 functions in centriole duplication. *Nat Cell Biol* 7, 1140-1146.
- Hafner, M., Schmitz, A., Grune, I., Srivatsan, S. G., Paul, B., Kolanus, W., Quast, T., Kremmer, E., Bauer, I., and Famulok, M. (2006). Inhibition of cytohesins by SecinH3 leads to hepatic insulin resistance. *Nature* 444, 941-944.
- Hamanaka, R., Maloid, S., Smith, M. R., O'Connell, C. D., Longo, D. L., and Ferris, D. K. (1994). Cloning and characterization of human and murine homologues of the *Drosophila polo* serine-threonine kinase. *Cell Growth Differ* 5, 249-257.
- Hammond, S. M. (2005). Dicing and slicing: the core machinery of the RNA interference pathway. *FEBS Lett* 579, 5822-5829.
- Hanisch, A., Wehner, A., Nigg, E. A., and Sillje, H. H. (2006). Different Plk1 functions show distinct dependencies on Polo-Box domain-mediated targeting. *Mol Biol Cell* 17, 448-459.
- Hansen, D. V., Tung, J. J., and Jackson, P. K. (2006). CaMKII and polo-like kinase 1 sequentially phosphorylate the cytostatic factor Emi2/XErp1 to trigger its destruction and meiotic exit. *Proc Natl Acad Sci U S A* 103, 608-613.
- Hauf, S., Roitinger, E., Koch, B., Dittrich, C. M., Mechtler, K., and Peters, J. M. (2005). Dissociation of cohesin from chromosome arms and loss of arm cohesion during early mitosis depends on phosphorylation of SA2. *PLoS Biol* 3, e69.
- Holtrich, U., Wolf, G., Brauninger, A., Karn, T., Bohme, B., Rubsamen-Waigmann, H., and Strebhardt, K. (1994). Induction and down-regulation of PLK, a human serine/threonine kinase expressed in proliferating cells and tumors. *Proc Natl Acad Sci U S A* 91, 1736-1740.
- Holtrich, U., Wolf, G., Yuan, J., Bereiter-Hahn, J., Karn, T., Weiler, M., Kauselmann, G., Rehli, M., Andreesen, R., Kaufmann, M., *et al.* (2000). Adhesion induced expression of the serine/threonine kinase Fnk in human macrophages. *Oncogene* 19, 4832-4839.
- Hornig, N. C., and Uhlmann, F. (2004). Preferential cleavage of chromatin-bound cohesin after targeted phosphorylation by Polo-like kinase. *Embo J* 23, 3144-3153.
- Hudson, J. W., Kozarova, A., Cheung, P., Macmillan, J. C., Swallow, C. J., Cross, J. C., and Dennis, J. W. (2001). Late mitotic failure in mice lacking Sak, a polo-like kinase. *Curr Biol* 11, 441-446.

- Jang, Y. J., Lin, C. Y., Ma, S., and Erikson, R. L. (2002a). Functional studies on the role of the C-terminal domain of mammalian polo-like kinase. *Proc Natl Acad Sci U S A* *99*, 1984-1989.
- Jang, Y. J., Ma, S., Terada, Y., and Erikson, R. L. (2002b). Phosphorylation of threonine 210 and the role of serine 137 in the regulation of mammalian polo-like kinase. *J Biol Chem* *277*, 44115-44120.
- Jiang, N., Wang, X., Jhanwar-Uniyal, M., Darzynkiewicz, Z., and Dai, W. (2006). Polo box domain of Plk3 functions as a centrosome localization signal, overexpression of which causes mitotic arrest, cytokinesis defects, and apoptosis. *J Biol Chem* *281*, 10577-10582.
- Jones, S., and Thornton, J. M. (1996). Principles of protein-protein interactions. *Proc Natl Acad Sci U S A* *93*, 13-20.
- Johnson, T. M., Antrobus, R., and Johnson, L. N. (2008). Plk1 Activation by Ste20-like Kinase (Slk) Phosphorylation and Polo-Box Phosphopeptide Binding Assayed with the Substrate Translationally Controlled Tumor Protein (TCTP). *Biochemistry* *47*, 3688-3696.
- Jordan, M. A., Thrower, D., and Wilson, L. (1992). Effects of vinblastine, podophyllotoxin and nocodazole on mitotic spindles. Implications for the role of microtubule dynamics in mitosis. *J Cell Sci* *102 (Pt 3)*, 401-416.
- Jorissen, R. N., Walker, F., Pouliot, N., Garrett, T. P., Ward, C. W., and Burgess, A. W. (2003). Epidermal growth factor receptor: mechanisms of activation and signalling. *Exp Cell Res* *284*, 31-53.
- Kang, Y. H., Park, J. E., Yu, L. R., Soung, N. K., Yun, S. M., Bang, J. K., Seong, Y. S., Yu, H., Garfield, S., Veenstra, T. D., and Lee, K. S. (2006). Self-regulated Plk1 recruitment to kinetochores by the Plk1-PBIP1 interaction is critical for proper chromosome segregation. *Mol Cell* *24*, 409-422.
- Kaseb, A. O., Chinnakannu, K., Chen, D., Sivanandam, A., Tejawani, S., Menon, M., Dou, Q. P., and Reddy, G. P. (2007). Androgen receptor and E2F-1 targeted thymoquinone therapy for hormone-refractory prostate cancer. *Cancer Res* *67*, 7782-7788.
- Kiessling, A., Sperl, B., Hollis, A., Eick, D., and Berg, T. (2006). Selective inhibition of c-Myc/Max dimerization and DNA binding by small molecules. *Chem Biol* *13*, 745-751.
- Kim, S. J., Park, Y., and Hong, H. J. (2005). Antibody engineering for the development of therapeutic antibodies. *Mol Cells* *20*, 17-29.
- Kitada, K., Johnson, A. L., Johnston, L. H., and Sugino, A. (1993). A multicopy suppressor gene of the *Saccharomyces cerevisiae* G1 cell cycle mutant gene *dbf4* encodes a protein kinase and is identified as CDC5. *Mol Cell Biol* *13*, 4445-4457.

- Kleylein-Sohn, J., Westendorf, J., Le Clech, M., Habedanck, R., Stierhof, Y. D., and Nigg, E. A. (2007). Plk4-induced centriole biogenesis in human cells. *Dev Cell* *13*, 190-202.
- Kohler, G., and Milstein, C. (1976). Derivation of specific antibody-producing tissue culture and tumor lines by cell fusion. *Eur J Immunol* *6*, 511-519.
- Kothe, M., Kohls, D., Low, S., Coli, R., Cheng, A. C., Jacques, S. L., Johnson, T. L., Lewis, C., Loh, C., Nonomiya, J., *et al.* (2007a). Structure of the catalytic domain of human polo-like kinase 1. *Biochemistry* *46*, 5960-5971.
- Kothe, M., Kohls, D., Low, S., Coli, R., Rennie, G. R., Feru, F., Kuhn, C., and Ding, Y. H. (2007b). Selectivity-determining residues in Plk1. *Chem Biol Drug Des* *70*, 540-546.
- Laemmli, U. K. (1970). Cleavage of structural proteins during the assembly of the head of bacteriophage T4. *Nature* *227*, 680-685.
- Lake, R. J., and Jelinek, W. R. (1993). Cell cycle- and terminal differentiation-associated regulation of the mouse mRNA encoding a conserved mitotic protein kinase. *Mol Cell Biol* *13*, 7793-7801.
- Lampson, M. A., and Kapoor, T. M. (2005). The human mitotic checkpoint protein BubR1 regulates chromosome-spindle attachments. *Nat Cell Biol* *7*, 93-98.
- Lane, H. A., and Nigg, E. A. (1996). Antibody microinjection reveals an essential role for human polo-like kinase 1 (Plk1) in the functional maturation of mitotic centrosomes. *J Cell Biol* *135*, 1701-1713.
- Lansing, T. J., McConnell, R. T., Duckett, D. R., Spehar, G. M., Knick, V. B., Hassler, D. F., Noro, N., Furuta, M., Emmitte, K. A., Gilmer, T. M., *et al.* (2007). In vitro biological activity of a novel small-molecule inhibitor of polo-like kinase 1. *Mol Cancer Ther* *6*, 450-459.
- Lee, M., Daniels, M. J., and Venkitaraman, A. R. (2004). Phosphorylation of BRCA2 by the Polo-like kinase Plk1 is regulated by DNA damage and mitotic progression. *Oncogene* *23*, 865-872.
- Lenart, P., Petronczki, M., Steegmaier, M., Di Fiore, B., Lipp, J. J., Hoffmann, M., Rettig, W. J., Kraut, N., and Peters, J. M. (2007). The small-molecule inhibitor BI 2536 reveals novel insights into mitotic roles of polo-like kinase 1. *Curr Biol* *17*, 304-315.
- Leung, G. C., Hudson, J. W., Kozarova, A., Davidson, A., Dennis, J. W., and Sicheri, F. (2002). The Sak polo-box comprises a structural domain sufficient for mitotic subcellular localization. *Nat Struct Biol* *9*, 719-724.
- Levy, D. E., and Darnell, J. E., Jr. (2002). Stats: transcriptional control and biological impact. *Nat Rev Mol Cell Biol* *3*, 651-662.
- Lin, H. R., Ting, N. S., Qin, J., and Lee, W. H. (2003). M phase-specific phosphorylation of BRCA2 by Polo-like kinase 1 correlates with the dissociation of the BRCA2-P/CAF complex. *J Biol Chem* *278*, 35979-35987.

- Lindon, C., and Pines, J. (2004). Ordered proteolysis in anaphase inactivates Plk1 to contribute to proper mitotic exit in human cells. *J Cell Biol* *164*, 233-241.
- Lipinski, C. A., Lombardo, F., Dominy, B. W., and Feeney, P. J. (2001). Experimental and computational approaches to estimate solubility and permeability in drug discovery and development settings. *Adv Drug Deliv Rev* *46*, 3-26.
- Litvak, V., Argov, R., Dahan, N., Ramachandran, S., Amarilio, R., Shainskaya, A., and Lev, S. (2004). Mitotic phosphorylation of the peripheral Golgi protein Nir2 by Cdk1 provides a docking mechanism for Plk1 and affects cytokinesis completion. *Mol Cell* *14*, 319-330.
- Liu, J., and Maller, J. L. (2005). Calcium elevation at fertilization coordinates phosphorylation of XErp1/Emi2 by Plx1 and CaMK II to release metaphase arrest by cytostatic factor. *Curr Biol* *15*, 1458-1468.
- Liu, X., and Erikson, R. L. (2003). Polo-like kinase (Plk)1 depletion induces apoptosis in cancer cells. *Proc Natl Acad Sci U S A* *100*, 5789-5794.
- Liu, X., Zhou, T., Kuriyama, R., and Erikson, R. L. (2004). Molecular interactions of Polo-like-kinase 1 with the mitotic kinesin-like protein CHO1/MKLP-1. *J Cell Sci* *117*, 3233-3246.
- Liu, Y., Shreder, K. R., Gai, W., Corral, S., Ferris, D. K., and Rosenblum, J. S. (2005). Wortmannin, a widely used phosphoinositide 3-kinase inhibitor, also potently inhibits mammalian polo-like kinase. *Chem Biol* *12*, 99-107.
- Liu, Y., Jiang, N., Wu, J., Dai, W., and Rosenblum, J. S. (2007). Polo-like kinases inhibited by wortmannin. Labeling site and downstream effects. *J Biol Chem* *282*, 2505-2511.
- Llamazares, S., Moreira, A., Tavares, A., Girdham, C., Spruce, B. A., Gonzalez, C., Karess, R. E., Glover, D. M., and Sunkel, C. E. (1991). polo encodes a protein kinase homolog required for mitosis in *Drosophila*. *Genes Dev* *5*, 2153-2165.
- Lo Conte, L., Chothia, C., and Janin, J. (1999). The atomic structure of protein-protein recognition sites. *J Mol Biol* *285*, 2177-2198.
- Ma, S., Charron, J., and Erikson, R. L. (2003). Role of Plk2 (Snk) in mouse development and cell proliferation. *Mol Cell Biol* *23*, 6936-6943.
- Mahajan, S., Ghosh, S., Sudbeck, E. A., Zheng, Y., Downs, S., Hupke, M., and Uckun, F. M. (1999). Rational design and synthesis of a novel anti-leukemic agent targeting Bruton's tyrosine kinase (BTK), LFM-A13 [alpha-cyano-beta-hydroxy-beta-methyl-N-(2, 5-dibromophenyl)propenamide]. *J Biol Chem* *274*, 9587-9599.
- Manning, G., Whyte, D. B., Martinez, R., Hunter, T., and Sudarsanam, S. (2002). The protein kinase complement of the human genome. *Science* *298*, 1912-1934.
- Martin, B. T., and Strebhardt, K. (2006). Polo-like kinase 1: target and regulator of transcriptional control. *Cell Cycle* *5*, 2881-2885.

- Martin-Lluesma, S., Stucke, V. M., and Nigg, E. A. (2002). Role of Hec1 in spindle checkpoint signaling and kinetochore recruitment of Mad1/Mad2. *Science* 297, 2267-2270.
- Matsumura, S., Toyoshima, F., and Nishida, E. (2007). Polo-like kinase 1 facilitates chromosome alignment during prometaphase through BubR1. *J Biol Chem* 282, 15217-15227.
- May, P., Gerhartz, C., Heesel, B., Welte, T., Doppler, W., Graeve, L., Horn, F., and Heinrich, P. C. (1996). Comparative study on the phosphotyrosine motifs of different cytokine receptors involved in STAT5 activation. *FEBS Lett* 394, 221-226.
- McInnes, C., Mezna, M., and Fischer, P. M. (2005). Progress in the discovery of polo-like kinase inhibitors. *Curr Top Med Chem* 5, 181-197.
- McInnes, C., Mazumdar, A., Mezna, M., Meades, C., Midgley, C., Scaerou, F., Carpenter, L., Mackenzie, M., Taylor, P., Walkinshaw, M., *et al.* (2006). Inhibitors of Polo-like kinase reveal roles in spindle-pole maintenance. *Nat Chem Biol* 2, 608-617.
- Meyer, A., Auernheimer, J., Modlinger, A., and Kessler, H. (2006). Targeting RGD recognizing integrins: drug development, biomaterial research, tumor imaging and targeting. *Curr Pharm Des* 12, 2723-2747.
- Morgan, D. O. (1999). Regulation of the APC and the exit from mitosis. *Nat Cell Biol* 1, E47-53.
- Müller, J., Sperl, B., Reindl, W., Kiessling, A., and Berg, T. (2008a). Discovery of chromone-based inhibitors of the transcription factor STAT5. *Chembiochem* 9, 723-727.
- Müller, J., Schust, J., and Berg, T. (2008b). A high-throughput assay for signal transducer and activator of transcription 5b based on fluorescence polarization. *Anal Biochem* 375, 249-254.
- Mullis, K. B., and Faloona, F. A. (1987). Specific synthesis of DNA in vitro via a polymerase-catalyzed chain reaction. *Methods Enzymol* 155, 335-350.
- Mundt, K. E., Golsteyn, R. M., Lane, H. A., and Nigg, E. A. (1997). On the regulation and function of human polo-like kinase 1 (PLK1): effects of overexpression on cell cycle progression. *Biochem Biophys Res Commun* 239, 377-385.
- Nahta, R., and Esteva, F. J. (2006). Herceptin: mechanisms of action and resistance. *Cancer Lett* 232, 123-138.
- Nakajima, H., Toyoshima-Morimoto, F., Taniguchi, E., and Nishida, E. (2003). Identification of a consensus motif for Plk (Polo-like kinase) phosphorylation reveals Myt1 as a Plk1 substrate. *J Biol Chem* 278, 25277-25280.
- Nasir, M. S., and Jolley, M. E. (1999). Fluorescence polarization: an analytical tool for immunoassay and drug discovery. *Comb Chem High Throughput Screen* 2, 177-190.

- Nasmyth, K. (2005). How do so few control so many? *Cell* *120*, 739-746.
- Neef, R., Preisinger, C., Sutcliffe, J., Kopajtich, R., Nigg, E. A., Mayer, T. U., and Barr, F. A. (2003). Phosphorylation of mitotic kinesin-like protein 2 by polo-like kinase 1 is required for cytokinesis. *J Cell Biol* *162*, 863-875.
- Nigg, E. A. (2001). Mitotic kinases as regulators of cell division and its checkpoints. *Nat Rev Mol Cell Biol* *2*, 21-32.
- Nikolovska-Coleska, Z., Wang, R., Fang, X., Pan, H., Tomita, Y., Li, P., Roller, P. P., Krajewski, K., Saito, N. G., Stuckey, J. A., and Wang, S. (2004). Development and optimization of a binding assay for the XIAP BIR3 domain using fluorescence polarization. *Anal Biochem* *332*, 261-273.
- Ohkura, H., Hagan, I. M., and Glover, D. M. (1995). The conserved *Schizosaccharomyces pombe* kinase *plp1*, required to form a bipolar spindle, the actin ring, and septum, can drive septum formation in G1 and G2 cells. *Genes Dev* *9*, 1059-1073.
- Okada, H., and Mak, T. W. (2004). Pathways of apoptotic and non-apoptotic death in tumour cells. *Nat Rev Cancer* *4*, 592-603.
- Oshimori, N., Ohsugi, M., and Yamamoto, T. (2006). The Plk1 target Kizuna stabilizes mitotic centrosomes to ensure spindle bipolarity. *Nat Cell Biol* *8*, 1095-1101.
- Ouyang, B., Pan, H., Lu, L., Li, J., Stambrook, P., Li, B., and Dai, W. (1997). Human Prk is a conserved protein serine/threonine kinase involved in regulating M phase functions. *J Biol Chem* *272*, 28646-28651.
- Ouyang, B., Li, W., Pan, H., Meadows, J., Hoffmann, I., and Dai, W. (1999). The physical association and phosphorylation of Cdc25C protein phosphatase by Prk. *Oncogene* *18*, 6029-6036.
- Owicki, J. C. (2000). Fluorescence polarization and anisotropy in high throughput screening: perspectives and primer. *J Biomol Screen* *5*, 297-306.
- Peters, J. M. (2002). The anaphase-promoting complex: proteolysis in mitosis and beyond. *Mol Cell* *9*, 931-943.
- Peters, U., Cherian, J., Kim, J. H., Kwok, B. H., and Kapoor, T. M. (2006). Probing cell-division phenotype space and Polo-like kinase function using small molecules. *Nat Chem Biol* *2*, 618-626.
- Picksley, S. M., Vojtesek, B., Sparks, A., and Lane, D. P. (1994). Immunochemical analysis of the interaction of p53 with MDM2;--fine mapping of the MDM2 binding site on p53 using synthetic peptides. *Oncogene* *9*, 2523-2529.
- Pinsky, B. A., and Biggins, S. (2005). The spindle checkpoint: tension versus attachment. *Trends Cell Biol* *15*, 486-493.

- Qian, Y. W., Erikson, E., Li, C., and Maller, J. L. (1998). Activated polo-like kinase Plx1 is required at multiple points during mitosis in *Xenopus laevis*. *Mol Cell Biol* 18, 4262-4271.
- Quelle, F. W., Wang, D., Nosaka, T., Thierfelder, W. E., Stravopodis, D., Weinstein, Y., and Ihle, J. N. (1996). Erythropoietin induces activation of Stat5 through association with specific tyrosines on the receptor that are not required for a mitogenic response. *Mol Cell Biol* 16, 1622-1631.
- Rapley, J., Baxter, J. E., Blot, J., Wattam, S. L., Casenghi, M., Meraldi, P., Nigg, E. A., and Fry, A. M. (2005). Coordinate regulation of the mother centriole component nlp by nek2 and plk1 protein kinases. *Mol Cell Biol* 25, 1309-1324.
- Rauh, N. R., Schmidt, A., Bormann, J., Nigg, E. A., and Mayer, T. U. (2005). Calcium triggers exit from meiosis II by targeting the APC/C inhibitor XErp1 for degradation. *Nature* 437, 1048-1052.
- Ree, A. H., Bratland, A., Nome, R. V., Stokke, T., and Fodstad, O. (2003). Repression of mRNA for the PLK cell cycle gene after DNA damage requires BRCA1. *Oncogene* 22, 8952-8955.
- Rishi, V., Potter, T., Laudeman, J., Reinhart, R., Silvers, T., Selby, M., Stevenson, T., Krosky, P., Stephen, A. G., Acharya, A., *et al.* (2005). A high-throughput fluorescence-anisotropy screen that identifies small molecule inhibitors of the DNA binding of B-ZIP transcription factors. *Anal Biochem* 340, 259-271.
- Rooney, S., and Ryan, M. F. (2005). Effects of alpha-hederin and thymoquinone, constituents of *Nigella sativa*, on human cancer cell lines. *Anticancer Res* 25, 2199-2204.
- Roshak, A. K., Capper, E. A., Imburgia, C., Fornwald, J., Scott, G., and Marshall, L. A. (2000). The human polo-like kinase, PLK, regulates cdc2/cyclin B through phosphorylation and activation of the cdc25C phosphatase. *Cell Signal* 12, 405-411.
- Rowinsky, E. K. (1997). Paclitaxel pharmacology and other tumor types. *Semin Oncol* 24, S19-11-S19-12.
- Russo, A. A., Jeffrey, P. D., and Pavletich, N. P. (1996). Structural basis of cyclin-dependent kinase activation by phosphorylation. *Nat Struct Biol* 3, 696-700.
- Saldanha, S. A., Kaler, G., Cottam, H. B., Abagyan, R., and Taylor, S. S. (2006). Assay principle for modulators of protein-protein interactions and its application to non-ATP-competitive ligands targeting protein kinase A. *Anal Chem* 78, 8265-8272.
- Sambrook, J., Fritsch, E. F., and Maniatis, M. (1989). *Molecular cloning: A laboratory manual*. (Cold Spring Harbor, Cold Spring Harbor Laboratory Press).
- Santamaria, A., Neef, R., Eberspacher, U., Eis, K., Husemann, M., Mumberg, D., Prectl, S., Schulze, V., Siemeister, G., Wortmann, L., *et al.* (2007). Use of the novel Plk1 inhibitor ZK-thiazolidinone to elucidate functions of Plk1 in early and late stages of mitosis. *Mol Biol Cell* 18, 4024-4036.

- Scherer, L. J., and Rossi, J. J. (2003). Approaches for the sequence-specific knockdown of mRNA. *Nat Biotechnol* 21, 1457-1465.
- Schmidt, A., Duncan, P. I., Rauh, N. R., Sauer, G., Fry, A. M., Nigg, E. A., and Mayer, T. U. (2005). *Xenopus* polo-like kinase Plx1 regulates XErp1, a novel inhibitor of APC/C activity. *Genes Dev* 19, 502-513.
- Schmidt, M., Hofmann, H. P., Sanders, K., Sczakiel, G., Beckers, T. L., and Gekeler, V. (2006). Molecular alterations after Polo-like kinase 1 mRNA suppression versus pharmacologic inhibition in cancer cells. *Mol Cancer Ther* 5, 809-817.
- Schust, J., and Berg, T. (2004). A high-throughput fluorescence polarization assay for signal transducer and activator of transcription 3. *Anal Biochem* 330, 114-118.
- Schust, J., Sperl, B., Hollis, A., Mayer, T. U., and Berg, T. (2006). Stattic: a small-molecule inhibitor of STAT3 activation and dimerization. *Chem Biol* 13, 1235-1242.
- Seong, Y. S., Kamijo, K., Lee, J. S., Fernandez, E., Kuriyama, R., Miki, T., and Lee, K. S. (2002). A spindle checkpoint arrest and a cytokinesis failure by the dominant-negative polo-box domain of Plk1 in U-2 OS cells. *J Biol Chem* 277, 32282-32293.
- Shoieb, A. M., Elgayyar, M., Dudrick, P. S., Bell, J. L., and Tithof, P. K. (2003). In vitro inhibition of growth and induction of apoptosis in cancer cell lines by thymoquinone. *Int J Oncol* 22, 107-113.
- Sillje, H. H., and Nigg, E. A. (2003). Signal transduction. Capturing polo kinase. *Science* 299, 1190-1191.
- Simmons, D. L., Neel, B. G., Stevens, R., Evett, G., and Erikson, R. L. (1992). Identification of an early-growth-response gene encoding a novel putative protein kinase. *Mol Cell Biol* 12, 4164-4169.
- Smith, P. K., Krohn, R. I., Hermanson, G. T., Mallia, A. K., Gartner, F. H., Provenzano, M. D., Fujimoto, E. K., Goeke, N. M., Olson, B. J., and Klenk, D. C. (1985). Measurement of protein using bicinchoninic acid. *Anal Biochem* 150, 76-85.
- Smits, V. A., Klompaker, R., Arnaud, L., Rijksen, G., Nigg, E. A., and Medema, R. H. (2000). Polo-like kinase-1 is a target of the DNA damage checkpoint. *Nat Cell Biol* 2, 672-676.
- Spankuch-Schmitt, B., Wolf, G., Solbach, C., Loibl, S., Knecht, R., Stegmuller, M., von Minckwitz, G., Kaufmann, M., and Strebhardt, K. (2002a). Downregulation of human polo-like kinase activity by antisense oligonucleotides induces growth inhibition in cancer cells. *Oncogene* 21, 3162-3171.
- Spankuch-Schmitt, B., Bereiter-Hahn, J., Kaufmann, M., and Strebhardt, K. (2002b). Effect of RNA silencing of polo-like kinase-1 (PLK1) on apoptosis and spindle formation in human cancer cells. *J Natl Cancer Inst* 94, 1863-1877.

- Steehmaier, M., Hoffmann, M., Baum, A., Lenart, P., Petronczki, M., Krssak, M., Gurtler, U., Garin-Chesa, P., Lieb, S., Quant, J., *et al.* (2007). BI 2536, a potent and selective inhibitor of polo-like kinase 1, inhibits tumor growth in vivo. *Curr Biol* *17*, 316-322.
- Stevenson, C. S., Capper, E. A., Roshak, A. K., Marquez, B., Eichman, C., Jackson, J. R., Mattern, M., Gerwick, W. H., Jacobs, R. S., and Marshall, L. A. (2002). The identification and characterization of the marine natural product scytonemin as a novel antiproliferative pharmacophore. *J Pharmacol Exp Ther* *303*, 858-866.
- Strausfeld, U., Fernandez, A., Capony, J. P., Girard, F., Lautredou, N., Derancourt, J., Labbe, J. C., and Lamb, N. J. (1994). Activation of p34cdc2 protein kinase by microinjection of human cdc25C into mammalian cells. Requirement for prior phosphorylation of cdc25C by p34cdc2 on sites phosphorylated at mitosis. *J Biol Chem* *269*, 5989-6000.
- Strebhardt, K., and Ullrich, A. (2006). Targeting polo-like kinase 1 for cancer therapy. *Nat Rev Cancer* *6*, 321-330.
- Sumara, I., Gimenez-Abian, J. F., Gerlich, D., Hirota, T., Kraft, C., de la Torre, C., Ellenberg, J., and Peters, J. M. (2004). Roles of polo-like kinase 1 in the assembly of functional mitotic spindles. *Curr Biol* *14*, 1712-1722.
- Sunkel, C. E., and Glover, D. M. (1988). polo, a mitotic mutant of *Drosophila* displaying abnormal spindle poles. *J Cell Sci* *89 (Pt 1)*, 25-38.
- Tsvetkov, L. (2004). Polo-like kinases and Chk2 at the interface of DNA damage checkpoint pathways and mitotic regulation. *IUBMB Life* *56*, 449-456.
- Tsvetkov, L. M., Tsekova, R. T., Xu, X., and Stern, D. F. (2005). The Plk1 Polo box domain mediates a cell cycle and DNA damage regulated interaction with Chk2. *Cell Cycle* *4*, 609-617.
- Uckun, F. M., Dibirdik, I., Qazi, S., Vassilev, A., Ma, H., Mao, C., Benyumov, A., and Emami, K. H. (2007). Anti-breast cancer activity of LFM-A13, a potent inhibitor of Polo-like kinase (PLK). *Bioorg Med Chem* *15*, 800-814.
- van de Weerd, B. C., and Medema, R. H. (2006). Polo-like kinases: a team in control of the division. *Cell Cycle* *5*, 853-864.
- van Vugt, M. A., van de Weerd, B. C., Vader, G., Janssen, H., Calafat, J., Klompaker, R., Wolthuis, R. M., and Medema, R. H. (2004a). Polo-like kinase-1 is required for bipolar spindle formation but is dispensable for anaphase promoting complex/Cdc20 activation and initiation of cytokinesis. *J Biol Chem* *279*, 36841-36854.
- van Vugt, M. A., Bras, A., and Medema, R. H. (2004b). Polo-like kinase-1 controls recovery from a G2 DNA damage-induced arrest in mammalian cells. *Mol Cell* *15*, 799-811.
- Walter, S. A., Cutler, R. E., Jr., Martinez, R., Gishizky, M., and Hill, R. J. (2003). Stk10, a new member of the polo-like kinase kinase family highly expressed in hematopoietic tissue. *J Biol Chem* *278*, 18221-18228.

- Warnke, S., Kemmler, S., Hames, R. S., Tsai, H. L., Hoffmann-Rohrer, U., Fry, A. M., and Hoffmann, I. (2004). Polo-like kinase-2 is required for centriole duplication in mammalian cells. *Curr Biol* *14*, 1200-1207.
- Watanabe, N., Arai, H., Nishihara, Y., Taniguchi, M., Hunter, T., and Osada, H. (2004). M-phase kinases induce phospho-dependent ubiquitination of somatic Wee1 by SCFbeta-TrCP. *Proc Natl Acad Sci U S A* *101*, 4419-4424.
- Wong, O. K., and Fang, G. (2005). Plx1 is the 3F3/2 kinase responsible for targeting spindle checkpoint proteins to kinetochores. *J Cell Biol* *170*, 709-719.
- Wong, O. K., and Fang, G. (2007). Cdk1 phosphorylation of BubR1 controls spindle checkpoint arrest and Plk1-mediated formation of the 3F3/2 epitope. *J Cell Biol* *179*, 611-617.
- Xie, S., Wu, H., Wang, Q., Cogswell, J. P., Husain, I., Conn, C., Stambrook, P., Jhanwar-Uniyal, M., and Dai, W. (2001). Plk3 functionally links DNA damage to cell cycle arrest and apoptosis at least in part via the p53 pathway. *J Biol Chem* *276*, 43305-43312.
- Yaffe, M. B., Schutkowski, M., Shen, M., Zhou, X. Z., Stukenberg, P. T., Rahfeld, J. U., Xu, J., Kuang, J., Kirschner, M. W., Fischer, G., *et al.* (1997a). Sequence-specific and phosphorylation-dependent proline isomerization: a potential mitotic regulatory mechanism. *Science* *278*, 1957-1960.
- Yaffe, M. B., Rittinger, K., Volinia, S., Caron, P. R., Aitken, A., Leffers, H., Gamblin, S. J., Smerdon, S. J., and Cantley, L. C. (1997b). The structural basis for 14-3-3:phosphopeptide binding specificity. *Cell* *91*, 961-971.
- Yaffe, M. B., and Smerdon, S. J. (2004). The use of in vitro peptide-library screens in the analysis of phosphoserine/threonine-binding domain structure and function. *Annu Rev Physiol Biomol Struct* *33*, 225-244.
- Yap, A. S., Crampton, M. S., and Hardin, J. (2007). Making and breaking contacts: the cellular biology of cadherin regulation. *Curr Opin Cell Biol* *19*, 508-514.
- Yarm, F. R. (2002). Plk phosphorylation regulates the microtubule-stabilizing protein TCTP. *Mol Cell Biol* *22*, 6209-6221.
- Yuan, J., Kramer, A., Eckerdt, F., Kaufmann, M., and Strebhardt, K. (2002). Efficient internalization of the polo-box of polo-like kinase 1 fused to an Antennapedia peptide results in inhibition of cancer cell proliferation. *Cancer Res* *62*, 4186-4190.
- Zhang, J. H., Chung, T. D., and Oldenburg, K. R. (1999). A simple statistical parameter for use in evaluation and validation of high throughput screening assays. *J Biomol Screen* *4*, 67-73.
- Zhou, T., Aumais, J. P., Liu, X., Yu-Lee, L. Y., and Erikson, R. L. (2003). A role for Plk1 phosphorylation of NudC in cytokinesis. *Dev Cell* *5*, 127-138.

## 8. Publications

Parts of this thesis are published in:

Müller, J., Sperl, B., Reindl, W., Kiessling, A., and Berg, T. (2008). Discovery of chromone-based inhibitors of the transcription factor STAT5. *Chembiochem* 9(5): 723-727.

Reindl, W., Yuan, J., Krämer, A., Strebhardt, K., and Berg, T. (2008). Inhibition of polo-like kinase 1 by blocking polo-box domain-dependent protein-protein interactions. *Chem Biol* 15(5): 459-466.

Reindl, W., Strebhardt, K., and Berg, T. (2008). A high-throughput assay based on fluorescence polarization for inhibitors of the polo-box domain of polo-like kinase 1. *Anal Biochem*, in press.

## 9. Acknowledgements

In the end, I want to thank all people involved in the positive course of this project.

I am very thankful to Prof. Dr. Dr. h.c. Horst Kessler for supervising my thesis as my doctoral adviser at the Department of Chemistry of the Technical University of Munich.

Very special thanks go to Dr. Thorsten Berg for giving me the chance to work on this exciting project, for his excellent supervision, the constant discussions and suggestions, and all advice for writing this thesis. An entry for “perfect supervisor” in an encyclopedia would show his picture.

Many thanks also go to Prof. Dr. Axel Ullrich for providing me with the opportunity to work in the Department of Molecular Biology and for all support.

I am grateful to Prof. Dr. Klaus Strebhardt, Dr. Juping Yuan and Andrea Krämer from the University of Frankfurt for the successful collaboration and the many stimulating discussions.

Furthermore, I extend my thanks to Prof. Dr. Thomas Mayer from the University of Konstanz for providing access to his chemical library.

I want to say thanks to all my current and former lab mates Bianca Sperl, Judith Müller, Angela Berg, Anke Kiessling, Martin Gräber, Hüseyin Cavga and Jochen Schust for all their help and discussions regarding experiments and for creating such a pleasant working atmosphere. Additionally I want to thank Anke Kiessling for introducing me so well to the lab's working techniques, and Angela Berg for proof-reading this thesis, ensuring that the “German-English” does not get too dominant. I am really happy I had such nice colleagues. And I apologize for all the lectures on football, capital cities, etc. they had to endure.

Many thanks also to all of my current and former office mates, especially Stephan Busche, for the discussion of problems, for distractions in times of disappointment, and for broadening the mind beyond science.

I want to thank all people of the Department of Molecular Biology for their help. And thanks to the department's football team for their enthusiasm, their sportsmanship, and for giving me the chance to be part of the team, winning the institute's football trophy twice. Cheers, lads!

Finally, special thanks go to my parents and Sophia for all their support and constant help during the last years, and for giving me the best opportunities to focus on this thesis.